Evaluation and Improvement of a Modified Permeameter to Characterize Dual Porosity Media

by
Beatriz Fidalgo Valverde

Diploma, Mining Engineering (1999)
Oviedo School of Mines, Spain

Submitted to the Department of Civil and Environmental Engineering
in Partial Fulfillment of the Requirements for the degree of
Master of Science in Civil and Environmental Engineering

at the

Massachusetts Institute of Technology
February 2002

Signature of Author.....
Department of Civil and Environmental Engineering
January 28, 2002

Certified by.....
Prof. Patricia J. Culligan
Associate Professor of Department of Civil and Environmental Engineering
Thesis Supervisor

Certified by.....
Dr. John T. Germaine
Principal Research Associate of Department of Civil and Environmental Engineering
Thesis Co-Advisor

Accepted by.....
Prof. Oral Buyukozturk
Chairman, Departmental Committee on Graduate Studies

Evaluation and Improvement of a Modified Permeameter to Characterize Dual Porosity Media

by
Beatriz Fidalgo Valverde

Submitted to the Department of Civil and Environmental Engineering
On January 28, 2002 in Partial Fulfillment of the Requirements for the degree of
Master of Science in Civil and Environmental Engineering

ABSTRACT

A modified permeameter had been developed at MIT for the physical characterization of wetland soils, which are often assumed to be Dual Porosity Media. The inconsistent results obtained from tests without specimens and with well-characterized sand specimens indicated a poor performance of some elements of the permeameter, and the influence of others on the measured parameters. In this research, the permeameter performance has been improved and its capabilities have been expanded to allow for better testing of dual porosity soils.

To improve the performance of the permeameter new electrical conductivity probes were made and a second set was re-platinized, which allowed more precise and accurate readings of the solution concentrations. Several sets of experiments were carried out with no specimen in the permeameter. In each set, one or more of the equipment elements were examined. The results indicated that the porous stones, which are used to distribute solution evenly over a specimen's cross-section, have a significant effect on solution dispersion. This, in turn, influences the measured soil dispersion coefficients. While this influence might not be substantial for sand specimens, it could be important for organic soils. Approximate Equations are presented to account for the permeameter dispersion and mathematically separate it from the soil dispersion.

Thesis Supervisor: Prof. Patricia J. Culligan
Title: Associate Professor of Dpt. of Civil and Environmental Engineering

Thesis Co-Advisor: Dr. John T. Germaine
Title: Principle Research Associate of Dpt. of Civil and Environmental Engineering

TABLE OF CONTENTS

TABLE OF FIGURES

TABLE OF TABLES

LIST OF SYMBOLS

A: specimen cross-section area [L^2]

C = C/C_0: normalized concentration

C_{im}: solute concentration [ML^{-3}] per unit volume of immobile water.

C_m: solute concentration [ML^{-3}] per unit volume of mobile water.

C^*: solute flux due to sources or sinks.

D: dispersion tensor [L^2T]

D_d: diffusion coefficient [L^2T^{-1}]

D^*: dispersion coefficient [L^2T^{-1}].

f: fraction of adsorption sites that equilibrates with the mobile liquid phase.

h: head [L].

i: hydraulic gradient [-].

K_d: partition coefficient [L^3M^{-1}]

K_x: hydraulic conductivity in x direction [LT^{-1}]

P = u.L/D: Peclet Number

Q: flow rate [L^3/T]

q_x: specific discharge in x direction [L^3T^{-1}]

S: solute adsorbed per bulk dry mass of soil [MM^{-1}]

T = u.t/L: dimensionless time variable

T: dimensionless mass transfer coefficient

u: pore or seepage velocity [MT^{-1}]

u_a : average velocity [LT^{-1}]

v_x : linear velocity [LT^{-1}]

x: distance between points [L]

Z = x/L: dimensionless space variable

GREEK SYMBOLS

α: dispersivity [L].

ι: zero-order production term

μ: first-order decay coefficient

Σ (or beta): Partition coefficient.

θ_m: effective porosity or water moisture content of mobile region [L^3L^{-3}].

θ_{im}: porosity or water moisture content of immobile region [L^3L^{-3}].

Chapter 1: Introduction

Over the past decades, manufacturing industries buried their refuse and waste as a common practice. There was no waste management and thus the normal practice was the disposal of waste in uncontrolled landfills or dumping it on surface soils. In addition to this, liquid hazardous waste was released to rivers and water streams. Wastes originating from metal treatments were, and are still, disposed of in lagoons closed by embankments or in large landfills. In addition, accidental spills from landfills, industries facilities or underground storage tanks released hazardous wastes into the environment.

This waste, exposed to climatic action, such as rain or snow, does not remain in place but rather moves through the subsurface deposits. Water percolating downwards through the soils can transport the waste or contaminant particles until they reach the groundwater table. Once in the groundwater movement through the soil pore can transports the contaminants to water supply wells as shown in figure 1.1.

Inadequate waste disposal practices have given rise to alarming consequences, primarily concerning human health. Many toxic wastes were dumped or buried in organic soil, since it was commonly thought that this type of soil could act as a barrier to waste transport, absorbing substances into its matrix and preventing then from migration. Wetlands, which contain organic soils, have been extensively used as toxic waste repositories (Shell, 1985). However, despite their wide-spread use as waste receptors, the nature of organic soils is not well known. Thereby their use as toxic waste repositories is not sensible until a better understanding of how these soils transport and detain chemicals is built.

Recent studies have found that contaminants do not remain trapped in organic soils but rather move slowly through them (Hag, 1995, Price, 1986). Although the rate of movement is very low in some cases, making them reasonable barriers for further contamination, in other cases, this low flow rate does not allow enough dilution of contaminants, and the result can be watershed contamination.

The main objective of this research is the improvement of the modified permeameter developed at MIT by Ramsay (1990) and used by Aref (1999) for the Aberjona River bed peat characterization. This permeameter was adapted to allow measurements of the hydraulic parameters that characterize, physically, wetlands deposits. Through this research work, the permeameter will be available for the characterization of any soil, including organic soils. The new procedures and developments will improve the accuracy of results obtained using this device.

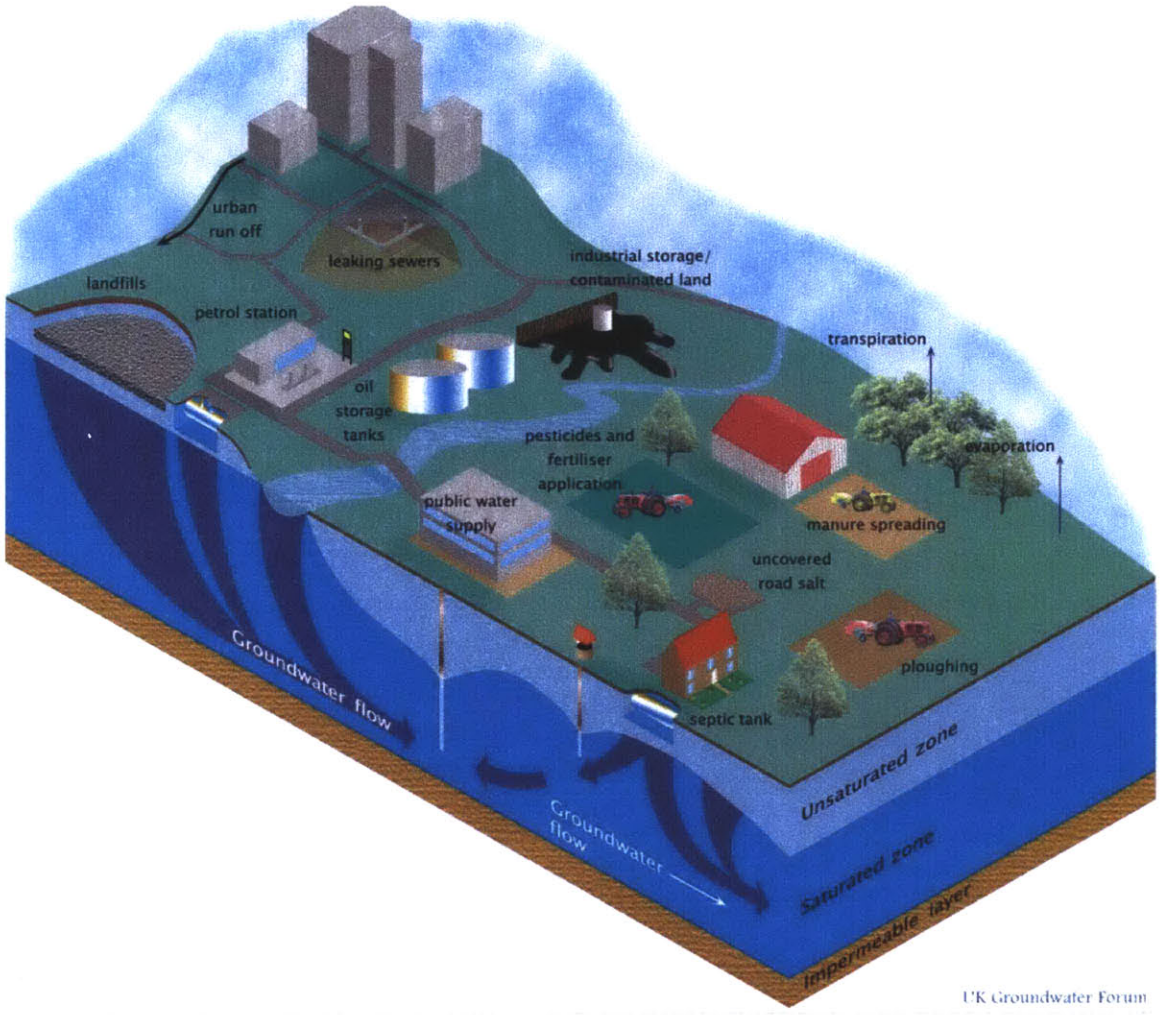

Figure 1.1: Contaminant movement towards the water table (Downing, 2000)

1.1. Background

Although it was thought that organic soils could retain and absorb the contaminants in their pore water, it has been proved, and well documented in the last decade, that contaminants move through organic soils (Price, 1986).

Organic soils constitute the upper layer of the earth crust, with the exception of glacial and coastal systems, where no organic matter is available for the formation of an organic layer. is easily contaminated.

An organic soil layer can have a 20 to 30 cm thickness, so accounting for contaminant transport through some organic layers could be unimportant. However, in some ecosystems, organic soil layers can be up to 160 cm thickness. In addition, they can be in contact with water bodies, which makes them an ideal route for contaminants from an origin source to reach a water body. There are several cases where this has happened. Some of these are highlight next.

1.1.1. Aberjona Watershed Case (US)

The Aberjona watershed is situated in the city of Woburn. In the early 1800's this region become an industrial center.

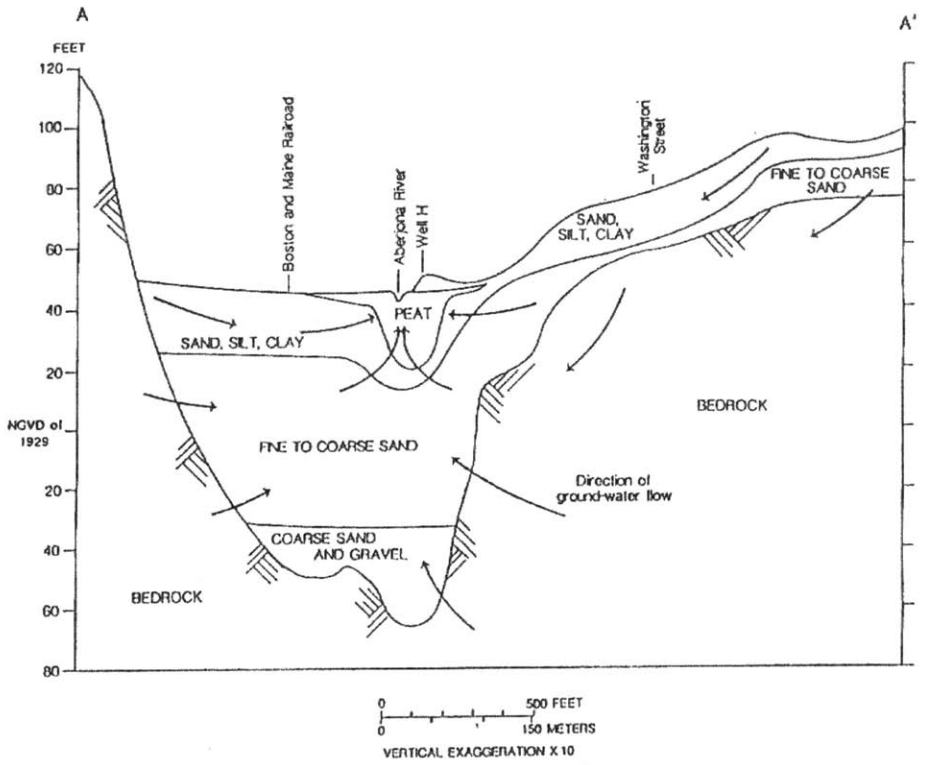

Figure 1.2: Stratigraphy at the pumping wells site in Woburn (After De Lima and Olimpio, 1989)

Industrial activity generated hazardous wastes that were either released into the Aberjona River that drains into the Aberjona watershed, or were buried on site. A wetland containing peat soils forms part of the stratigraphy of the watershed.

High concentration levels of heavy metals, by-products of the former industrial processes, have been found in the Aberjona watershed, indicating that these elements traveled through the watershed via the surface soils or the river. Furthermore, high concentrations of Volatic Organic Compounds have been detected in the drinking water extracted with pumping wells in the watershed (Myette, 1987). These pumping wells are tapped into a sand and gravel aquifer as shown in figure 1.2.

De Lima and Olimpo (1989) found that, when the pumping wells are not in use, the regional groundwater flows into the river through the wetlands, but when pumping wells are in use they induced flow of water from the river into the wetlands that surround the extracting wells. This means that the contaminants released in the Aberjona river passed through the surrounding wetlands, which form the riverbed, into the lower aquifers towards the drinking wells.

Extensive studies on the area have been carried at the MIT. The main objectives of these studies were the identification of wastes released in the area, identification of pathways through which toxic elements can reach humans, and determination of health effects. The permeameter improved through this research work was also developed as a part of this study.

1.1.2. Doñana Natural Park Case (Spain)

Doñana is considered the most important wetland in Europe. In April 1998, the tailing dam of the Los Frailes zinc mine lagoon, close to the wetland zone, collapsed. Billions of gallons of water with heavy metals escaped towards the Guadiamar River, eliminating aquatic life and depositing heavy metals throughout the area. The spill covered 10000 hectares of farmland and contaminants reached groundwater storages, then ruining the drinking water sources in the zone (figure 1.3)

Although the avalanche of water and sludge was stopped just before arriving at the Doñana National Park (thanks to the rapid construction of an emergency dam), the contamination has already reached the tropic chain and stork malformations and tumors have been subsequently detected. This suggests that contaminants have reached some water sources, and that the wetlands, rather than storing the contamination, have acted as a by-pass allowing contaminants to move to the storks drinking water zones.

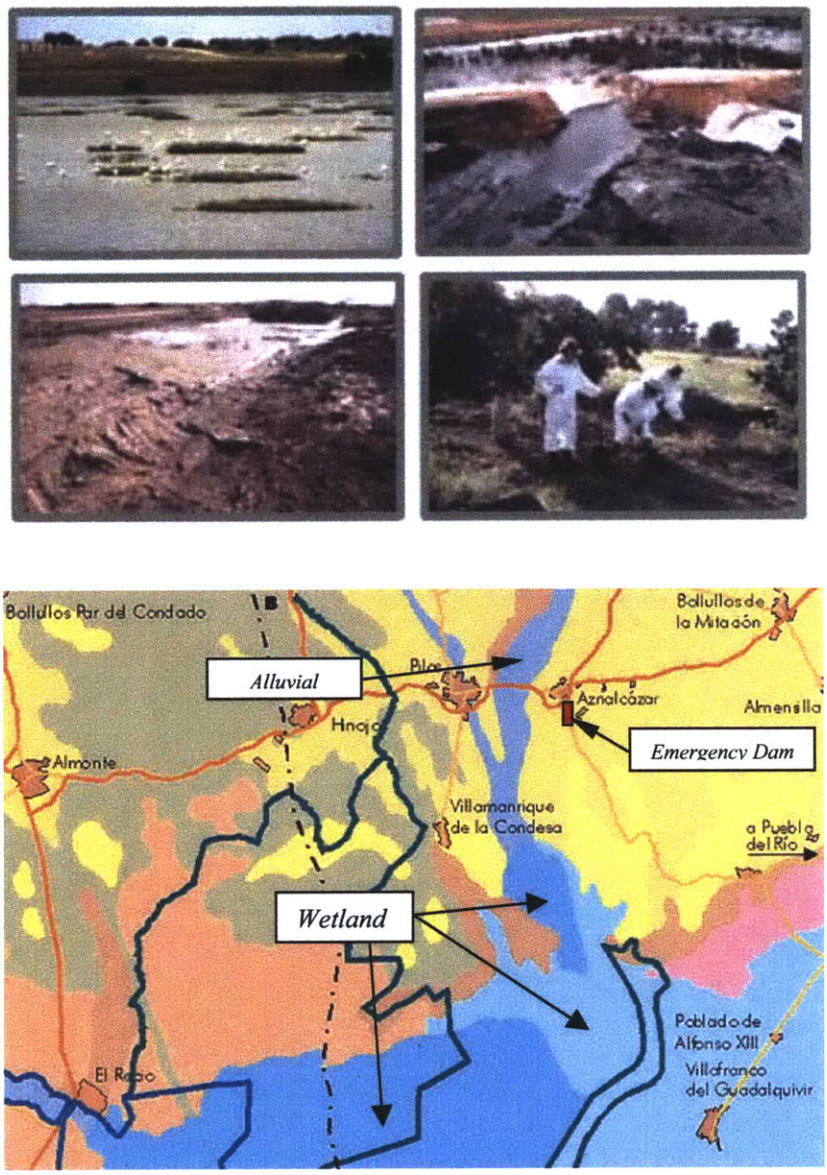

Figure 1.3: Doñana Natural Park (Consejería de Medio Ambiente. Junta de Andalucía, 1999)

1.2. Organic soils' main characteristics

Organic soils are porous and humid material. The mechanism of water flowing through these soils is complicated and not well known. Often, it is assumed that organic soils behave as a Two-Pore medium. Two-pore, or Dual porosity, means that the soil contains two kinds of pores (figure 1.4):

1. Pores that are connected and therefore form channels through which water can flow (mobile region).

2. Pores that are half isolated from the flow channels, where contaminants can move in and out by diffusion alone (immobile region). These type of pores are named dead-end pores.

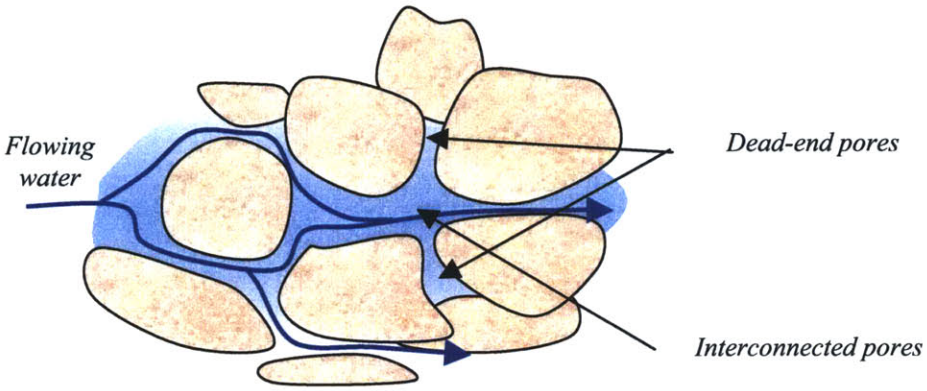

Figure 1.4: Mobile and immobile regions

Organic soils are a mixture of sediments and organic substances of dark brown color in colloidal form. These organic substances are the result of organic material decomposition. The organic material in soils is continuously decomposing and its composition is very complex and varies with environments and ecosystems.

Microscopy examination of organic soils shows a group of heterogeneous components consisting of organic elements with mineral material. For a detailed structural explanation of organic soils refer to Chapter 2.

The existence of dead-end pores is what makes organic soils a potential "long-term" contaminant storage soil. First, the contaminants carried by the water in solution will diffuse into the dead-end pores until the contaminant concentration in end pores equals the concentration of solute in the water. Contaminants will then remain in the pores until the contaminant concentration in the water decreases below the concentration level in the end pores. The same process that made solute accumulate in these pores will then reverse, and the contaminants will then diffuse back into the flowing water. Thus, once the contaminant source is removed or disappears, the organic soil itself becomes the contaminant source. However, since the process of diffusion is inherently slow, this may occur over a time-scale that is

acceptable is terms of contaminant mass release into the environment. Moreover, contaminant degradation itself might occur over this time scale.

1.3. Previous research

Previous research at MIT has been conducted to develop a better understanding of the mechanisms that control transport through organic deposits (Bialon, 1995). Column experiments were run on wetland samples from a contaminated Superfund site, the Aberjona watershed (see section 1.1), in order to investigate the factors that influence flow in wetland soils. These experiments were run with a modified permeameter that allows measurement of the hydraulic conductivity as well as breakthrough curves resulting from pulses of a conservative tracer introduced into the soil (Ramsay, 1996 and Aref, 1999).

Earlier results indicate that, although wetland soils are often classified as Two-Region soils, breakthrough of sodium chloride in the soil can be described with a One-Region Model using a mobile porosity that is less than the total porosity of the soil. This outcome indicates that sodium chloride did not interact with the immobile regions of the soil (Aref, 1999), probably due to the combination of a short injection time of solute and a high flow rate that limited the solute diffusion into and out of the immobile pores. Thus, it is suspected that some of the test procedures followed by Aref might have lead to false conclusions.

In addition, previous work indicated that the changes in the hydraulic conductivity of the wetland specimen were produced by changes in pore channel distribution. These changes in the hydraulic conductivity of the soil during column experiments were thought to be due to the increase and decrease of the number of flow channels in the soil and not to changes in pore size as it was be theorized (Aref, 1999). These results again indicate the complexity of transport mechanisms in organic soils.

1.4. Goals and chapters of the thesis

Previous research at MIT pointed out the need for improved experimental methods to measure flow characteristics using the modified permeameter developed for the research of wetland soils. The main goal of this research is to improve the permeameter so as to have more

accurate and precise measurements of contaminant flow in organic soils. The thesis has been divided in seven chapters. This chapter provides background material and a description of research goals.

Chapter 2 describes the genesis and resulting structure of organic soils and their classification.

Flow characteristics of soils can be described by differential equations that are developed in Chapter 3 for the particular case of a Dual Porous Media.

Chapters 4 and 5 describe the testing equipment and experimental procedures for the permeameter testing program, respectively. Testing results, which refer mainly to the influence of equipment parts on testing results and permeameter flow characteristics, are given in Chapter 6. An analytical computer program, CXTFIT 2.0, is used to analyze the experimental results. The CXTFIT 2.0 program performance is also described in Chapter 6.

Finally, Chapter 7 presents the research conclusions and enumerates several recommendations for future researchers.

Chapter 2: Organic soil Characterization

2.1. Introduction

In general, a soil consists of three phases: solid, liquid and gaseous. Liquid and gaseous phases make up the pore space, which allows contaminant movement through the soils. Contaminants will move in suspension or a dissolved state with the flowing water through the soil pores in fully saturated soils. In unsaturated soils, contaminants can also appear in gaseous state and move through the empty channels of the soil structure.

The solid phase can also influence contaminant transport. It is responsible for the interaction between the contaminant and the soil. In organic soils, the solid phase includes both organic and inorganic components and they both tend to adsorb contaminant particles from the solution or in suspension (Shackelford, 1994). The structure of soils defines the type of flow through them, and the principal element that influences an organic soil structure is the content of organic matter (Tank, 1994). The influence of organic matter in water movement and transport processes in organic soils has not been well studied and measured. In the literature, preferential flow is discussed as an effect of macrospore heterogeneity, pore size and space continuity, and the Two Region Model, whose derivation only incorporates physical but not chemical processes, has been used widely to describe macrospore transport mechanisms through organic soils (Reiken, 1996).

The organic matter in soils is not a stable, immobile element, but rather changes over short periods of time due to the continuous activity of the aerobic and anaerobic bacteria that decompose the large organic chains in shorter, simple ones (Buol, 1997). The chemical decomposition of the organic matter leads to changes in the structure, pore spaces and flow channels. These changes obviously influence the permeameter testing results and breakthrough curves, since the permeability, immobile and mobile zones can change during the tests.

Previous research at MIT with the modified permeameter has shown that the hydraulic conductivity of organic soils changes over the long periods necessary for organic soils testing, probably due to the activity of the organic matter (Aref, 1999). The bonding of soil particles, as described above, can close existing flow paths or increase the pore size, increasing or decreasing the hydraulic conductivity of the soil, respectively.

This chapter gives a brief description of the structure of organic soils, their formation and influence in flow patterns. Since this research concentrates on the behavior of non-reactive contaminants. Chemical reactions that might occur between the soil elements and the contaminant are not discussed.

2.2. Organic matter

2.2.1. Definition of organic matter (Everett, E. 1983):

Organic soil matter is a substance that either:

1. Is saturated with water for long periods and, excluding live roots, has an organic-carbon content (by weight) of:

    a) 18% or more if the mineral fraction contains 60% or more clay, or
    b) 12% or more if the mineral fraction contains no clay, or
    c) 0.1 x (% of clay)% or more if the mineral fraction contains less than 60% of clay, or

2. Is never saturated with water for more than a few days and contains 20% or more, by weight, organic carbon.

This definition includes mud and peat.

Organic matter has several components (figure 2.1). These include

- Raw plant residues and microorganisms – 1 to 10%
- Active organic fraction – 10 to 40%
- Resistant or stable organic matter also referred to as humus – 40 to 60%.

Organic matter and humus are terms that describe different, but related, things. Organic matter is the fraction composed by living organisms and once-living residues in decomposition. Humus is the end product of organic matter decomposition, and it is

a relatively stable substance. Humus is then a substance in the group named organic matter (Sullivan, 2001).

The stabilized organic matter comprises large, complex substances produced in the decomposition of plants and animal tissues that very few microorganisms can degrade. These hard-to-decompose substances make up a third, or even half, of the soil organic matter. Science divides them into three groups:

1. Humic acids
2. Fulvic acids
3. Humins

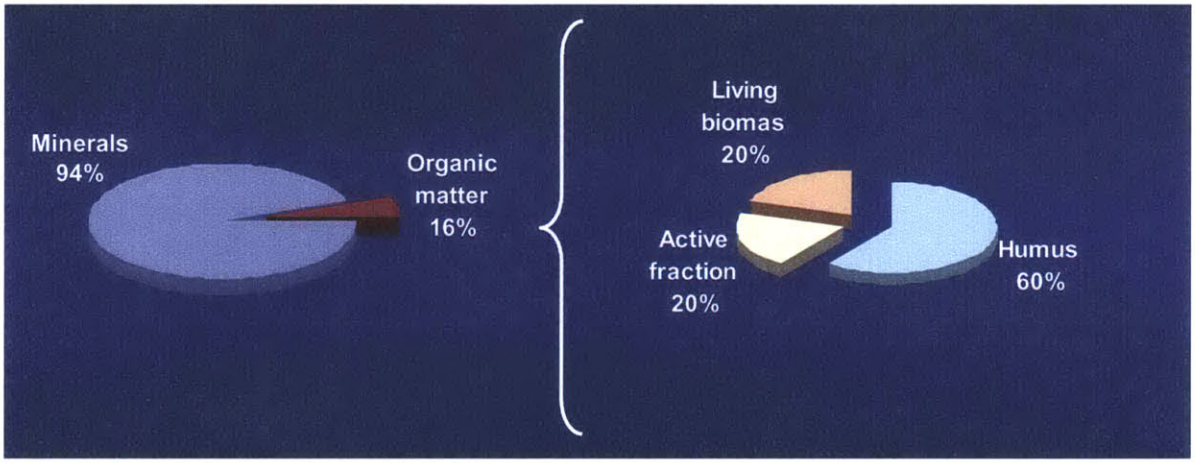

Figure 2.1: Organic compound in soils (Lewandowski, A. 2000)

Some of these hard-to-decompose compounds are bonded to clay particles and are important as cementing agents, which glue together tiny aggregates of soil particles improving aggregation and preventing compaction. This stabilized organic matter acts like a sponge. It can absorb and store six times its weight in water, increasing the water holding capacity of the soil, especially of sandy soils.

Note, that fine-grained soils can hold much more organic matter than sandy soils. First, clay particles form electrochemical bonds that hold organic compounds together. Second, decomposition occurs faster in well-aerated soils, as sandy soils.

There are several classifications of organic soil matter: Topographical classification (Hammond 1981), Classifications based on surface vegetation (Canada and northern

Europe), Classifications based on botanical origin (Anderson 1964) and classifications based on physical characteristics (Von Post, 1981). The classification system description is beyond the scope of this research. However, it is noteworthy that none of these systems use any parameters related to the flow characteristics of the soils.

2.2.2. Soil profile

Horizons are mineral and/or organic strata of varying thickness, differing among themselves and from the lithologic substratum for some morphologic, physical, chemical and mineralogic properties and for biological features. They are pointed out by the following initials: O, possible organic horizon; A, horizon containing either organic matter, decomposed and humified, or mineral substances resulting from disaggregated and alterated rock; E, horizon impoverished of soluble chemical compounds and those removable in suspension such as clay; B, horizon rich of alteration minerals or where some elements from E horizon are concentrated; C, horizon composed of "soft" substratum or disaggregated rock; R, "hard" and not alterated rock (Everett, 1983).

The description of soil profiles will indicate at which depth under the soil subsurface organic matter is present. The soil profile consists of different *horizons* numbered alphabetically beginning at the ground surface and going downwards.

2.2.3. Formation of organic matter

Dead vegetable matter and plants remain accumulated in-situ or are transported by water long distance. Under wet conditions, this matter is subjected to bacterial action that break the long organic chains resulting in the formation of organic fraction and humus, and in some cases peat (partially carbonized vegetable tissue formed in wet conditions by decomposition of various plants and mosses). This geochemical process is named "the humidification stage". After the humidification stage the bacterial action comes to an end.

In the humidification stage the vegetable matter is subjected to biochemical and chemical changes. The main trends of the chemical changes are the removal of the major percentage of oxygen and the enrichment of the carbon content, hydrogen and sulfur (figure 2.2).

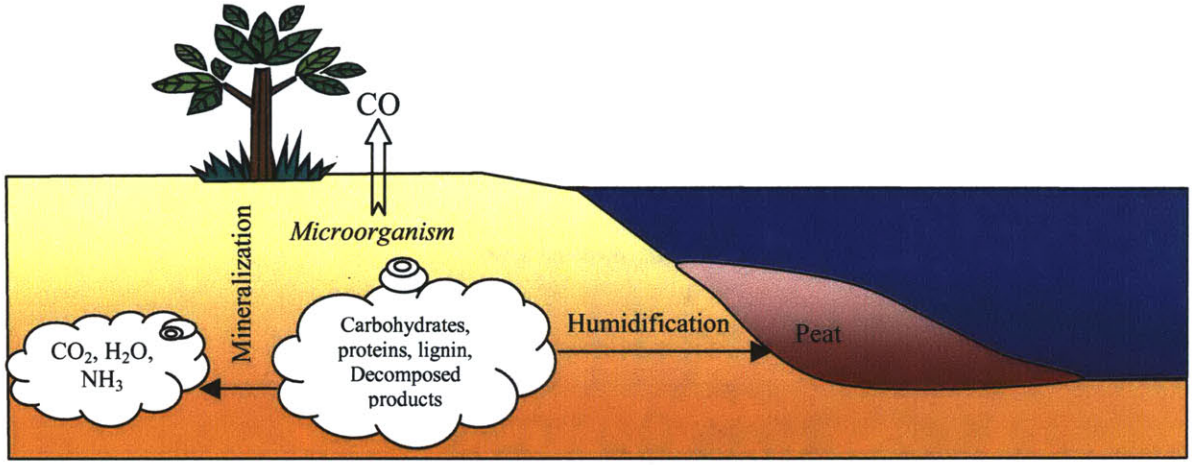

Figure 2.2: Origin of organic matter

Green plants, in the photosynthesis process, form carbohydrates such as glucose (figure 2.3), combining CO_2, water and solar energy through photochemical reactions. These molecules of glucose are linked together to form cellulose (figure 2.4), starch, etc, that allow plants to grow. These processes take place under oxidizing conditions. The organic compounds are characterized by high molecular weight and complicated structure.

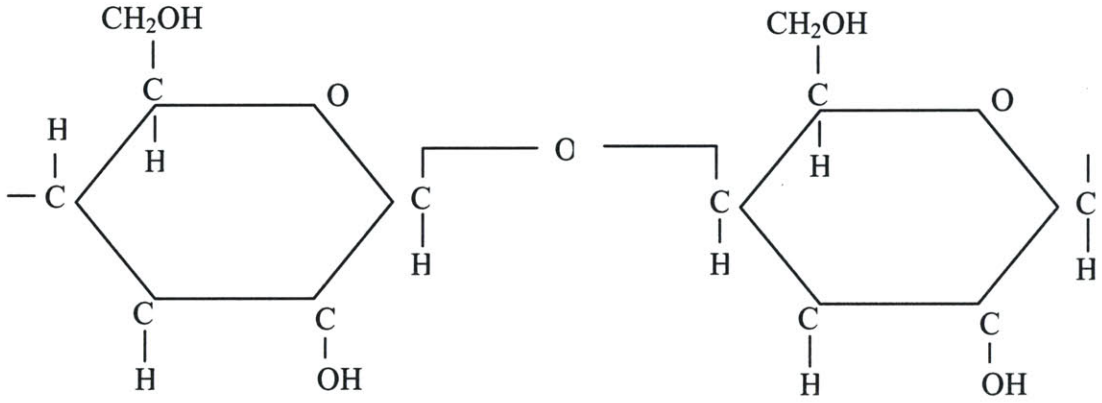

Figure 2.3: Molecule of glucose (Paustian, 2000)

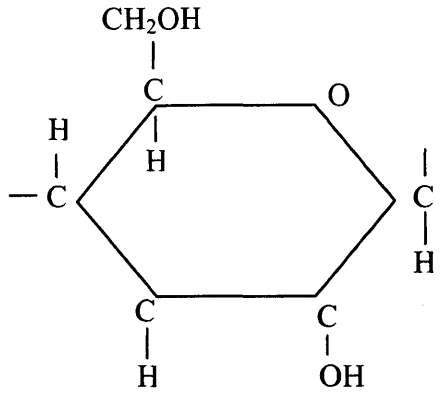

Figure 2.4: Molecule of cellulose (Paustian, 2000)

2.2.4. Interaction between the organic matter and the contaminants

Organic molecules are formed principally by carbon bonds. These molecules have ringed or chain structures. Carbon and nitrogen combine with oxygen and hydrogen to form what is called functional groups. The activity of these groups controls the activity of the molecules. They develop negative or positive charges depending on the pH of the environment/soil, and thus they interact not only with the contaminants dissolved, or in suspension, but also with the water that transports these contaminants.

2.2.5. Formation of the inorganic matter present in organic soils

Inorganic matter in the organic soils comes from weathering of rocks, and can remain in place or be transported to a new location where the soil is formed. Weathering is a physical and chemical process. The rocks are physically disintegrated, or reduced to smaller particles, and chemically transformed into new materials.

Due to cycles of heat, cold and humidity, rocks crack because their different constituents have different thermal expansion and contraction coefficients. Water comes into these cracks, and when it freezes its volume increases tearing the rock.

In the chemical process hydrolysis, hydration, carbonation and oxidation reactions produce new minerals from the former material of rocks. The new minerals that are formed and constituent the soil are mainly composed of alumina silicates.

2.3. Soil organic matter structure

The organic matter in the soil can appear in any of the next stages:

1. free particles of organic matter
2. occluded organic matter bonding soil particles
3. colloidal or clay associated organic matter.

The amount of organic matter in each group changes constantly since, as noted, the organic matter undergoes decomposition and is an unstable element. Thus, the structure of soils with organic matter changes within short periods of time if compared to non-organic soils. This means that soil porosity, grain size and shape, also change when soil grains aggregate or disaggregate.

Organic matter plays an important role in forming soil aggregates named peds (figure 2.5). Sand, silt and clay particles in the soils are bonded together mainly by organic matter. The organic matter in the soils acts as a glue that holds soil particles together into aggregates. This means that the soil will behave as a coarse-grained soil, although its real grain size is lower (Sullivan, 2001).

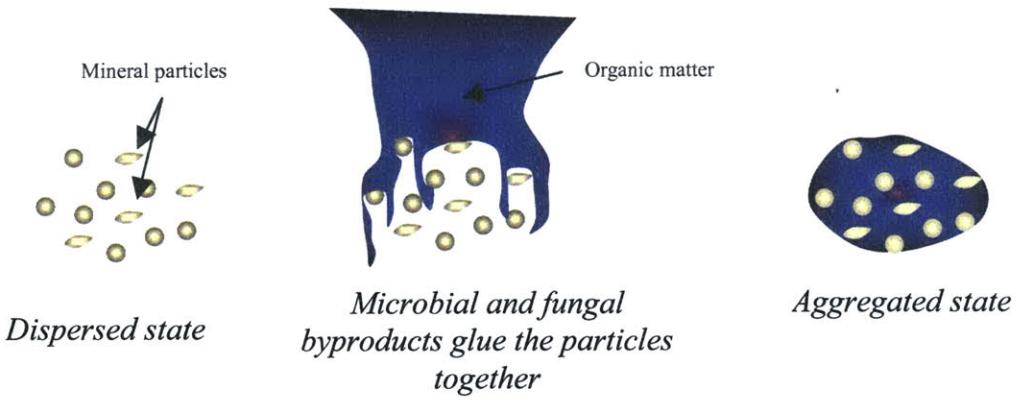

Figure 2.5: Aggregates or ped formation (after Sullivan, 2001)

The bonding of the soil particles by the organic matter forms an arrangement of pores and spaces within the soil. Water will flow through the pore spaces, and within the aggregates (figure 2.6). The breakdown of aggregates, named dispersion, can result in the release of fine

grains that block large pores, thereby restricting the entry and flow of water in and out of the soil flow paths and even leading to much fine-grained soil, with a decrease in hydraulic conductivity and an increase in dead-end pores.

As the clay content of the soil increases, it requires a higher content of organics to maintain the level of aggregate formation and stability.

The dead-end pores can appear in the peds due to their uneven shape, or in the inorganic particles where cracks are formed on the particle surface.

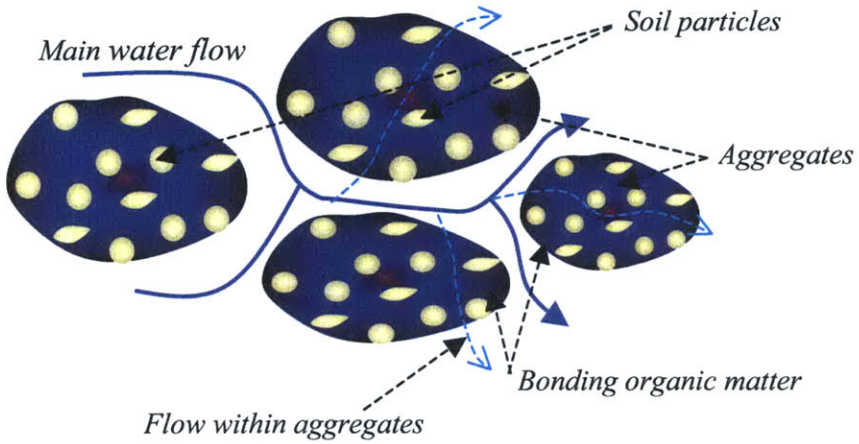

Figure 2.6: Flow paths through peds

2.3.1. Types of organic soil structure

Soil Structure reflects how the individual soil particles clump or bind together or aggregate. Natural aggregates that can be clearly seen in the field are the peds. Structure is important since (along with texture) it affects the pore space of the soil.

The structure of soils with organic matter can be classified into six groups, based on type and size (figure 2.7):

1. Structureless.
2. Platy: arranged around a horizontal plane, with the faces of the soil particles horizontal.
3. Prismatic: soil particles arranged around vertical line.
4. Columnar: same as prismatic, except that now the horizontal faces are not well defined.

5. Blocky: three dimensions all similar, arrange around a point.
6. Granular: refers to spherically peds. They can be porous or non-porous.

Obviously, these structures determine the type of flow thought the soil. The columnar or prismatic structure produces vertical flow, while flow through platy soils would be predominantly horizontal. In granular soil, flow can be in any spatial direction depending on the hydraulic gradient.

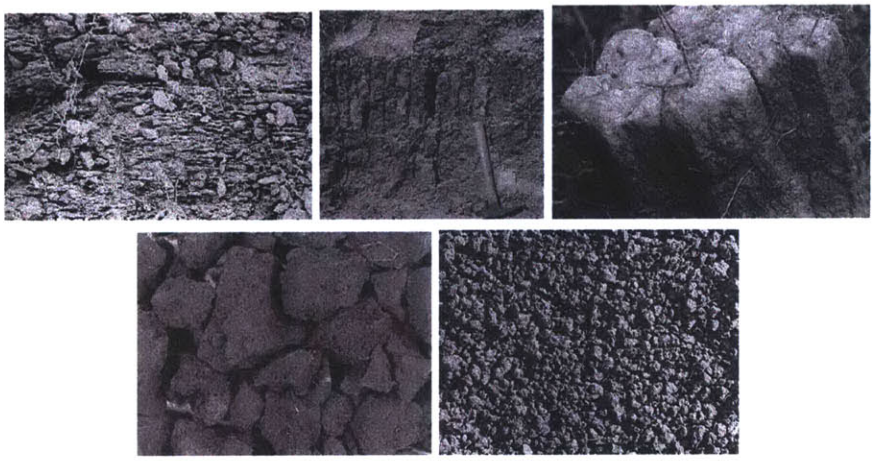

Figure 2.7: Different types of organic soils structures (from left to right, and up down): platy, prismatic, columnar, blocky and granular

Chapter 3: Advective-diffusion equation for Two Region Model

3.1. Introduction

This chapter discusses contaminant transport in groundwater flow. The data from experimental tests are analyzed with the advection-diffusion equation for a Two-Region model. In this chapter, only the Two-Region equations are given since the One-Region equation can be considered as a particularization of the Two-Region equation. The Advection-diffusion equation is a partial differential equation with multiple solutions depending on the initial and boundary conditions. The solution given by the computer program CXTFIT2.0 used in this research is an analytical solution for the conditions in which a contaminant is injected for a defined period of time (pulse).

Note that, although the solute used in the experimental procedures is a non-reactive element, the equation includes a first-order degree parameter to account for solute degradation.

3.2. Water flow through porous media

Soil is a porous media with inter-connected pores that form channels that allow water to flow through. The water flows through the soil pore paths according to Darcy's Law (1856):

$$q_x = -K_x . A . \frac{dh}{dx} \tag{1}$$

where

K_x: hydraulic conductivity in x direction [LT^{-1}]
q_x: flow rate in x direction [L^3T^{-1}]
h: head [L]
x: distance between points [L]
A: cross-section area [L^2]

Darcy's' Law indicates that water discharge is directly proportional to the driving force, the gradient, produced by the variation in hydraulic head between two points separated by a distance x (figure 3.1).

Equation 1 accounts for the water volume discharge. For the case of water running through a pipe with cross-section A the linear, or seepage velocity, v_x is:

$$v_x = \frac{q_x}{A} \tag{2}$$

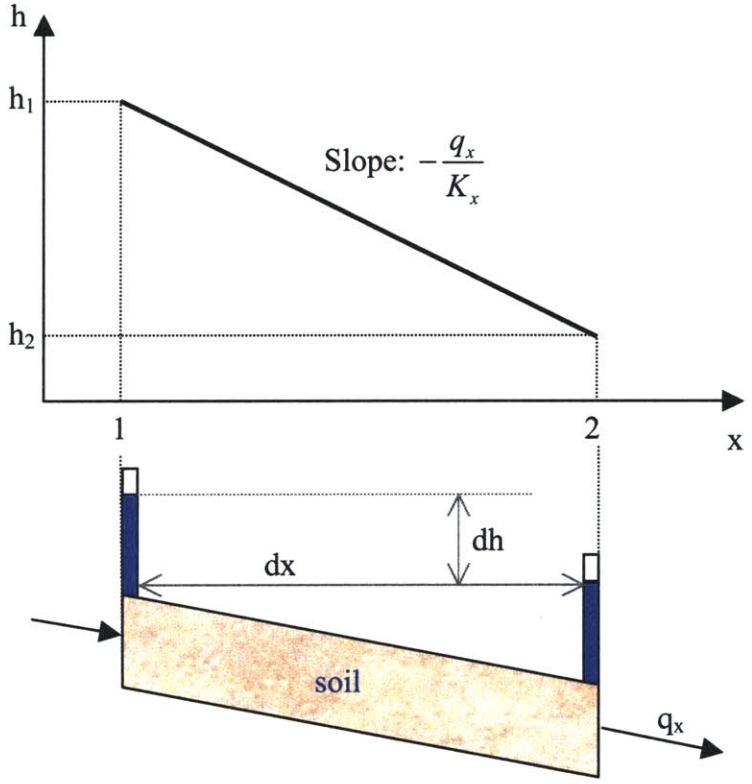

Figure 3.1: Darcy's Law

However, this is not the real velocity of the water flow through a soil because the cross-section area of the pore space is smaller than the soil cross-section. The actual velocity u_a, called the average or pore velocity, is the linear velocity divided by the porosity of the medium, n. The porosity refers to the real space through which water can flow.

$$u_a = \frac{v_x}{n} \tag{3}$$

3.2.1. The immobile water region

For the case of a soil with Two-Region behavior, there are two types of pores. One type of pore is interconnected and allows water to flow and a second type, named "dead-end pores", is connected to the flow paths but the water in these pores is immobile, therefore contaminants go in and out of these pores by means of the diffusion process alone. In this case, not all the pore volume is available for water to flow through the soil. Thus, the average velocity (or pore velocity) for this case would be:

$$u_m = \frac{v_x}{n_m} \tag{4}$$

where n_m (m refers to the mobile water) is the effective porosity and is defined as the ratio of the volume of pores through which water can flow to the total volume of soil. Note, that for a saturated soil the porosity equals the volumetric moisture content.

It is not presently possible to easily measure the effective porosity of a sample and only the total porosity is generally found. The total porosity can be measured after the specimen weight and volume, when dry, is measured. With the specimen's weight and the specific gravity, the volume of the solid particles of the specimen is calculated. The porosity is the ratio between the volume of voids (in this case the differences between the total volume and the solids volume) to the volume of solid particles. The effective porosity can be estimated using tracer pulse tests. The comparison between the measured average velocity and the one obtained from interpreting the tracer breakthrough curve will give the ratio of the total to the effective porosity (Aref, 1999).

3.3. Contaminant transport phenomena

3.3.1. Main factors controlling contaminant transport

The main elements that affect the contaminant transport through porous soils are:

1. Velocity distribution – flow through the channels formed by soil particles. This distribution is likely to be parabolic distribution rather than uniform as shown in figure 3.2.

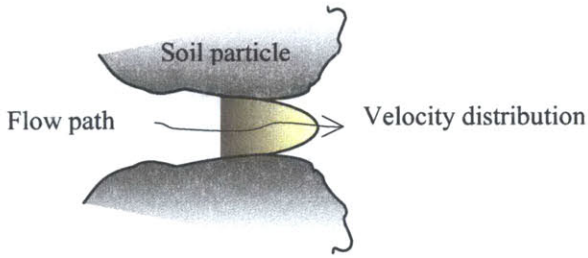

Figure 3.2: Flow Velocity distribution

2. Diffusion process: solute will migrate from high concentration zones to low concentration zones until concentration equals in both zones (figure 3.3).

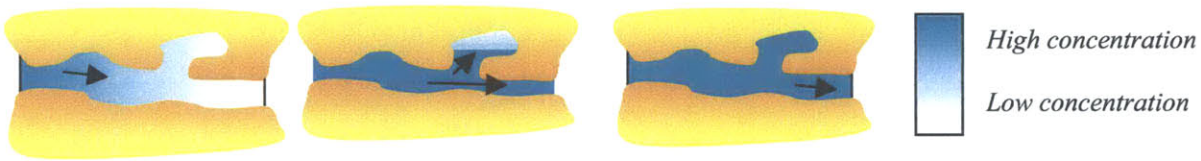

Figure 3.3: Diffusion process

3. Heterogeneities: the heterogeneities in the medium can create variations in flow velocities and flow paths due to friction of fluid with pore walls and the presence of soil grains. Furthermore, due to the different flow path diameters, the average velocity changes from one channel to another. Finally, changes in the soil type from one are to another at a site will cause different average velocities at different points.

3.3.2. Equations describing the contaminant transport mechanism for a Two-Region Soil

The main mechanisms involved in contaminant transport are:

1. *Advection* – moving of contaminant along with water flow through the porous media at the seepage or linear velocity. The mass flux per cross-section area [$ML^{-2}T^{-1}$] due to advection equals the product of average velocity and concentration of solute (C [ML^{-3}]) expressed as mass of solute per unit volume of mobile water. For consistency, this flux is multiplied by the effective porosity and then the resulting concentration in expressed as mass of solute per total soil volume:

$$F_{advection} = u.(C.n_m) \tag{5}$$

The effective porosity n_m is defined as the volume of mobile water per unit volume of soil.

2. *Diffusion* – as noted, diffusion is a microscopic process that causes spreading of solute from an area of high concentration to an area of lower concentration. Diffusive transport can thus occur in the absence of velocity. Mass flux due to diffusion can be described through Fick's First Law of Diffusion (1855):

$$F_{diffusion} = -D_{dm} \frac{d(C.n_m)}{dx} \tag{6}$$

where

D_{dm}: diffusion coefficient for the mobile fluid [L^2T^{-1}]
dC/dx: concentration gradient [ML^{-4}]

The molecular diffusion coefficient depends on the properties of the solute and water.

3. *Mechanical Dispersion* – dispersion is cause by heterogeneities in the medium. Dispersion can be longitudinal and or normal to the flow direction. It is assumed that mass flux due to dispersion can be described through Fick's First Law too:

$$F_{dispersion} = -D^*_m \frac{d(C.n_m)}{dx} \tag{7}$$

where

D^*_m: dispersion coefficient in the mobile zone [L^2T^{-1}]

Laboratory studies indicate that the dispersion coefficient is a function of the average velocity and a factor called dispersivity, α [L]. Dispersivity factors are often set constant in transport models.

$$D^*_m = \alpha.u^k_m \tag{8}$$

Usually k =1 for simplicity.

3.3.3. Transport model for a Two-Region Soil

Flow and transport processes are often represented by a differential equation. Pollution transport in many porous media models is based on the advective-diffusion equation, which is an equation of continuity. Water must satisfy continuity since it is conserved in flow through the porous media. The general form of this equation, expressed in three-dimensions for the mobile water, is obtained by considering the three mechanisms described in the previous section in the contaminant movement through a unit volume of soil in the mobile zone.

$$\frac{\partial(C_m.n_m)}{\partial t} + u_m \nabla(C_m.n_m) - D_m \Delta(C_m.n_m) = \pm C^* \qquad (9)$$

where

$\frac{\partial(C_m.n_m)}{\partial t}$: rate of change in solute concentration expressed as mass of solute per volume of mobile water with time

C_m: solute concentration [ML^{-3}] per unit volume of mobile water.

n_m: effective porosity or water moisture content of mobile region [L^3L^{-3}]

u_m: pore or average velocity in the mobile zone[MT^{-1}]

D_m: dispersion coefficient for the mobile zones [L^2T]

C^*: solute flux due to sources (+) or sinks (-) [ML^{-3}]

This equation is a statement of mass conservation for a conservative solute. The fact that there is an immobile region from which contaminants can diffuse in and out can be modeled as a sink term in the equation as:

$$C^* = \frac{\partial(C_{im}.n_{im})}{\partial t} \qquad (10)$$

where

C_{im}: solute concentration [ML^{-3}] per unit volume of immobile water

n_{im}: porosity or water moisture content of immobile region [L^3L^{-3}]

Very often, the term that gives the rate of contaminant exchange between the immobile and mobile zones is expressed as:

$$C^* = \frac{\partial(C_{im}.n_{im})}{\partial t} = \alpha(C_m - C_{im}) \quad (11)$$

where α is the transfer coefficient that describes the rate of mass transfer between the immobile and mobile zones, and depends on the coefficient of molecular diffusion D_d, a retardation factor, the distance traveled by the contaminant and the flow velocity. This is the equation for the immobile region.

Transport Models can be divided into:

- Stochastic – any quantity in the mathematical model is a random variable with a probabilistic distribution.

- Deterministic – any non-stochastic model can be regarded as deterministic. However, a deterministic problem can be considered as a limiting case of a stochastic model where all variables are well defined rather than follow a probabilistic distribution.

For this research, a deterministic model is considered since all parameters, boundary and initial conditions are well known.

3.3.4. The effects of Sorption

One of the most important reactions that contaminants can undergo is sorption. This term refers to the removal of tracer from the solution onto the soil particles where they are retained. There are different mechanisms that can lead to tracer sorption onto the soil matrix: hydrophobic partition of organic chemicals, absorption due to electrostatic forces, ion exchange, etc.

It is often assumed that the solute sorbed onto the solid phase is directly proportional to its concentration in solution. The proportionality is carried by a distribution coefficient K_d that is an empirical value obtained in field or laboratory testing from the Freudlich isotherm. When sorption occurs it does so in both the mobile and immobile region so the corresponding isotherms are:

- Mobile region: $S_m = f.\ K_d.C^b_m$ (12)

- Immobile region: $S_{im} = (1\text{-}f).K_d.C^b_{im}$ (13)

Where

S: solute adsorbed per bulk dry mass of soil [MM^{-1}]

K_d: partition coefficient [L^3M^{-1}]

$C_{m/im}$: solute concentration per unit volume of mobile/immobile water respectively

b: empirical coefficient. It is considered 1 for simplicity.

f: fraction of adsorption sites that equilibrates with the mobile liquid phase

Thus, due to sorption the solute concentration in the solution will decrease:

$$K_d \frac{\partial C_{m/im}}{\partial t}.n_{m/im} = \frac{\partial S}{\partial t} \tag{14}$$

This effect is incorporated in the equation for mobile water as:

$$\begin{aligned} &D_m.\Delta(C_m.n_m) - u_m \nabla(C_m.n_n) - \alpha.(C_m - C_{im}) = \frac{\partial(C_m.n_m)}{\partial t} + \rho_b \frac{\partial S}{\partial t} = \\ &\frac{\partial(C_m.n_m)}{\partial t} + \rho_b.f.K_d.\frac{\partial C_m}{\partial t} = \frac{\partial(C_m.n_m)}{\partial t}\left(1 + \frac{\rho_b.f.K_d}{n_m}\right) = R_m.\frac{\partial(C_m.n_m)}{\partial t} \end{aligned} \tag{15}$$

where R_m [-] is the retardation factor, defined as $R_m = 1 + \frac{f.\rho_b.K_d}{n_m}$ and ρ_b the dry bulk density of the soil. For the immobile water:

$$\begin{aligned} \alpha.(C_m - C_{im}) &= \frac{\partial(C_{im}.n_{im})}{\partial t} + \rho_b \frac{\partial S}{\partial t} = \\ \frac{\partial(C_{im}.n_{im})}{\partial t} + \rho_b.(1-f).K_d.\frac{\partial(C_{im}.n_{im})}{\partial t} &= R_{im}.\frac{\partial(C_{im}.n_{im})}{\partial t} \end{aligned} \tag{16}$$

If there is degradation and/or production of solute, two new terms are added to the equation:

- For mobile water:

$$D_m.\Delta(C_m.n_m) - u_m.\nabla(C_m.n_m) - \alpha(C_m - C_{im}) = R_m \frac{\partial(C_m.n_m)}{\partial t} + n_m.R_m.\mu.C_m + n_m\iota \tag{17}$$

- For immobile water:

$$\alpha.(C_m - C_{im}) = R_{im}.\frac{\partial(C_{im}.n_{im})}{\partial t} + n_{im}.R_{im}\mu.C_{im} + n_{im}.\iota \tag{18}$$

where

μ: first-order decay coefficient

ι: zero-order production term

3.4. CXTFIT2 Equation

The program CXTFIT (Toride, 1985) gives the analytical solution of the One-Dimension Equation described in this chapter for pulse and continuous tracer input. It can solve both the direct and the inverse problem:

- Direct problem: prediction of solute distributions versus time and/or space.
- Inverse problem: estimation of transport parameters by fitting the parameters observed in laboratory column experiments.

This program reduces the differential equations (17) and (18), where the production and decay terms are ignored since these processes are not likely to occur for the experimental cases carried out, so all parameters in them will become dimensionless. It is assumed than the porosity, $n_{m/im}$, remains constant. Multiplying the equations (17) and (18) by L, a characteristic length, and dividing by the average linear velocity, u, and the total porosity n, the equations become:

- For mobile water: $\frac{1}{P}.\frac{\partial C_m^{\,2}}{\partial Z^2} - \frac{\partial C_m}{\partial Z} - \omega.(C_m - C_{im}) = \Sigma.R.\frac{\partial C_m}{\partial T}$ (19)
- For immobile water: $\omega.(C_m - C_{im}) = (1-\Sigma).R.\frac{\partial C_{im}}{\partial T}$ (20)

where:

T = u.t/L: dimensionless time variable

$C = C/C_0$: normalized concentration

$P = u.L/D$: Peclet Number

$Z = x/L$: dimensionless space variable

Σ (or beta) $= n_m/n$: Partition coefficient for a non-reactive solute.

$\omega = \alpha.L/nu$: dimensionless mass transfer coefficient

R: retardation factor [-]

The CXTFIT program uses as input parameters D and u instead of D_m ($D = \frac{n_m.D_m}{n}$) and u_m ($u = \frac{n_m.u_m}{n}$), that are included in the equations (17) and (18) to obtain the dimensionless form shown in equations (19) and (20).

Input and Output files for the CXTFIT program are given in Appendix C. Input files format is explained in section 5.4.2.

Chapter 4: Equipment used for column tests

4.1. Introduction

The permeameter developed for column tests on organic soils was originally used for measuring the hydraulic conductivity of the Aberjona wetland deposits (Bailon, 1995). This permeameter was afterward modified (Ramsay, 1996) so it allows determination of other hydrological properties of the specimen such as effective porosity and dispersivity. The modified permeameter has conductivity and temperature probes in the influent and effluent lines that measure the concentrations of ionic solutions as well as temperature. Originally, pH and Oxidation-Reduction potential probes were epoxed in the cell pedestal but now they are disabled.

The equipment has been modified in the course of this research to improve its performance and avoid problems with water aeration and salt accumulation in the water line system. The conductivity probes, which are a major component of the permeameter, were re-plated so measurements are actually more accurate and reliable. Figure 4.1 shows a picture of the equipment, which is described in this chapter.

Tests were conducted with sand specimen, and without specimen to better understand how the equipment characteristics affect result interpretations. Test results are discussed in Chapter 6.

4.2. Type of test

4.2.1. Selection of type of test

Flexible versus rigid wall permeameter

There are two general test methods used to determine the hydrological characteristics of soils. Tests can be divided into rigid wall permeameter and flexible wall permeameter tests. The flexible wall approach was chosen for the permeameter over the rigid wall because it allows control over the confining pressure, lets free specimen deformation and eliminates sidewall leakage.

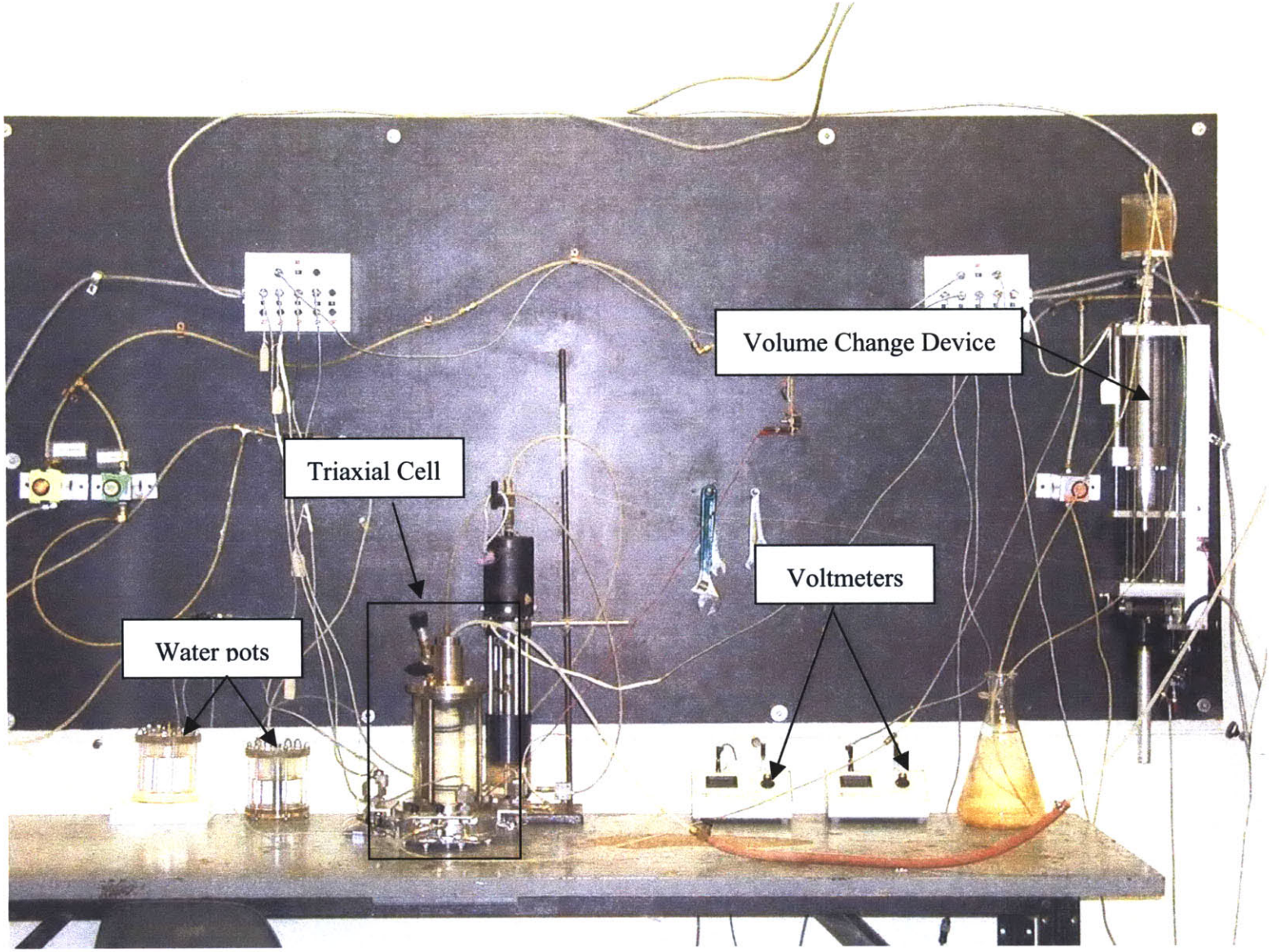

Figure 4.1: Equipment used in the permeability tests

In a fixed wall permeameter, separation of the soil from the membrane walls will lead to new flow paths for the fluid that do not pass through the specimen (figure 4.2); and so the hydraulic conductivity values would be much larger than the real ones. It was observed that organic soils compress during hydraulic testing resulting in specimen separation from the sidewalls in the case of a rigid wall system. A flexible wall system follows the specimen deformation and no separation between specimen and membrane occurs. For these reasons, it is the preferred test.

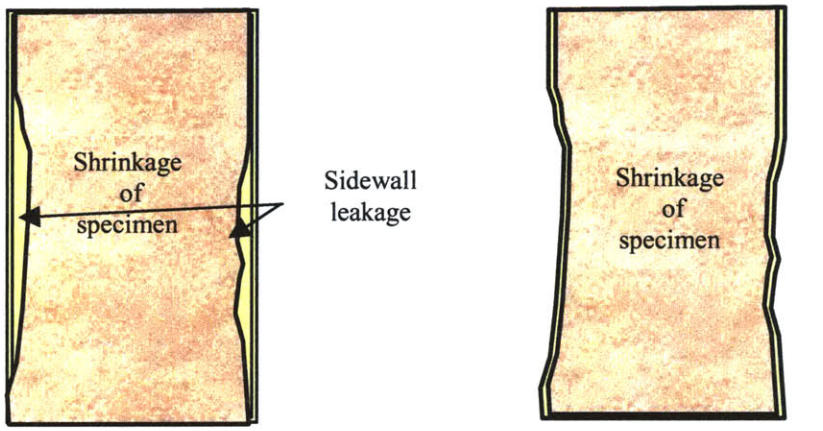

Sidewall leakage for a rigid Wall permeameter

No sidewall leakage in a flexible permeameter

Figure 4.2: Example of sidewall leakage

The flexible wall test is performed in a pressure chamber. The specimen is encapsulated with a latex membrane and an outside pressure, named the cell pressure, is applied to keep the membrane in contact with the soil. In cases where the specimen can shrink or an undisturbed specimen is tested, the cell pressure ensures full contact between the specimen and the membrane.

The main disadvantage of the flexible wall test is that positive effective pressure is required to maintain specimen particles in place and keep membrane in contact with soil during testing. Therefore, the cell pressure should be always higher than the pore pressure applied to the specimen.

For the water solution to flow through the specimen at a desirable pressure gradient, pressure at the inlet and outlet of the specimen must be different but always lower than the cell pressure. The higher the desirable gradient, the larger the difference between

top and bottom pore pressures. On some occasions the coordination of all these parameters leads to a high pore pressure at the inlet, low at the outlet and high cell pressures. These pressures can produce differential consolidation leading to changes in the hydraulic conductivity.

Flow Control system

The flow through the specimen can be controlled in two ways:

1. Flow-controlled system (figure 4.3): a flow pump maintains a constant flow through the specimen and the gradient through the specimen is measured.

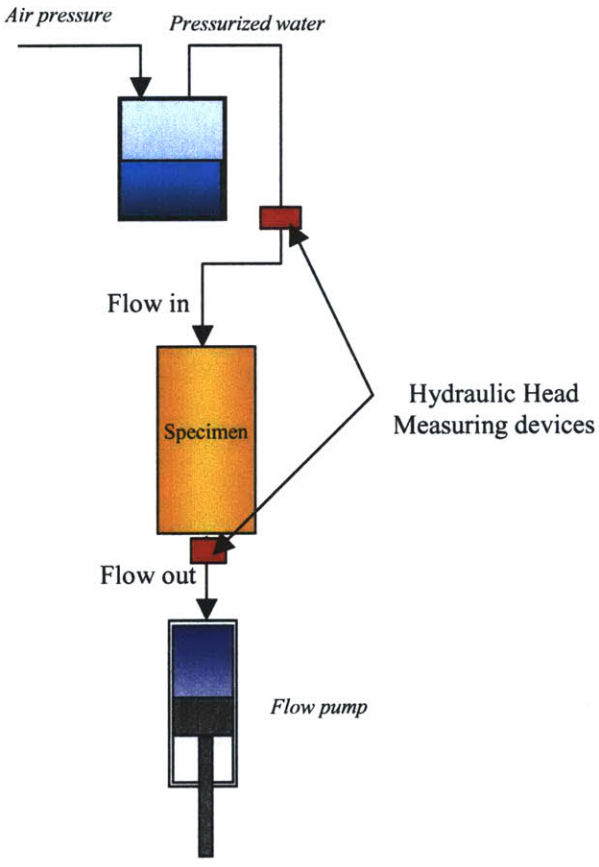

Figure 4.3: Flow-controlled system

2. Pressure-controlled system: the gradient across specimen is controlled with a constant head configuration, as shown in figure 4.4, and kept constant, while the flow rate is measured.

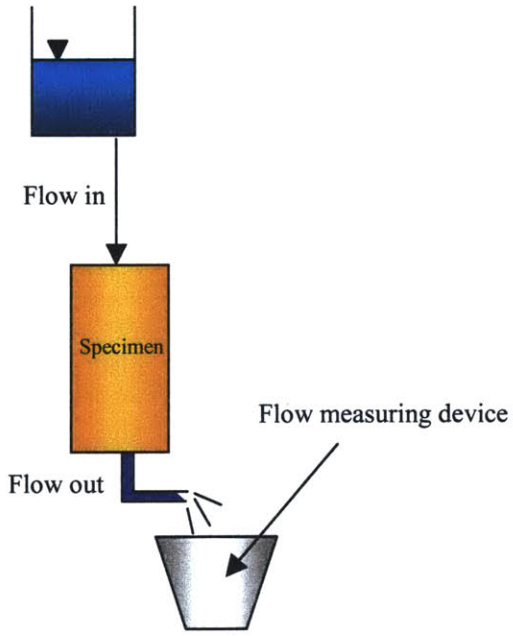

Figure 4.4: Gradient-controlled system

For these experiments, the flow-controlled system is preferable since it allows stabilization of flow in a short period. Furthermore, the analyses of the breakthrough curve with the computer program CXTFIT 2.0 does not allow the input of variable flow rate values.

Tracer tests

A tracer test consists of the injection of a measurable solution concentration of a non-reactive contaminant in the main flow while running a common hydraulic conductivity test. The input and output concentrations versus time are compared. Differences between them allow calculation of the transport parameters of the soil.

The tracer used in the tracer test is a non-reactive (conservative) solute, NaCl. The solute is injected into the fresh water stream that goes into the specimen during the hydraulic conductivity test. The input and output concentration of solute in water is measured with electric conductivity probes and plotted versus time as shown in figure 4.5.

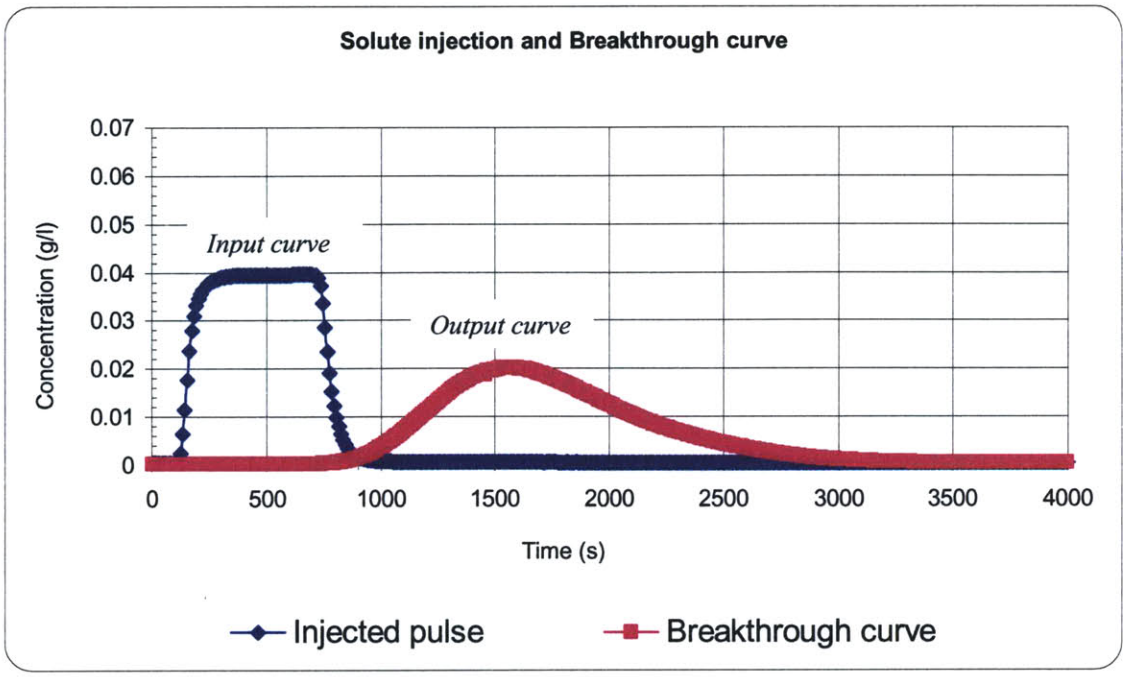

Figure 4.5: Example of input pulse and breakthrough curve

A conservative solute is a substance that does not interact with the soil. Thus the input mass of input solute should be equal to the output mass. This provides a quality control measure for each individual test.

4.3. Equipment

The equipment consists of:

- Pressure regulators
- Pipes and lines of pressurized air and water
- Water reservoirs
- A triaxial cell were the specimen is placed, or permeameter and accessories (distribution caps, porous stone, nylon papers)
- Conductivity probes to measure solution conductivity
- Flow pump that creates the necessary flow rate through the system.
- Data Acquisition System that records all the data

Figure 4.6 shows a sketch of the equipment

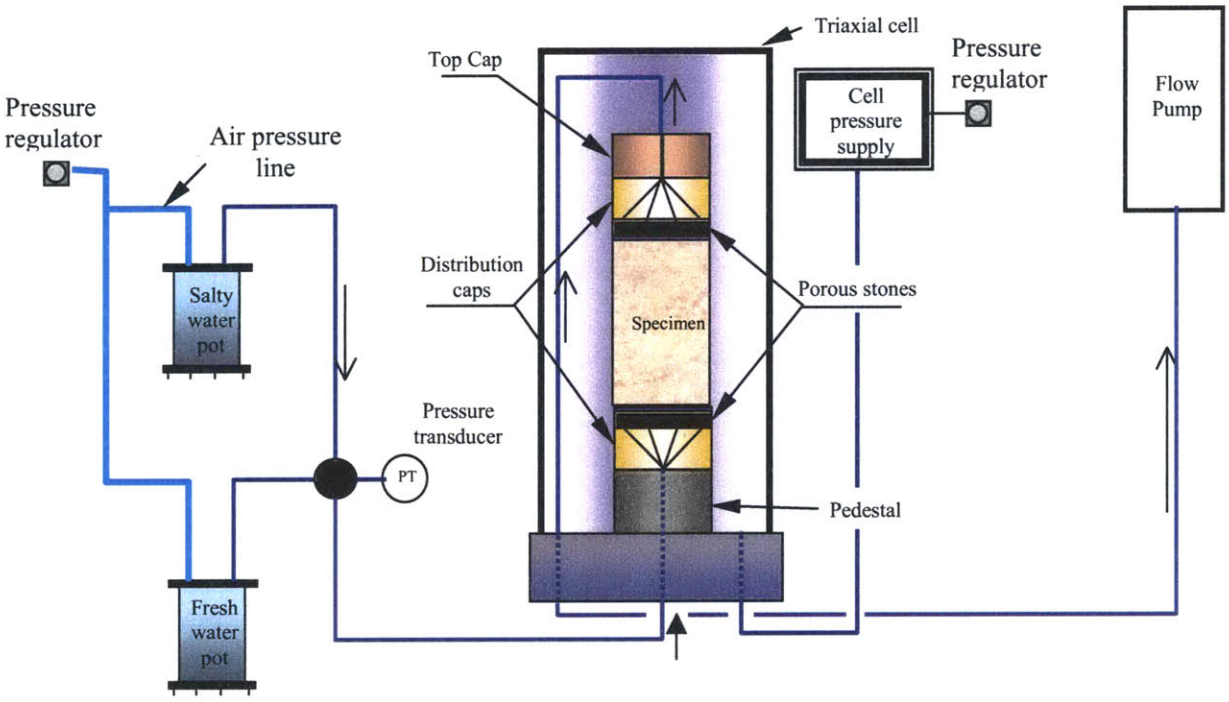

Figure 4.6: Sketch of equipment

4.3.1. Triaxial cell or permeameter

The triaxial cell has two main parts: a removable pedestal where the specimen is placed and a covering chamber that is filled with water to apply confining stress to the specimen.

Pedestal

The pedestal was designed for a specimen of 35.6 millimeters diameter and variable height. Along the pedestal drainage line (0.159cm diameter) are the four pin conductivity probes and a temperature probe. They are in a machined epoxy tube that forms part of the drainage line (figure 4.7). Section 4.3.3 gives a physical description of the conductivity probes.

Chamber

The chamber is made of transparent acrylic that allows visual observation of the specimen. It is filled with distilled water and pressurized until the desirable confining pressure. Pressure is applied using an air pressure to water pressure regulator. This prevents diffusion of air into the specimen through the membrane.

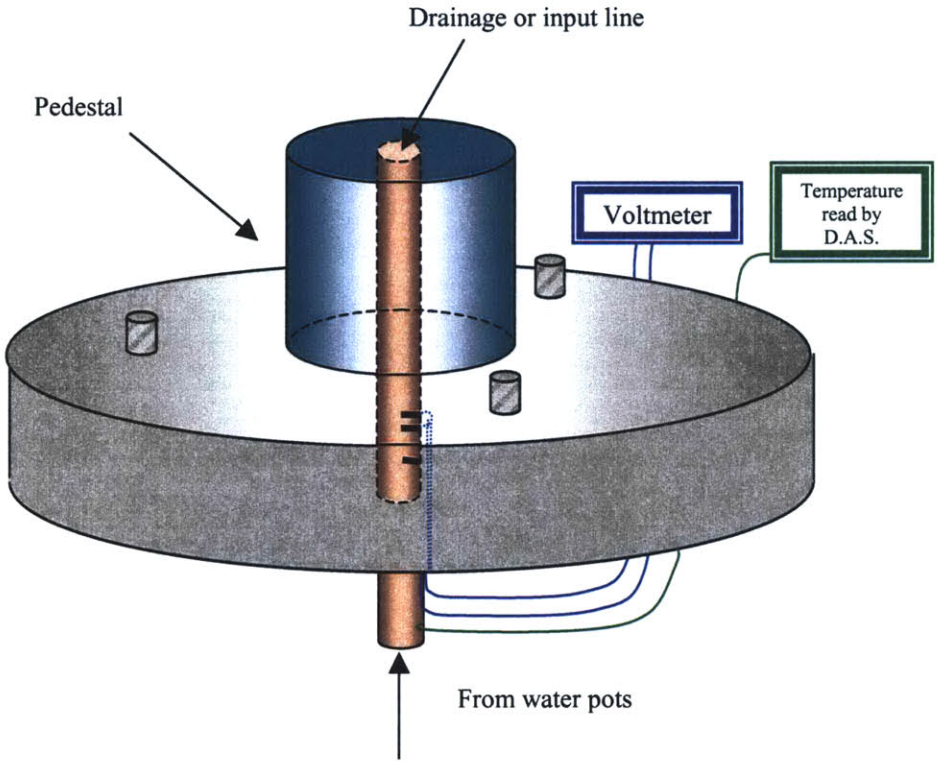

Figure 4.7: Sketch of pedestal

Figure 4.8 shows the pedestal and chamber. There is an o-ring under the pedestal that ensures a watertight conection during tests.

4.3.2. Fluid lines

Figure 4.9 illustrates the water and air lines. Water flow through the specimen can be upward or downward. Given that the conductivity probe situated at the top cap line was found to be more precise than the one situated in the pedestal line, the first is used to measure the breakthrough curve and therefore the flow is upward.

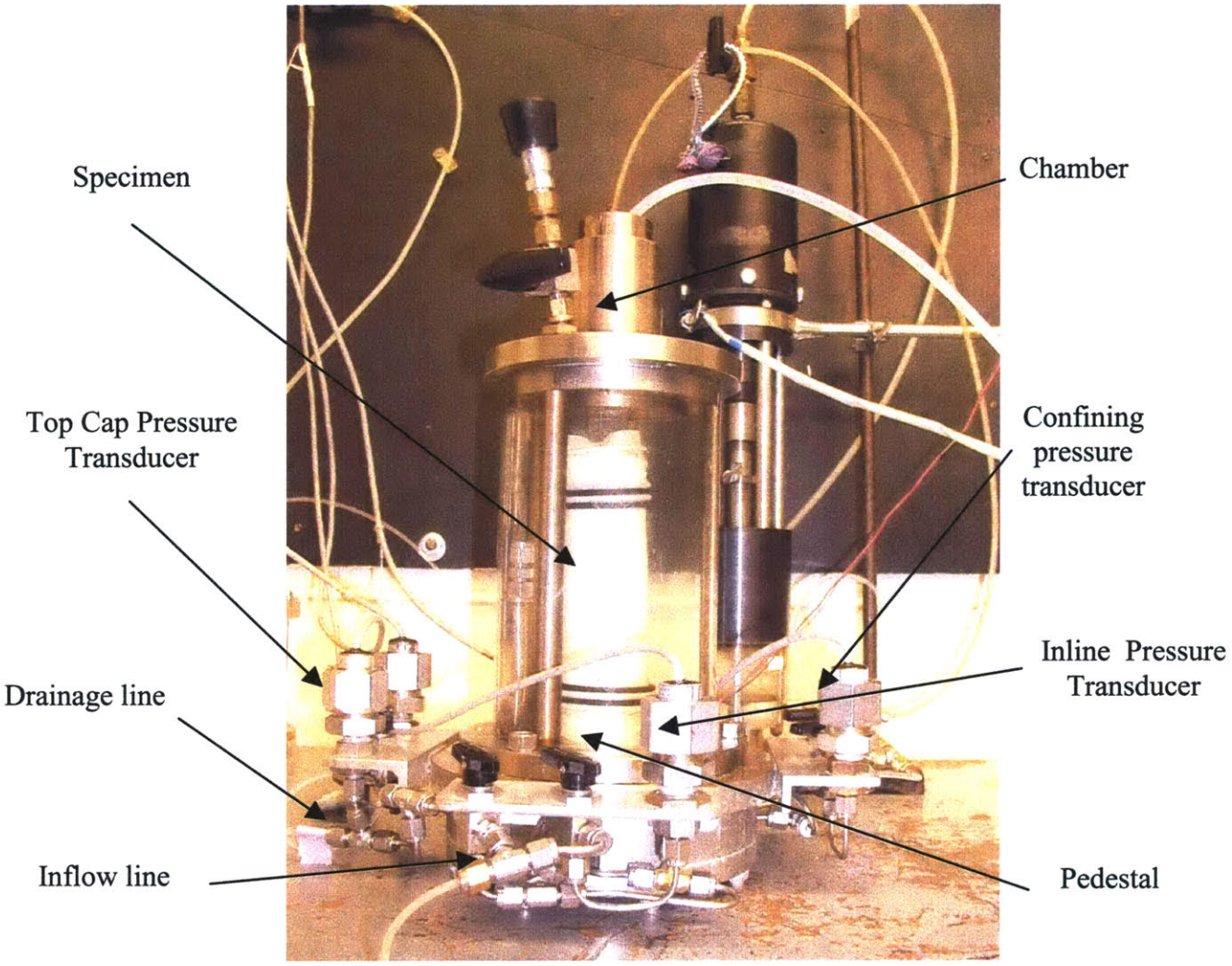

Figure 4.8: Picture of pedestal and chamber

The water line that goes to the bottom of the specimen is connected to the two pressurized water reservoirs, one containing fresh water and the other a salty solution for the tracer tests. Pressure is applied to the water in the water pot by an air-water interface and the air pressure controlled by a Fairchild regulator that restrains the air volume going into the water pots.

The salty water reservoir is connected to the same regulator that controls the pressure in the fresh water reservoir to avoid pressure fluctuations when the salty water line is opened to the specimen. The salty water line goes into the fresh water line through a three-way valve (figure 4.10), which is the salt/fresh water selector valve. A similar regulator controls the air pressure in the volume change device used to apply the confining or cell

pressure. In this case, the air pressurizes the water that goes into the cell chamber through a piston in the volume change device.

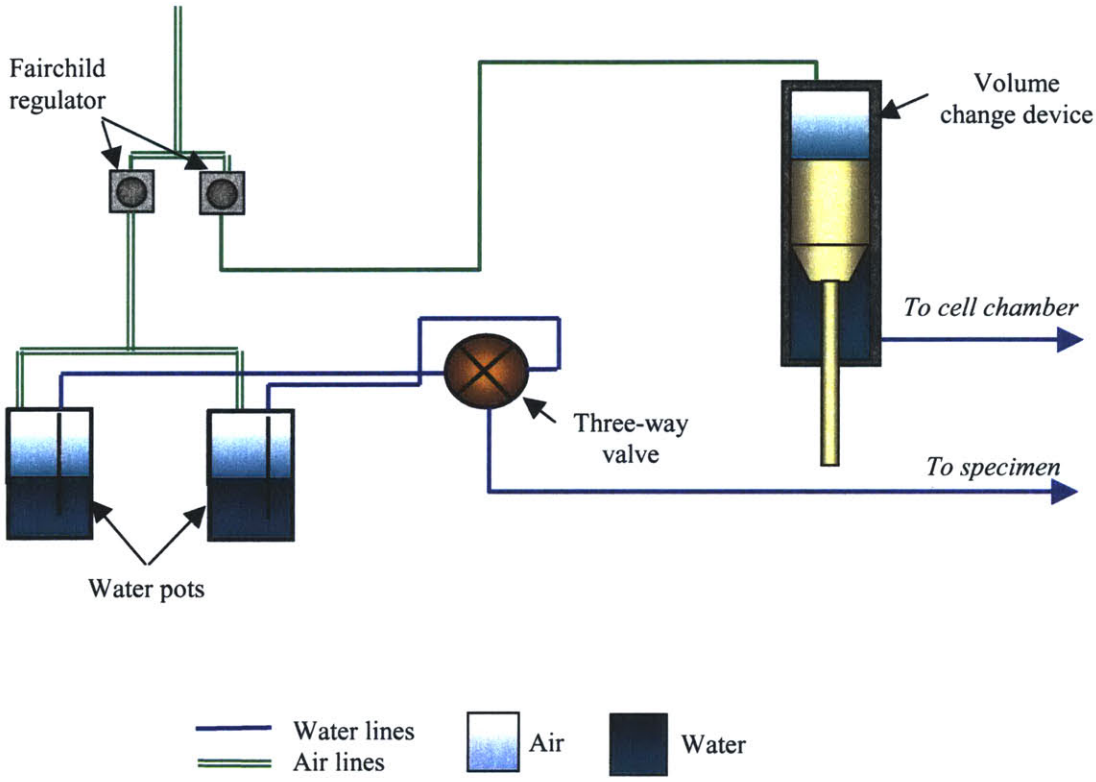

Figure 4.9: Sketch of fluid lines

Note, that the water pressurized in the volume change device is not in direct contact with the air to avoid aeration of the cell water. In a system with an air-water surface under pressure, air can dissolve into the water and diffuse through the specimen membranes into the soil and the specimen will be de-saturated.

The specimen bottom line can be opened to the specimen top line through a three-way valve, so the specimen can be backpressure-saturated.

Pressure transducers

Pressure transducers record the pressures of the inflow and outflow lines. These pressures are the pressures on the top and bottom of the specimen, and they are intended for calculating the pore pressures and hydraulic gradient through the

specimen. Another pressure transducer registers the pressure in the chamber, which is the confining pressure, applied to the specimen (figure 4.8). These transducers are also used to calculate the back saturation pressures.

The three transducers have a range of 0 to 14 ksc with a sensitivity of 100mV and 5.5 volt input.

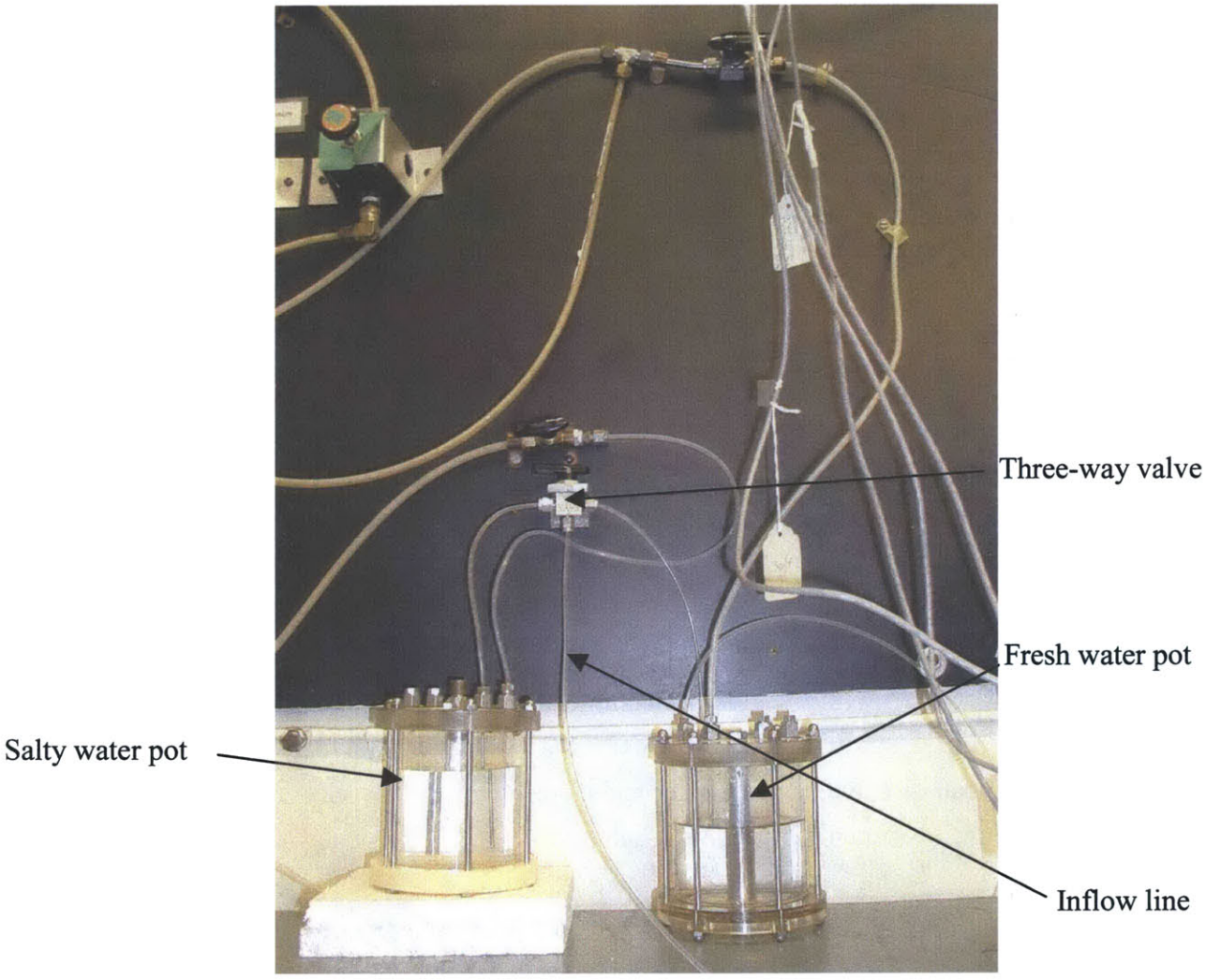

Figure 4.10: Water reservoirs fluid lines

4.3.3. Conductivity probes

The conductivity probes measure the concentration of the input and effluent solutions. Each of these probes consists of two electrodes connected to a conductivity meterYSM Model-35 2-pin. This model calculates and displays the conductivity of the solution.

The voltmeter has a reference resistance and it applies a known current to the circuit, where all elements are connected in series. The current through the circuit induces a difference in voltage between the two pins proportional to the resistance of the solution, which then can be calculated easily (figure 4.11).

The resistance of the solution indicates its concentration. Higher resistances imply lower concentrations of an ionic solute. Because resistance is directly proportional to voltage (V=R.I) and current is kept constant, a measure of the voltage can be used to calculate the solution concentration with calibration curves. The probe calibration is a relationship between the solution concentration and the voltage corresponding to that concentration.

Both pedestal and top cap probes are similar in their physical components. The pins are made of platinum wire of 0.05cm diameter and spaced 0.159cm apart. The probe installed on the inlet was cast, and platinum wires drove across the entire section in pairs and were maintained in place with epoxy (figure 4.12). The probe in the pedestal was made by "Electrochemical, INC." and consists of four platinum wires epoxed into the drainage line.

Maintenance

The platinum coating of the electrode pins suffers corrosion over time and the readings become meaningless. The electrodes need to be plated every year or two, depending on their frequency of use, in order to maintain their reading accuracy.

In order to diminish corrosion, the electrodes should be kept into distilled water while they are not in use. If electrodes are dry, they need to be soaked in distilled water for 24 hours before use.

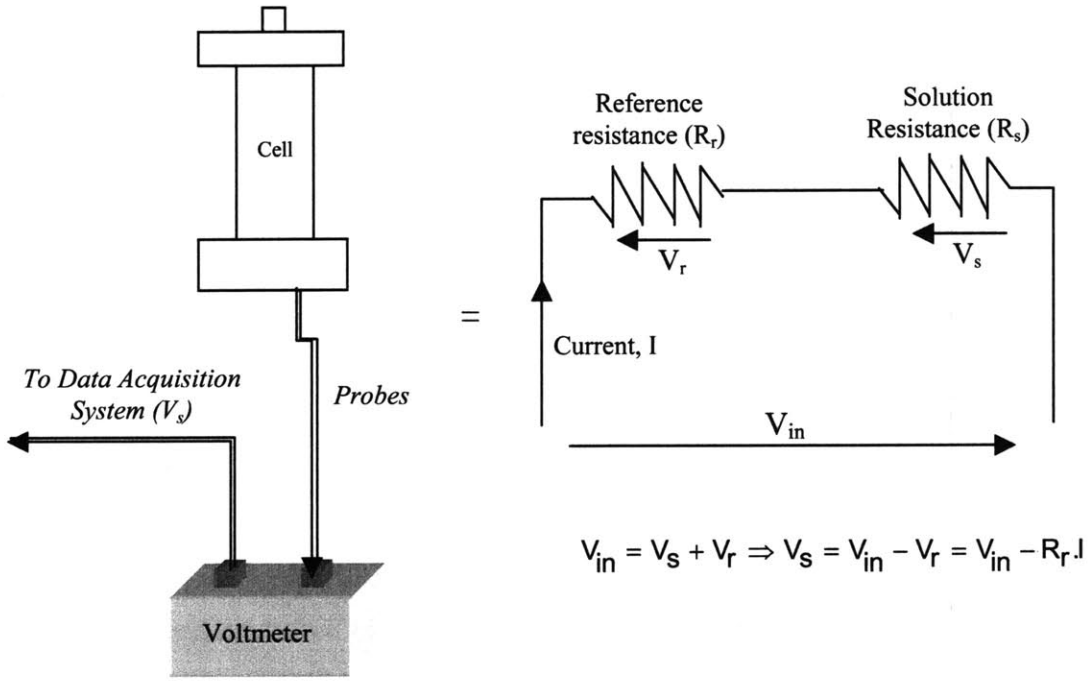

Figure 4.11: Conductivity Probes operation (Two Pins)

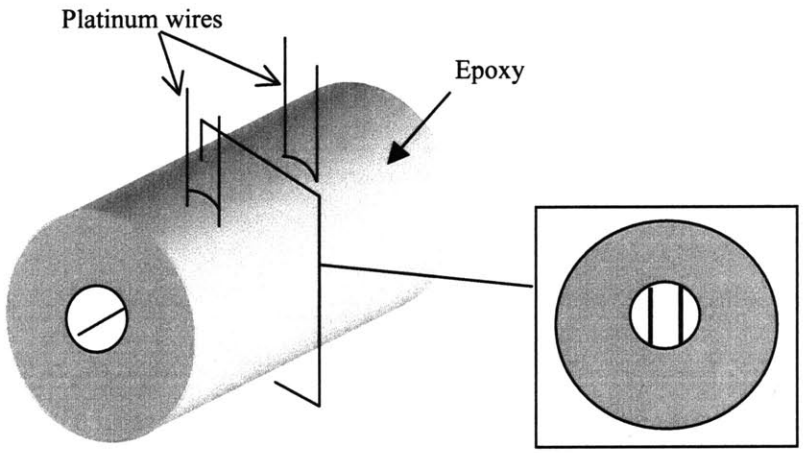

Figure 4.12: Top Cap Conductivity probe

4.3.4. Flow-Control System

This device consists of a stainless steel cylinder with two stainless steel end caps. A stainless steel piston runs up and down in the cylinder (figure 4.13). The flow-control device was modified to allow a wider range of flow rates of 10^{-5} to 10^{-1} cc/s, as well as larger volume flows of 270 cc approximately. To increase the flow rate, the piston diameter was increased to 4.128 cm, and to increase the flow volume the stroke was increased to 20.32 cm.

When the piston moves down it draws water from the specimen into the cylinder of the flow control device. The piston is driven by a DC motor and a transmission system. The motor can be placed in two different locations to achieve 5:1 and 400:1 reductions. Flow rates can be modified either by replacing a gear reducer that is attached to the motor to achieve reductions of 100:1, 50:1, 25:1 and 180:1, or by substituting the ball screw units that move the piston.

One ball screw moves the piston 2.54 cm per each 25 revolutions of the drive shaft. The second one reduces the flow rate by a factor of four, i.e., it moves the piston 2.54 cm per each 100 revolution of the drive shaft. The first one is used for sand testing, while the latter one is used when testing organic soils.

The motor has a tachometer, which outputs 3.5 volts per 1000 rpm. A rheostat, which is actuated manually until the desired flow rate is attained, controls the motor. A displacement transducer measures the piston vertical displacement.

A displacement transducer is attached to the pump that measures the linear displacement of the piston. This value and the cross-section area of the piston are used to calculate the interval of volume that goes into the VCD.

4.3.5. Data Acquisition System

The outputs from the pressure and displacement transducers, conductivity probes and the input voltage is recorded with the Central Data Acquisition System (D.A.S.) used in the geotechnical laboratory at MIT. Data are recorded in a computer through a software package (EASYDAT) developed by Dr. John T. Germaine (MIT) and Mr. R. S. Ladd.

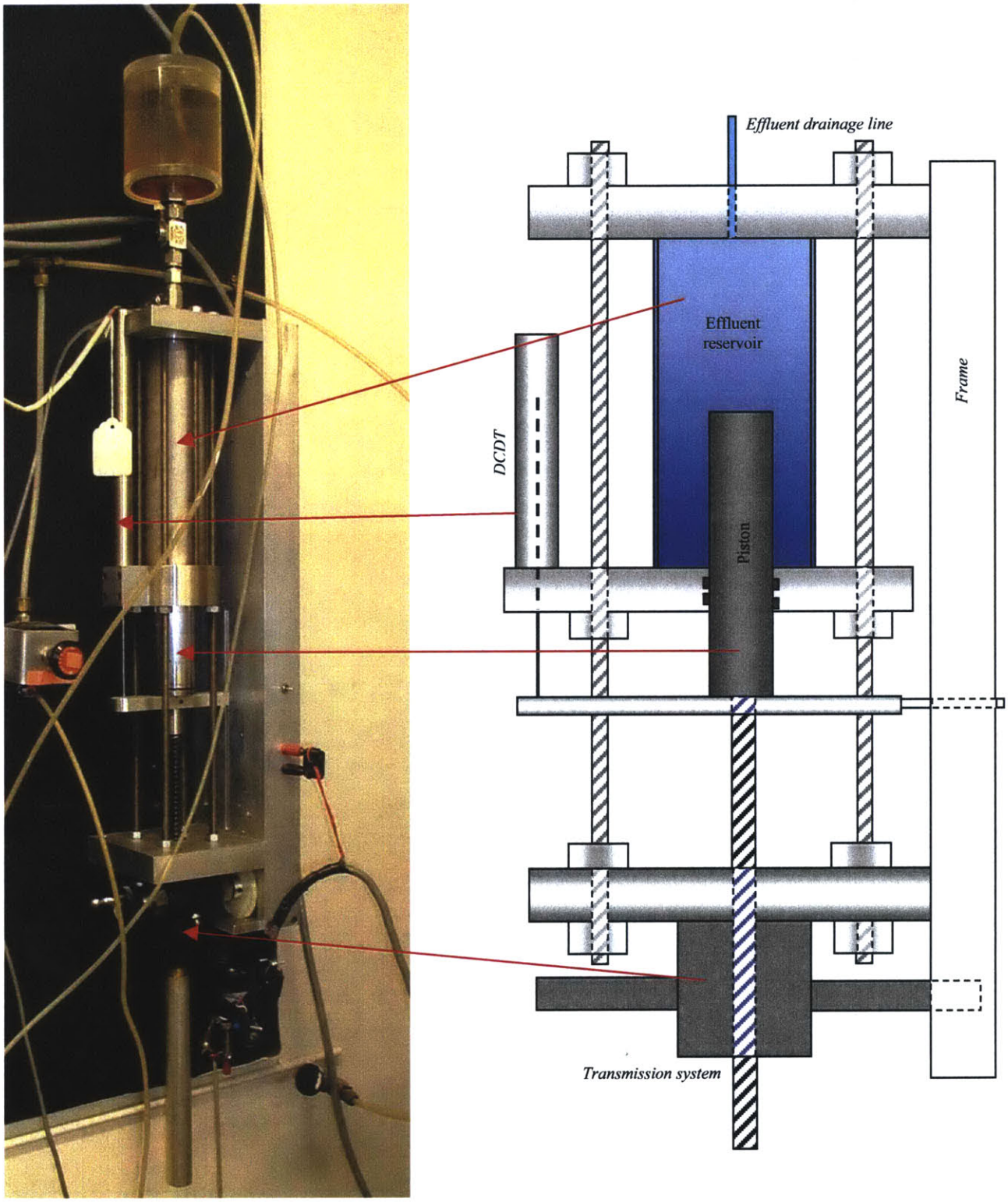

Figure 4.13: Volume control device

Chapter 5: Experimental procedures and data analysis

5.1. Introduction

The solute or contaminant transport parameters that characterize a soil are obtained experimentally from tests in the modified permeameter described in Chapter 4, but the value of these parameters can be affected by different factors. These factors can be divided in two groups:

1. Factors associated with the permeameter.
2. Factors associated with the physical and chemical properties of the soil.

The focus of this research is to understand the influence of the permeameter on the solute transport parameters obtained in column testing. Once these parameters are identified, the testing protocol and the permeameter can be modified to avoid their influence in the testing results.

This chapter is divided in two main parts. The first part describes specimen preparation, back-saturation procedures and parameter calculations. The second part explains data reduction calculations. Sand was the only soil type used in this research; sand is a One-Region material and its transport characteristics are well known. Therefore, when testing sand specimens it is possible to determine if the specimen geometry and set up influence the transport parameters.

5.2. Testing of sand specimens

Before the start the column experiments with the sand, it is important to identify the physical properties of the soil. Sand was characterized with the next series of test:

- Sieve analysis
- Specific Gravity
- Sorption coefficient
- Column experiments in modified permeameter

The ASTM standard procedures were used for the sieve and specific gravity analyses. The results of these tests are given in Appendix A. Although sorption phenomenon is not likely to occur in sands, sorption experiments were carried to confirm this assumption.

5.2.1. Sorption experiments

Contaminants in groundwater can undergo sorption onto the soil particles surfaces. Sorption mechanisms consist of the association of a dissolved contaminant with a solid material. Sorption usually refers to two different processes: absorption and adsorption. It is difficult to distinguish between these since they may occur simultaneously. Thus, sorption is usually used to describe the overall phenomena.

Sorption is an important process. It can decrease the contaminant concentrations dissolved in water, delaying the contaminant movement.

Evaluation of sorption

The most common method for evaluating sorption phenomena is through the partition coefficient (K_d), which is defined as the ratio between the contaminant concentration sorbed onto the soil solid phase to the contaminant concentration in aqueous phase:

$$K_d = \frac{[C]_{solid}}{[C]_{aqueous}} \Rightarrow [C]_{solid} = K_d \cdot [C]_{aqueous} \quad (1)$$

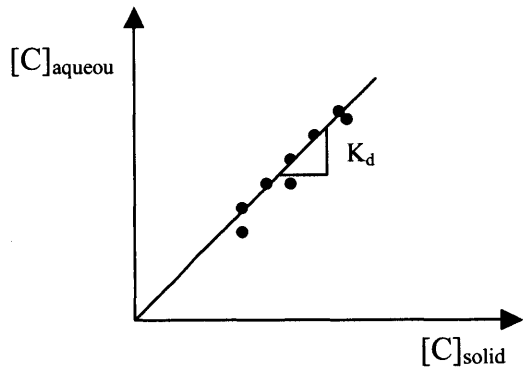

Figure 5.1: Linear sorption isotherm

Typical test results yield a straight line named an isotherm where concentrations of the solid phase are represented versus concentrations of the aqueous phase. The slope of this line is the Partition Coefficient (figure 5.1). There are also more complicated cases where a linear result is not obtained.

The sorption of non-organic molecules, as NaCl in the experiments, is primarily due to an interaction with solid-phase natural organic matter (Bedient, 1994), so its values depend on the amount of organic matter in the soil. Sands are almost devoid of organic matter so they will not undergo sorption (or it will be so low that we can ignore its effects on the overall transport process). The results from the sorption experiments, where the partition coefficient was found to be 0, are outlined in Appendix A.

5.2.2. Column experiment

An extensive description of the specimen set up procedure is given in Appendix B.

5.3. Column experiments

The column experiment procedures can be divided into the next six steps:

1. Travel Time calculations
2. Conductivity probes calibration
3. Preparation and set up of specimen in triaxial cell
4. Back saturation of specimen
5. Hydraulic conductivity test
6. Tracer test and breakthrough curves

All these steps require careful procedures to optimize the accuracy of the results, and they are described below.

5.3.1. Travel Time

The time that the solute travels through the specimen is an important factor for solving the advective-diffusion equation given in Chapter 3. Conductivity probes are located

in the influent and effluent lines at a fixed distance upward and downward, and not at both ends, of the specimen. For this reason, the input and output curves are spaced by the time the solute travels through the sample plus the time the solute travels between the sample ends and the probes (figure 5.2). The reason for this set up is to avoid running cables through the sample.

It is necessary to subtract the travel time between probes and sample ends (t_t) in order to have a real time scale in the plot of concentration-time for the breakthrough curves (t_s).

To find the travel time, tracer experiments were conducted on the permeameter that was set up with only the distribution cap, porous stones and nylon papers, and the time between the input and output concentration curves was measured. This time is the travel time. Since it is dependent on the flow rate, tests were carried at different flow velocities and an equation relating the travel time and flow rates was developed. The time between the half–areas under the curves was determined for each test, and the equation was obtained from the linear regression on these data.

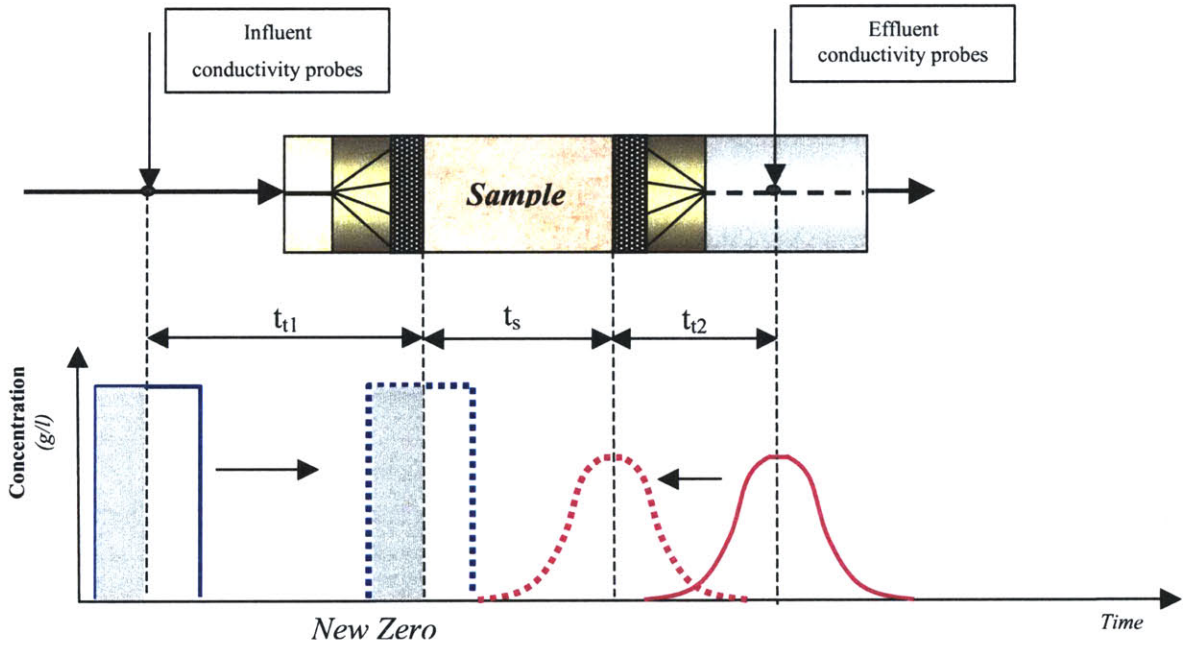

Figure 5.2: Eliminating Travel Time effect

Appendix B gives the Time Travel calculations and results.

5.3.2. Conductivity Probe calibrations

Calibration procedure

The conductivity probes are calibrated before and after each experiment since their values are time sensitive. This means that each set of experiments has their own calibration values.

Three different salt solutions are used for each calibration, with concentrations in the range of those to be used during the column experiments. A certain amount of each solution is put in contact with the probes, and the output values of the probes (conductivity and temperature probes) are recorded. The concentration values are affected by temperature and they need to be modified to avoid this temperature effect.

Temperature correction

Correction of temperature is made with the Hewit's equation (Head, 1985), which converts a conductivity value at any temperature into a conductivity value at a reference temperature of 18°C. The equation is:

$$\frac{\text{Conductivity at any T}^{\circ}}{\text{Conductivity at } 18^{\circ}} = 1 + b\left(T - 18^{\circ}\right) \tag{2}$$

where the temperature T (°C) is the measured temperature of the solution in the tracer tests and:

$$b = \sum_{0}^{4} a_n T^n \tag{3}$$

$$a_0 = 2.1179818 \times 10^{-2}$$

$$a_1 = 7.8601061 \times 10^{-5}$$

$$a_2 = 1.5439826 \times 10^{-7}$$

$$a_3 = -6.2634979 \times 10^{-9}$$

$$a_4 = 2.2794885 \times 10^{-11}$$

Calibration curves

Once conductivity values are corrected, they are represented versus the concentration. The resultant calibration curve is a straight line whose slope and intersection with the axis that represent the concentrations, are the calibration factors. The equation of this line relates the solute concentrations with the adjusted conductivity. There are different calibration curves for different experiments. Instead of a log-log scale, a normal scale is used so a value of zero concentration can be included in the calibration equations.

The calibration equations of several experiments are shown in Appendix B.

Calibration troubles

Ramsay (1996) conducted the first experiments to evaluate the equipment performance. With a sand sample in the triaxial cell, he injected salt solutions and studied the mass recovery comparing the mass of salt that went into the specimen with the mass of salt that came out. He found that the recovery was always lower than 100%.

Aref (1999) conducted twenty similar experiments and found that the recovery was not only lower than 100% but it also decreased with time. This behavior suggests that the pedestal probe becomes less sensible with time. To corroborate this theory, she injected soap into the system to rinse the probe before tracer experiments, and it was found that the recovery improved. Additional physical sampling of effluent gave higher values than the ones registered by the pedestal probes.

During different column experiments performed during the course of this research, a random variation of the calibration factors was observed. First, it was theorized that the permeameter geometry, pressures, flow rates or all of these factors were responsible of this variations and that several parameters could affect calibration factor values. Results of several tests and conclusions are given in Chapter 6.

5.3.3. Preparation and set up of specimen in triaxial cell

Specimen set up procedures are given next. For a guide sheet refer to Appendix B.

5.3.3.1. Sand specimen

The sand is poured directly on the pedestal using the following steps:

1. Permeameter lines are filled with the appropriate liquid. Meanwhile, filter papers and porous stones are sonicated in distilled water to reduce the entrapped air.
2. Pedestal pressure transducer zero is read when a pool of water is maintained on it. With the pedestal line linked to the Top Cap line record the inlet and outlet water pressure.
3. Rubber membranes are used to protect the top cap and the pedestal. A large membrane is placed on to maintain the specimen on place.
4. A specimen mold is assembled on the pedestal and vacuum is applied to it so that the membrane is flushed with the mold wall. Inner diameter and height is recorded.
5. Sand in poured into the mold using the Raining Method.
6. When the mold is full, the top of the sand specimen is leveled with a straight edge. The top cap, with a rubber membrane to protect it, and the distribution cap are placed on top and the membrane roll over it. The mold is disassembled.
7. A prophylactic membrane is rolled over the specimen and secured with o-rings. Another prophylactic membrane is rolled over the first one and secured with o-rings.
8. Pedestal and surroundings are cleaned of any sand grains.
9. Permeameter chamber is screwed on the base and filled with distilled water. Cell pressure zero is taken when water is half way up.

5.3.4. Back saturation of specimen

Initially, the specimen will have air and water in the pore spaces. The air phase can give erroneous pore pressure values. Instead of eliminating the air in the water, the air

is dissolved into the water by applying high pore pressures up to 4 ksc (kg/cm^2). This process is named backpressure-saturation (Head, 1985).

In this process, pressure in the drainage lines and cell is increased to 4 ksc applying intervals of 0.5 ksc. In order to maintain an effective pressure in the specimen, the cell pressure is always maintained 0.1 ksc higher than the pore pressure.

The specimen is completed back-saturated when B-value is about 95% or larger (Head, 1985). The B value is the ratio between the increase of the pore pressure and the increase of the cell pressure increases when no drainage is allowed. With the pore pressure lines closed, the cell pressure is increased 0.25 ksc. If the specimen is saturated and no air is left in the specimen pores, the increase in the cell pressure will produce an increase in the pore pressure of equal value, i.e, B=1. If there is still air in the water it will compress preferentially with respect to the water and no change, or a small change, in pore pressure will be seen. Once the specimen has been saturated, the pore and cell pressures remain at that level during the tracer tests. Reduction of pore pressure can lead to the air coming out from solution.

Backpressure-saturation procedure

Saturation is attained by following these steps:

1. Calculate the milivolts equivalent to 0.5 ksc increments for the pore and cell pressures. Calculate the equivalent of 0.1 ksc for the cell pressure. Maintaining the cell pressure value at least 0.1 ksc over the pore pressure, there is always a positive effective pressure within the specimen.
2. Increment both pressures at the same time. First, with all valves closed, increase pressure in water pots and VCD chamber to the desirable values. Then open at the same time fresh water and cell water lines to the specimen and chamber. Next, open the pedestal valve to the inlet line so the same pressure obtained on the top of the specimen is applied to its bottom.
3. Let pressures equilibrate and repeat the operation as necessary to reach 4 ksc for the pore pressure and 4.1 ksc for the cell pressure.

4. Check the B value. First, close drainage valves. Increase the cell pressure by 0.25 ksc and record the increase in the pore pressure. The B value will be the rate of pore pressure increment to the rate of cell pressure increment:

$$B = \frac{\Delta\sigma_{\text{Pore pressure}}}{\Delta\sigma_{\text{Cell pressure}}} \tag{4}$$

B values between 0.95 and 1 are acceptable.

Transducer calculations

First, it is necessary to calculate the pressures from the voltage that the transducers give as readings. Calibration Factors give the relationship between the pressure and the voltage (figure 5.3)

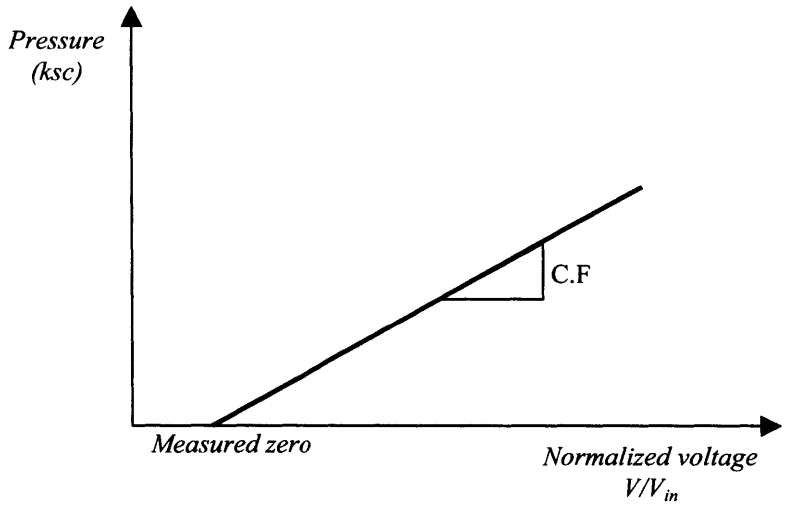

$$\text{Voltage (mV)} = \text{Pressure (ksc)} \times \frac{V_{in}}{C.F.} + Zero.V_{in}$$

$$\text{Pressure (ksc)} = \text{C.F.} \times \left[\frac{V}{V_{in}} - \frac{\text{Zero}}{V_{in}}\right]$$

Figure 5.3: Pressure transducer calculations

The same principle for the displacement transducer applies. Table 5.1 gives the Calibration Factors for the actual pressure transducers on the cell.

Pressure transducer	Calibration Factor (ksc/(V/V_{in}))
Inlet line	-701.7593
Pedestal line	-701.7412
Cell	-701.8224

Table 5.1: Calibration Factors

5.3.5. Hydraulic conductivity test

Once the specimen has been back-saturated, the outlet line, which is the one that goes to the top cap, is connected to the flow pump, which induces water flow through the specimen.

Pump operation

There are two ways of controlling water flow through the specimen:

- Maintaining a gradient during the experiments: the VCD is operated to create the necessary pore pressure at the specimen outlet. The hydraulic gradient is defined as:

$$i = \frac{\Delta h}{L} \tag{5}$$

where

h: pressure head [L]

L: sample length [L]

The relation between pressure head and the equivalent pore pressure in the specimen is:

$$\Delta h = \frac{\text{Pore pressure Top - Pore pressure Bottom}}{\text{Unit weight of water } (\gamma_w)} \tag{6}$$

Note, that 1 ksc ~ 98.6 kPa and 1 Pa = 1 N/m^2

Since the pore pressure at the top of the specimen is constant and the gradient values are known, from Equation (6) the pore pressure at the specimen bottom can be calculated. The motor velocity will be increased slowly with the tachometer until the pressure at the pedestal is the required one.

- Maintaining a desirable flow rate during experiments: for a defined flow rate, the linear velocity of the piston can be calculated since its cross-sectional area is known:

$$v = \frac{Flow\ rate}{Piston.\ x\text{-}section\ area} \tag{7}$$

The actuator needs 25 revolutions to move the piston 2.54 cm, so the r.p.m. can be calculated (note that with the reduction gears, one with a constant reduction of 180:1 and the other two exchangeable for reductions of 4:1 - slow seepage - and 5:1 - fast seepage- , the actual revolutions for 2.54 cm of piston displacement will be much larger). The motor gives 1000 r.p.m. for an input voltage of 3.5 volts. With these data the input voltage is calculated. The motor input voltage is again controlled with the tachometer.

Flow rate calculations

The D.A.S. records the data from the linear displacement transducer that is transformed into values of length through the Calibration Factor. Therefore, the piston displacement with time is known. If the linear displacement for each interval of time is multiplied by the piston cross-section area, the result is the volume of water that passes through the specimen for that interval of time, or the flow rate (cm^3/s). For VCD Calibration Factor values, refer to Appendix B.

Hydraulic conductivity values

Using Darcy's Law:

$$Q = A.k.i \tag{8}$$

where

Q: flow rate [L^3/T]

A: specimen cross-section area [L^2]

i: hydraulic gradient [-].

k: hydraulic conductivity [L/T]

All the parameters are known except the hydraulic conductivity k, which is easily calculated from Equation (8).

5.3.6. Tracer test and breakthrough curves

A tracer test consists of the injection of a non-sorbing solution with a known concentration into the water flow. The conductivity probes will record the electrical conductivity of the solution that goes in and comes out the specimen. Then, conductivity is transformed into concentration values with the corresponding calibration factors, and concentrations are represented versus time.

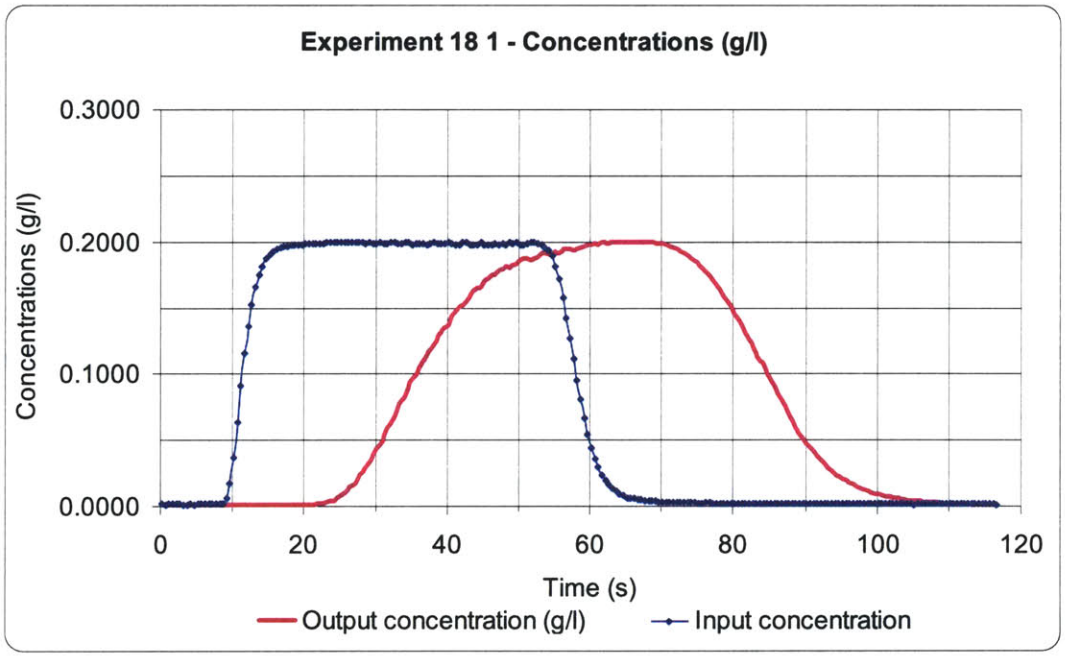

Figure 5.4: Example of a tracer test with a pulse input

The final output are two curves, one that reads the concentration of the solution going into the specimen, named *pulse* since the solution is injected for an interval of time, and the second one gives the concentration values of the solution coming out from the specimen, named *breakthrough curve* (figure 5.4).

There are different parameters that can be deduced from the shape, area and time of travel of the breakthrough curve. The breakthrough curve is analyzed with the program CXTFIT in order to obtain these parameters.

On some occasions, the injection of a solution for an infinite time is preferred. For these cases, the input curve has a step shape, and so has the breakthrough curve (figure 5.5).

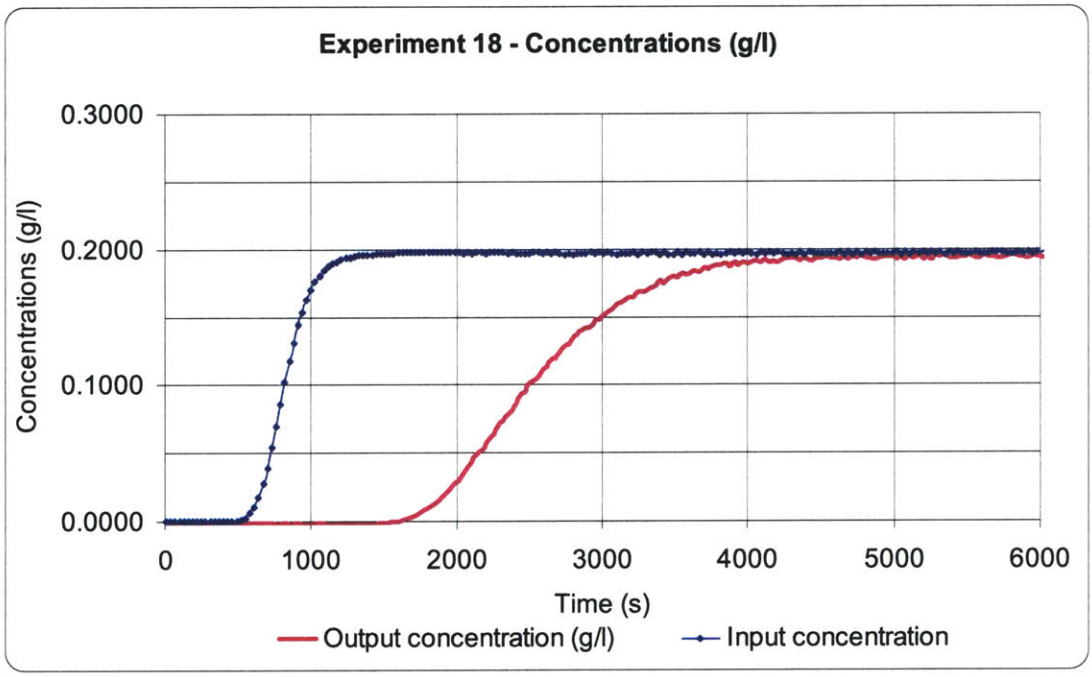

Figure 5.5: Example of tracer test with a step input

5.4. CXTFIT program

Parker and Van Genuchten (1984) developed the CXTFIT program, and Toride and Genuchten (1995) updated the program to the version named CXTFIT 2.0. This last version

can be used to fit parameters of steady, equilibrium and non-equilibrium one-dimensional transport using the One Region and Two Region models.

The program analyses the input data and the experimental breakthrough curve to obtain the values of several transport parameters: dispersion coefficient (D), retardation coefficient (R), mass transfer coefficient (α) and percentage of mobile to total volumetric water content (β).

5.4.1. Adjusting the travel time

Before the breakthrough curve is used in the input file of the CXTFIT program, the curve must be adjusted for the travel time. The initial part of the output curve includes the time the solute takes to travel from the three-way valve where it is injected to the top of specimen, passing through the top cap and porous stones. Using the travel time equation given in Appendix B, the travel time was calculated for each test and the curve shifted to the origin, being the origin the time at which the input probe detects the input pulse (figure 5.2).

5.4.2 Input parameters

The input data must follow a specific format. The ASCII input file has eight blocks. Each block is described below. Refer to Appendix C for examples of input and output CXTFIT files for both types of injection, pulse or step, and for both types of problems, direct and indirect.

Block A: Model description

This block defines the type of problem to be solved. The numbers in brakets refer to ORM/TRM cases.

- NCASE (1/1): Cases to be considered, usually 1.
- INVERSE (1/1): the program solves the direct and inverse problem. In the direct problem it calculates a breakthrough curve from the transport parameters (D, R, β, α). In the inverse problem it calculates the transport parameters from the experimental BTC, that is the actual case.

- MODE (1/2): from the 7 models that the program can analyze, the deterministic equilibrium (ORM) and the deterministic non-equilibrium (TRM) are used.
- NREDU (1/1): this parameter defines which of the input variables, time, position or concentration, are dimensional or not. For this case, the time and position are dimensional and concentration is dimensionless.
- MODC (1/1): the concentration mode is a flux average.
- ZL (DUM VALUE): characteristic length of dimensionless parameters.

Block B: Inverse problem parameters

This block contains the necessary data for the estimation of parameters.

- MIT (30 TO 50 both): number of iterations
- ILMT (0/0): the user can choose to place maximum and minimum to the parameters being estimated. For all cases no constraints are given
- MASS (0/0): this function allows the program to calculate the total tracer mass from the breakthrough curve. This option is not used.
- MNEQ (0): this function is only used for Two-region Model. The user can choose between the two Two-Region mechanisms, physical or chemical. For all cases, the physical TRM is used.
- MDEG (0): this parameter is used if any degradation of the tracer occurs in the TRM. For all cases it does not.

Block C: Transport parameters

The user introduces here the known or estimated parameters and defines which one the program should estimate.

- V: this value is the average flow velocity that is measured from the experiments.
- D: dispersion coefficient. The input value is the molecular diffusion of NaCl which is $1.5_x\ 10^{-5}$ cm^2/s at 25°C. The program is allowed to fit this value.

- R(1/1): the retardation factors are calculated in the sorption experiments. Note that, since there is no sorption for sand specimens, the retardation factor becomes 1.
- β (0/0.5): a dimensionless form of the partition coefficient $\sum$. It is zero for sands.
- ω (0/1): a dimensionless form of the mass transfer coefficient α.

Block D: boundary value problem

In this block the user can select the time and the tracer input method. For all cases, tracer is defined as a pulse through a function that relates concentration with time.

- MODB (2/2 OR 3/3): there are seven types or modes of tracer input. Only pulse (3) and step (2) inputs were used.
- PULSE: input concentration. Since concentrations are normalized with respect to the input concentrations this value will be 1.
- TPULSE: length of pulse in seconds. This value is not included for step inputs.

Block E: Initial value problem

In this block the user defines the conditions before the tracer is injected into the system. The initial conditions can be a zero initial concentration, exponential initial distribution, etc.

- MOD1 (0/0): The initial input concentration is zero.

Block F: Production value problem

In this block, the user defines the type of production term. For all cases, no production of tracer is considered and thus, the values for both cases ORM and TRM are zero.

Block G: Observed data for inverse problem

In this block the user input the breakthrough curve data

- INPUTM (1/1): this term defines the form the data is given. The 1 indicates time versus normalized concentrations.
- DUMTZ: specimen length.

In Appendix C the input and output CXTFIT files for an experiment are shown as example.

Chapter 6: Experimental Results

6.1. Introduction

This chapter presents the experimental results and gives a discussion of their significance. It includes equipment modifications and improvements, as well as new steps in testing procedures. There are also explanations of the CXTFIT program capabilities and the effect of platinization on conductivity probe performance.

The experiments are numbered from 1 to 22. Each Experiment consists of a separate permeameter set up and they are subdivided into sub-experiments that correspond to the tracer test number. For example, experiment 12 5 refers to the 12th permeameter set up and the fifth tracer test with that set up. Table 6.1 summarizes all Experiments carried out, their objectives and specifications.

Experiment No	No of tracer test	Objectives	Comments
1	14	Familiarization with permeameter and protocol	Peak due to salt accumulations
2	3	Find source of peak	Sand specimen
3	3	Characterization Porous stones	No specimen
4	1	Characterization Nylon papers	No specimen. No porous stones
5	12	Travel time calculation	No specimen. Leak
6	2	Characterization Drainage lines	Long cap only
7	1	Nylon papers ORM or TRM?	Long cap + nylon papers
8	1	"	Long cap between nylon paper
9	4	Travel time calculations	No specimen. Some peaks
10	1	"	"
11	1	Cell cleaned	No specimen. Peak
12	1	"	"
13	18	New travel time	Salt pressure transducer bypassed
14 and 15	30	Influence of pressure and flow rate on probes readings	Probes need replatinization
16 and 17	8	Check platinization of pedestal probe	-
18	9	Upwards flow. BTC measured with top cap probe	Good calibration. D of equipment
19	4	Sand specimen (2 cm)	Influence of equipment in D
20	2	Sand specimen (5 cm)	Influence of equipment in D
21	1	No specimen	Influence of equipment in D

Table 6.1: Experiments and tracer tests objectives

Notice that the last improvement consisted of the re-platinization of both conductivity probes. Results from this point forward, which include Experiments 16 to 21, are used to obtain the permeameter transport parameters.

6.2. Permeameter improvements

6.2.1. Effects of salt accumulation in flow lines

Solute can accumulate in dead zones in the permeameter flow lines, such as those lines that go from the main flow line to the pressure transducers. A dead zone was located in the salty pressure transducer line, so solute could diffuse in this dead zone during a tracer test and it had access to the main flow lines while the valves were open to the salty water pot only. After a tracer test was finished, the specimen is rinsed but because the fresh water had no access to the salty pressure transducer, the salt accumulation could not be cleaned. During the next tracer test, the accumulated solute diffused into the main fresh water flow, as is explained in Chapter 3 (figure 3.3), causing two mayor problems. First, the mass balance did not fit for the current experiment, and neither for the next one. Second, the consecutive solute injections were not square pulses as shown in figure 6.1.

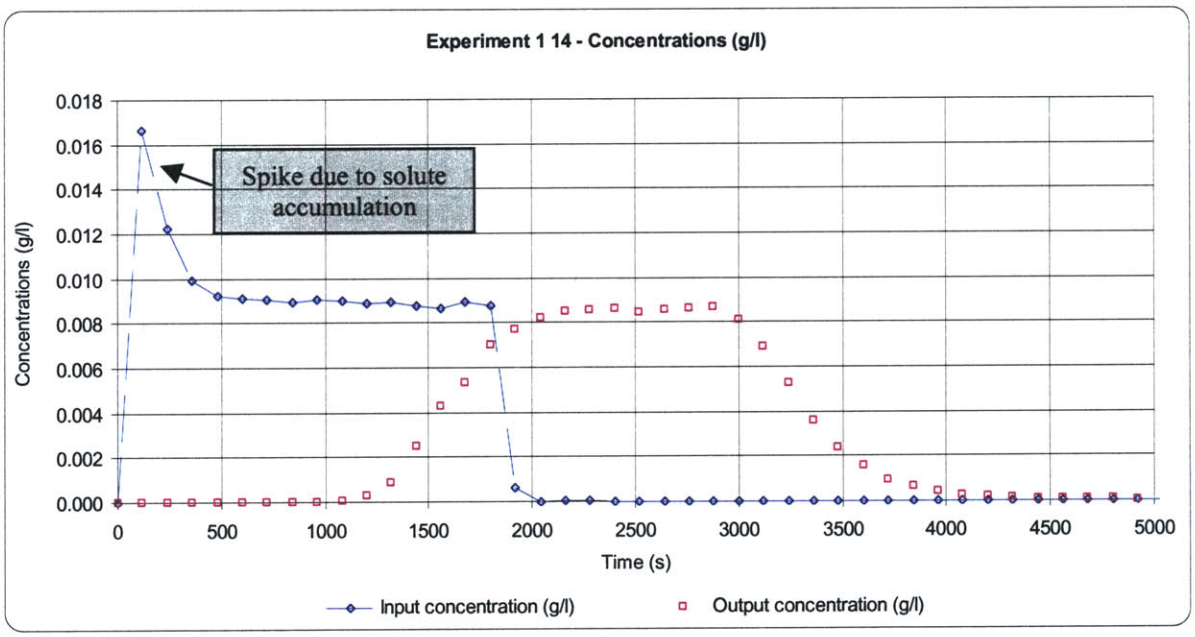

Figure 6.1: Effect of solute accumulation in water lines

These solute accumulations are detected from the input pulse shape. The peak on the input pulse, shown in figure 6.1, suggests that there is an increase in solute concentration.

This peak always appeared at the beginning of the pulse regardless of the time the specimen and lines were flushed with fresh water. Thus, it was deduced that the accumulation was in the water line that was going to the salty water transducer.

As a result of this, the salty pressure transducer was by-passed and is no longer used. A three-way valve was installed in the fresh water line upstream of the fresh water transducer, and the salty water pot connected directly to this water line through the new valve, as in figure 6.2. This new configuration solved the problem.

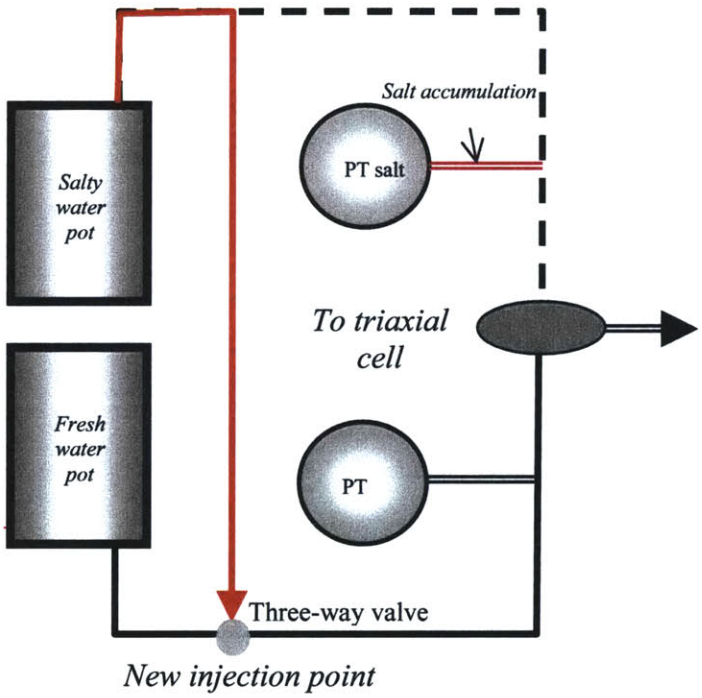

Figure 6.2: New solute injection point

6.2.2. Air diffusion through membranes

During tracer tests, inconsistent pressure readings were observed with the cell and pedestal pressure transducers. It was deduced that air was diffusing through the latex membranes that separate the specimen from the cell fluid, and passing into the specimen fluid (pore fluid).

The cell fluid was pressurized through a water-air interface, as it was for the fresh and salty water pots that feed the flow lines. This water is constantly under air pressure so air diffuses easily into the cell water. Air then diffuses through the membranes and comes out of solution because the pore pressure is lower than the cell pressure.

This pressurizing system was substituted with a volume change device, where air pressure is applied through a piston that acts as an interface between the pressurized air and the cell fluid (figure 6.3).

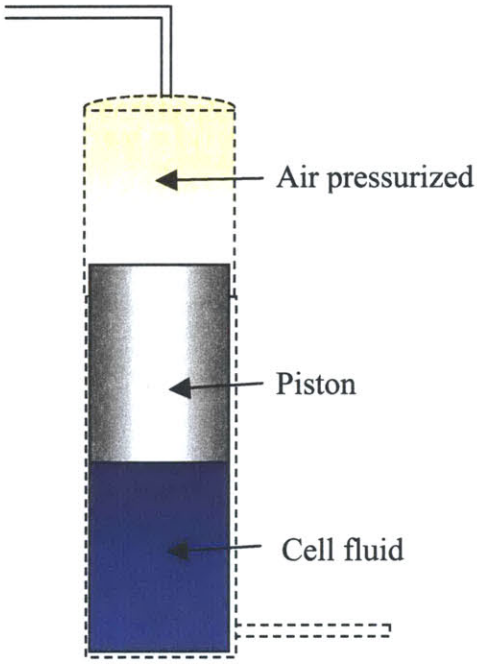

Figure 6.3: Air/water separator used to apply cell pressure

6.3. Evaluation of probe stability

Probes that are not plated regularly give inconsistent readings. The re-platinization process will fix any platinum lose from the electrodes, and it will create a uniform platinum cover. Electrodes should be plated every year or two depending on the frequency of use and the type of storage. Dry storage electrodes will require more plating.

Figures 6.4 and 6.5 shows a tracer test before probes were plated, where the permeameter is set up without a specimen. Although the injection time is long enough to obtain a constant value equal to the input solution concentration, the pedestal probe readings, which are the output solution concentrations, do not equal the input concentrations. Several factors that

could affect the solution conductivity and/or probes reading were investigated and are presented in the following paragraph:

a) *Sensitivity to pressure:* since the probes calibration is carried out without any pressure in the system, the changes in conductivity of the salty solution could be due to the pressure applied to the solution in the back-saturation process (figure 6.4).

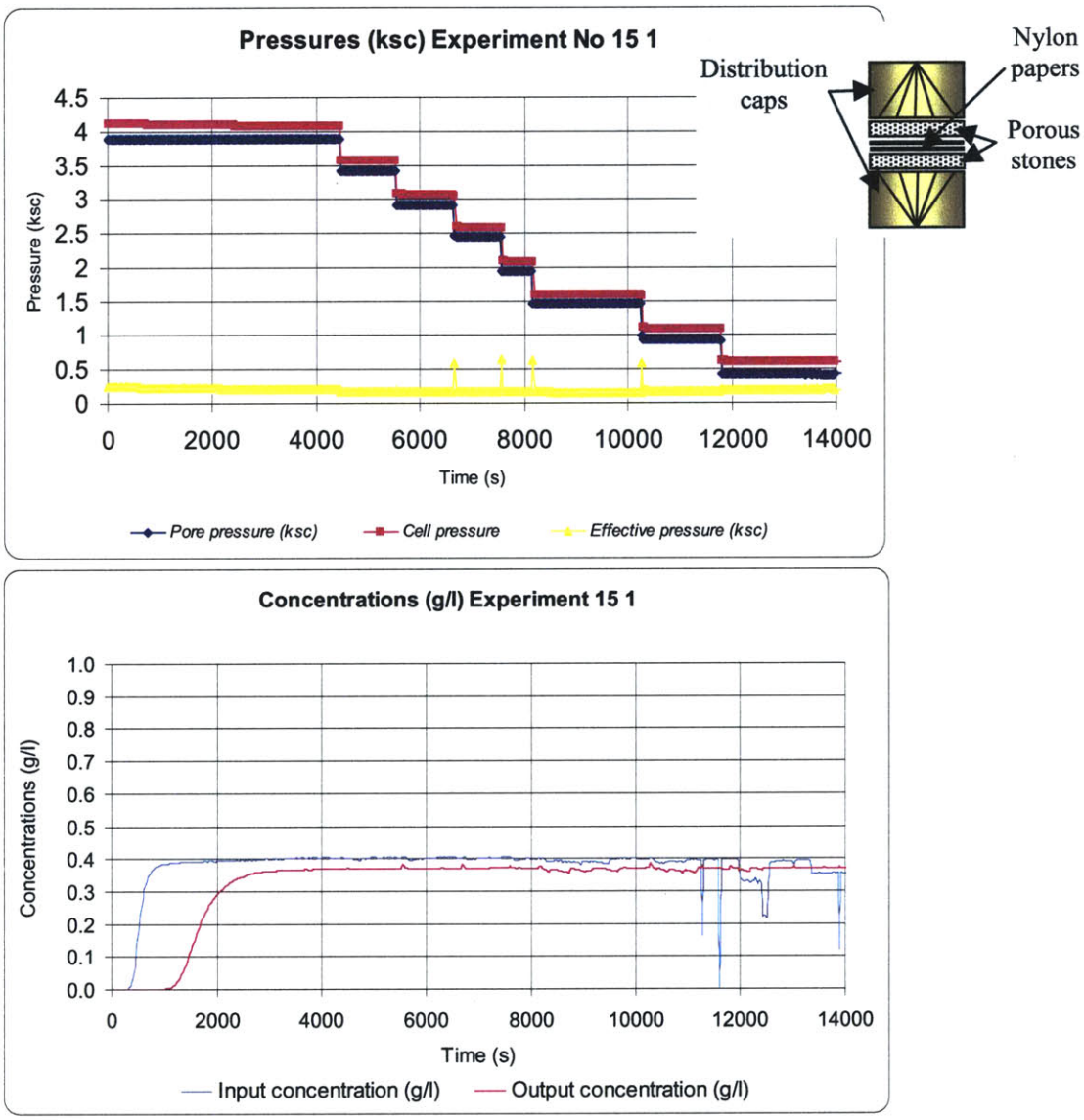

Figure 6.4: Experiment No 15 1 – Influence of pressure on probes readings

In Experiment 15 1 the permeameter was set up without a specimen, only the distribution caps, porous stones and nylon papers were in place. After back-saturation,

and during a constant flow, the pore pressure and cell pressure values were decreased in several steps and probes readings recorded. Pressures were dropped in increments to maintain the effective pressure unchanged during this test. No change in conductivity was observed, and it was concluded that the pressure does not affect conductivity readings (figure 6.4). Note the drastic drops in the concentration curves due to the formation of air bubbles when pressures fall under the back-saturation pressure and the air comes out the solution.

b) *Sensitivity to flow rate*: as with Experiment 15 1, the permeameter was set up without a specimen and a permeability test was carried out.

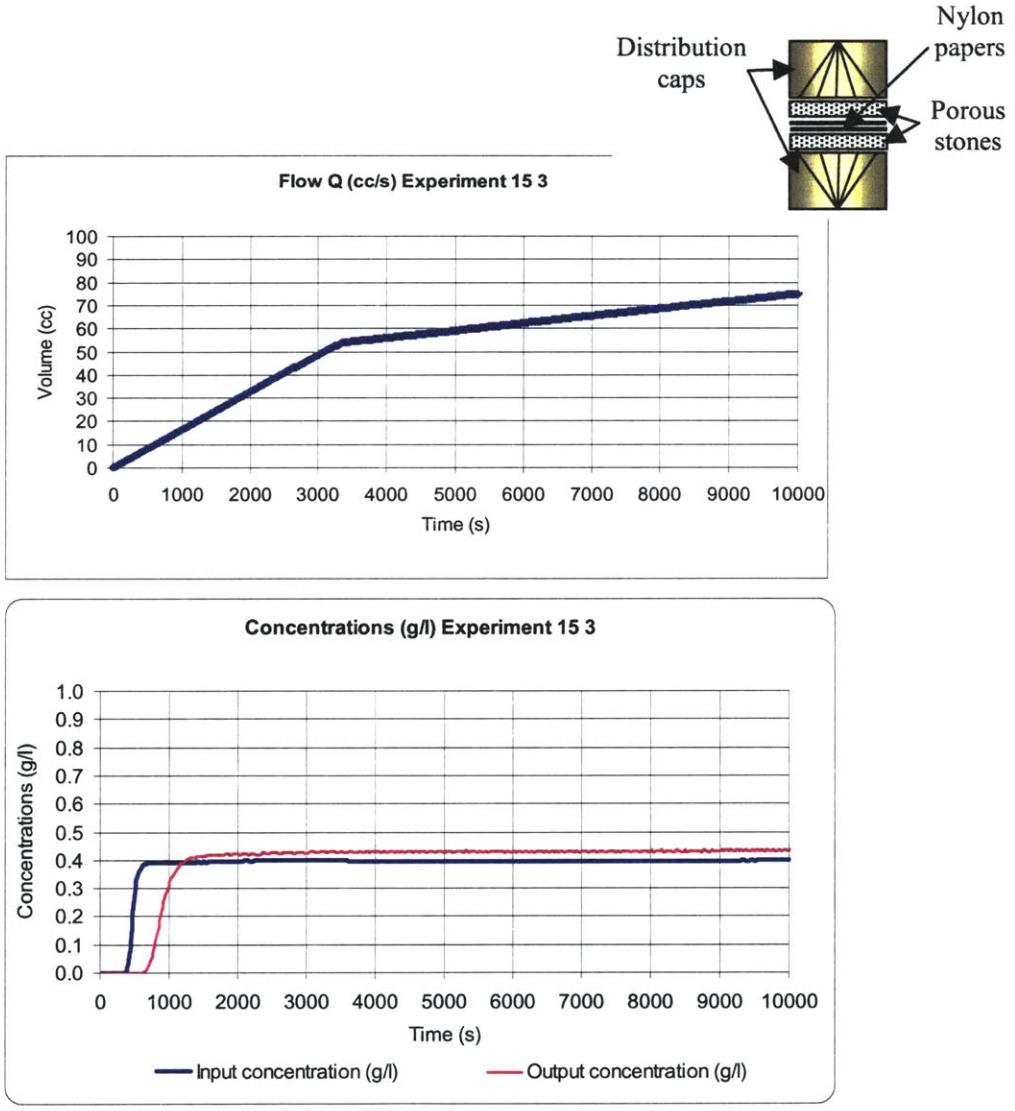

Figure 6.5: Experiment 15 3 – Influence of flow rate on probes readings

By changing the speed of the motor attached to the volume change device, the flow rate was modified maintaining constant pressures. Results are shown in figures 6.5 that correspond to Experiment 15 3. There is no influence of flow rate on probe readings.

c) *Probes readings affected by the geometry of the system*: Previous experiments did not generate changes in probe readings with the different set up geometries. Different geometries were shown in the preceding sections. Some elements in the permeameter, such as the porous stones or nylon papers, were placed in different positions along the solute flow path. Furthermore, some of them were removed. Flow lines were exchanged and flow direction was reversed. None of the different configurations tested modified the probes readings. This indicates that probe readings are not influenced by the geometry of the system.

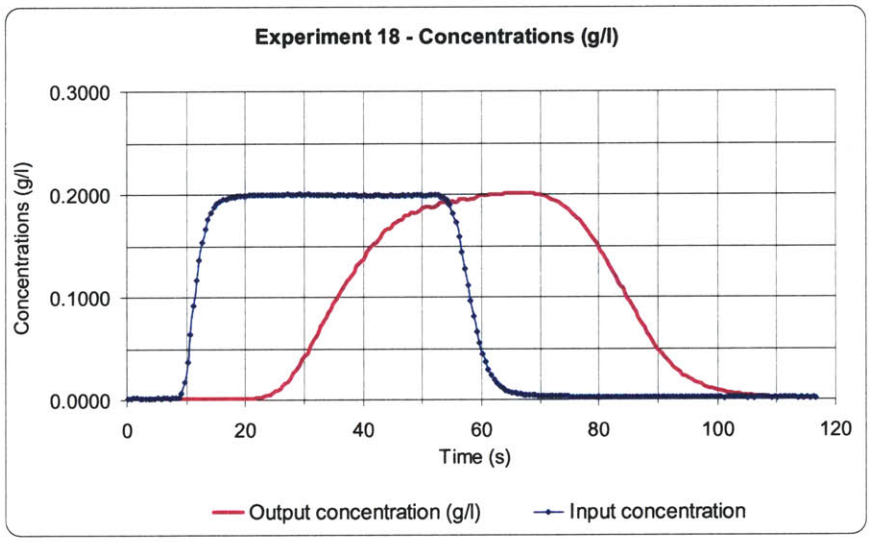

Figure 6.6: Experiment 18 – New inlet probe and re-platinized pedestal probe

Since there are no sinks or sources of solute in the system, or any geometric or pressure effects that could disturb the probes readings, it was theorized that the conductivity probes surface was altered and they needed platinization. Pedestal probes were re-platinized by Microelectrodes, Inc. (Manchester, NH) and new inlet probes were made. Experiment 18 is carried with the new probes (figure 6.6). As a result of several consecutive tests, it was assumed that:

1. Sensitivity of pedestal probe decreases with time. The time at which pedestal probes read lower concentrations is about 5 days from the set up of equipment.

2. Inlet probes readings are very reliable with time. For some column tests, tracer tests were carried out for a two-weeks period. During the tests, it was observed that the inlet probe readings were consistent with the input solute concentration while the pedestal probe was giving lower values for the same input concentration (figure 6.7).

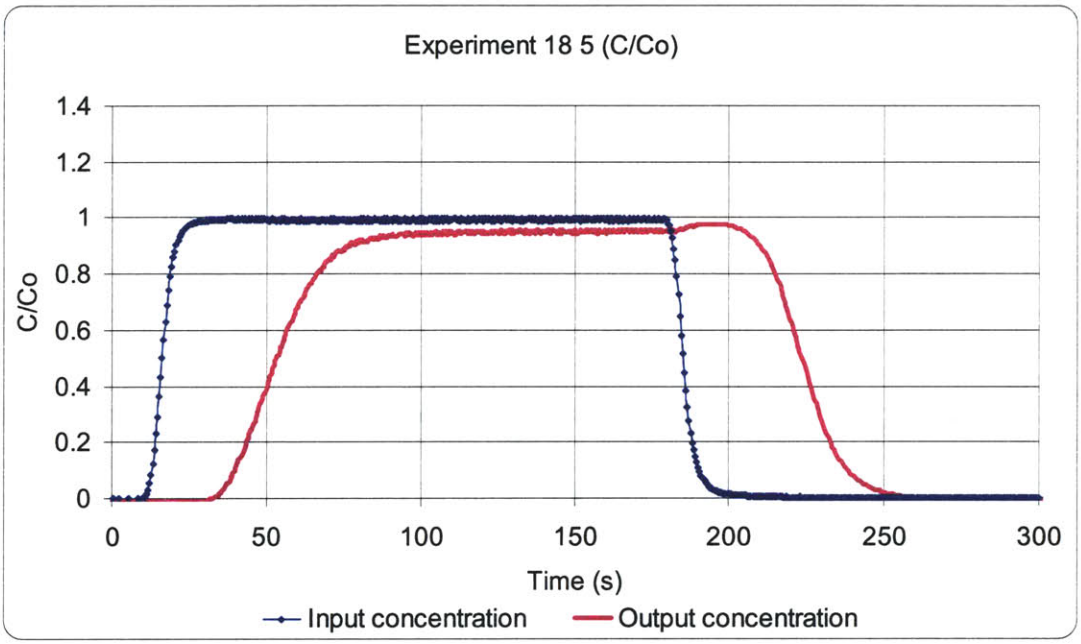

Figure 6.7: Breakthrough curve at the 7th day of test.

Since the breakthrough curve is the one used in calculating transport parameters is was decided to use the inlet probe as the probe used to read the breakthrough curve since its sensibility is constant with time. As a result, the flow direction was inverted for the next experiments (Experiment 18 8, figure 6.8).

6.4. Influence of pulse length and specimen length

Previous research shows that, although wetland soils are considered as Two-Region soils, the One-Region model with $n_m < n_{total}$ was able to describe sodium chloride breakthrough in these soils (Aref, 1999). This means that the solute moving through the mobile pores did not interact with the immobile zones of the soils.

One reason for this could be that the injection time in the tracer test was not long enough to input reasonable solute mass into the specimen, and solute did not have time to diffuse into the immobile pores. Note, that for an average flow velocity between 10^{-4} and 10^{-5} cm/s and a solute concentration of 0.5 g/l, 10 minutes injection would input into the specimen about 0.16 mg of solute. The injected solution volume would be less than 1% of the specimen pore volume, which can vary between 4 to 80 cm^3 depending on its height and assuming a saturated specimen with 40% volumetric water content.

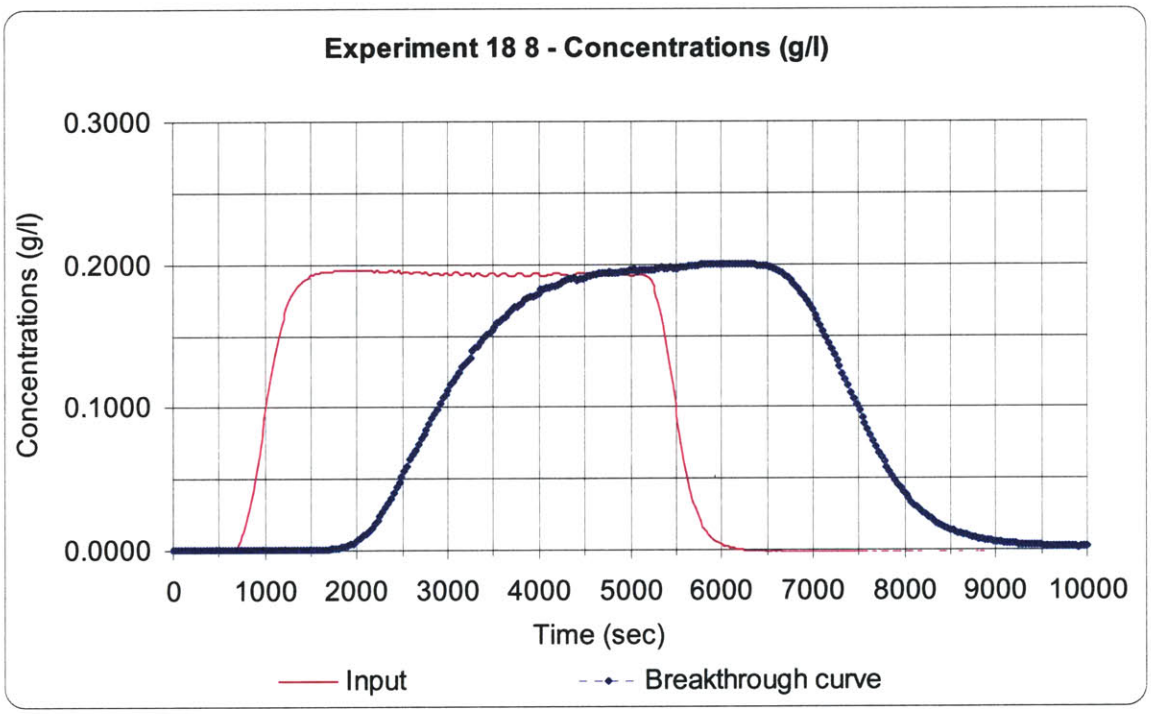

Figure 6.8: Experiment 18 – Inverted flow from pedestal to top of specimen

There should be a balance between the pulse volume and specimen volume that allows the solution to move through the effective flow paths and diffuse in and out of the dead-end pores. In this way, a Two-Region soil will not behave as a One-Region soil. Furthermore, since the pulse volume depends on the injection time and the specimen volume depends on its length, there should be equilibrium between pulse size and specimen length in such a way that these values do not influence breakthrough curve parameters.

To understand better which injection time and height values are the most reliable for interpretation of results using the CXTFIT program, several breakthrough curves were generated using the direct problem mode for typical organic soil parameters, listed in table

6.2. Later, the resulting breakthrough curves were fitted using the indirect problem mode. For all the simulations it was found that, the longer the specimen, the larger the input pulse should be to obtain a good fit of the breakthrough curve.

Flow velocity, v (cm/d)	5
Diffusion coefficient, D (cm/d)	1.3
Length (cm)	From 5 to 20
Beta, β (-)	0.75
Mass transfer dimensionless coefficient, ω (-)	0.259

Table 6.2: Theoretical soil parameters

For example, for a specimen of 5 cm, the best fit occurs at an injection time of at least 2 days, while for a 20 cm specimen length the best fit occurs at a minimum injection time of about 10 days. Appendix C lists the variations of the soil parameters (diffusion coefficient D, mobile zones percentage beta and mass transfer coefficient alpha) with injection time for each soil length. Figure 6.9 shows the fits for a specimen length of 5 cm and two different injection times.

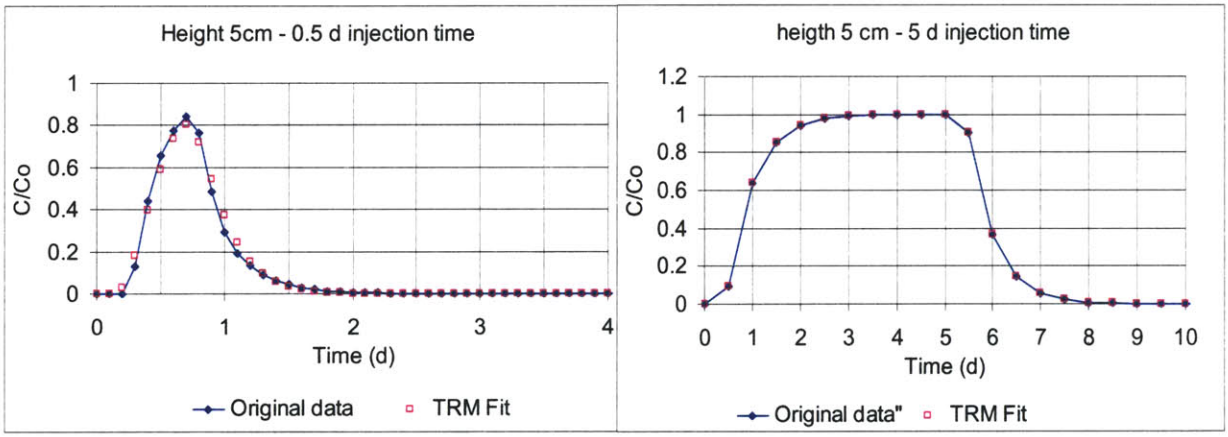

Figure 6.9: Fits for a specimen of 5 cm length and two different injection times

Figures 6.10 to 6.12 show the variation of each parameter with specimen height and injection time. The injection time is given in days and specimen height in centimeters. These charts show that, for longer specimens, the dispersion of the fitted values around the theoretical value increases with specimen height. The distances between the theoretical and the fitted values increase for short injection times. This is clear for the larger specimen heights.

The R^2 values, defined as the R square for regression of observed versus predicted data, indicate the goodness of the fit. These values were compared for all the fits, and the higher this value is the better the fit was. The best fit was defined as the fit that gave the highest R^2.

For a better view of the results, table 6.3 shows the relation between the input solution volume that allows the best fit (for best injection time refer to Appendix C charts) and the specimen volume, assuming a cross-section area of 10 cm^2 equal for all specimens. For all these cases R^2>0.999. Percentages are given as ratio of solution volume to specimen pore volume.

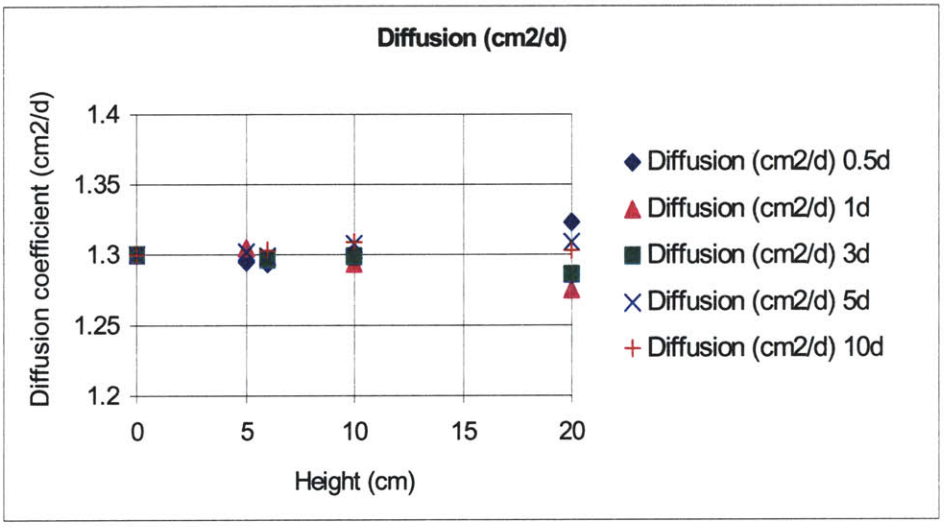

Figure 6.10: Variation of fitted diffusion coefficient D

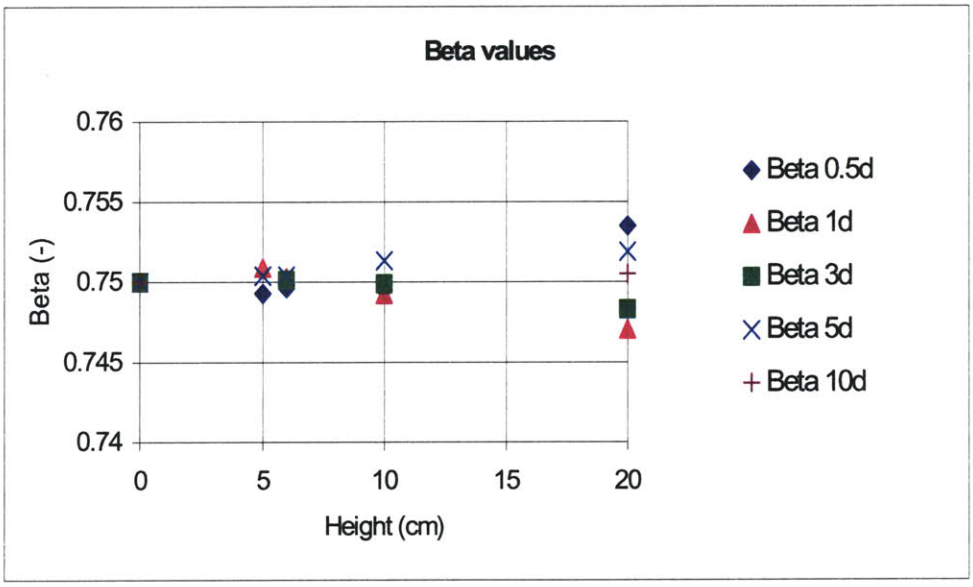

Figure 6.11: Variation of beta coefficient, β

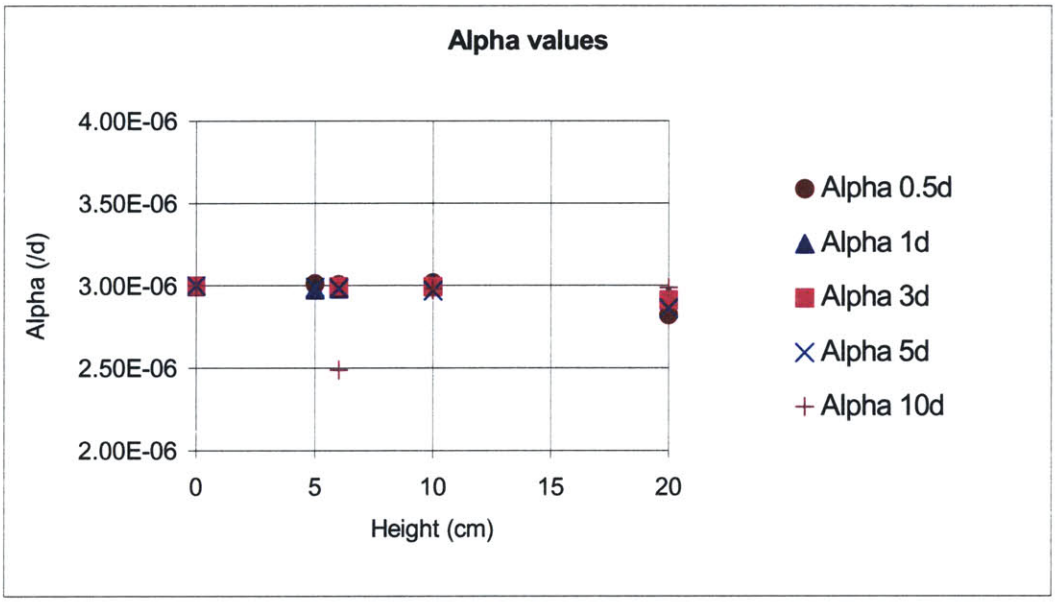

Figure 6.12: Variation of mass transfer coefficient, α

Note that percentage values lay between 20% and 30%. This means that, for a given soil, the best injection time is the one that inputs a solution volume approximately 25% that of the specimen pore volume.

Length (cm)	*Specimen Volume (cm^3)*	*Pore volume (cm^3)*	*Injection time (d)*	*% volume*
5	50	20	2	20
6	60	24	2	24
10	100	40	3	27
20	200	80	7	23

Table 6.3: Relation between solution volume and specimen pore volume

6.5. Influence of permeameter elements on breakthrough curve

Previous research showed the influence of some permeameter elements on breakthrough curve characteristics (Aref, 1999). Furthermore, some of these elements, like the porous stone and specimen end caps, can act as Two-Region material, creating a false tailing on the

breakthrough curve. The CXTFIT computer program would wrongly include these effects as inherent to the soil characteristics.

It was demonstrated that the end caps create a dead zone at the two ends of the specimen that act as immobile zones (Aref, 1999). Therefore, distribution caps were developed to diminish this effect.

In order to detect the influence of permeameter elements on the breakthrough curve the permeameter was set up without a specimen. These experiments were used to calculate the travel time too.

6.5.1 Experiments with porous stones, distribution caps and nylon papers

Experiments No 3 and 5 consisted of tracer tests with no specimen in the permeameter. In all of these tests, the breakthrough curve presented some tailing that became more prominent when the flow velocity decreased (figure 6.13). Hence, the porous stones, the nylon papers or both provide immobile space.

6.5.2. Influence of nylon papers

In Experiment No 7 the permeameter was set up only with the nylon papers. A long cylindrical cap with one central drainage line along it was used as an extension of the existing ones in the permeameter since the input drainage line was not long enough to connect both caps with nylon paper between them (figure 6.14).

Although these tracer experiments gave breakthrough curves with large tailing, there is no zone in the permeameter that acts as an immobile region. The immobile region was created when nylon papers were overlapped but fiber patterns are not coincident as showed in figure 6.15.

The resulting breakthrough curves from another tracer experiment in which nylon papers were placed on top and bottom of the long cap corroborated this theory, since no tailing were observed this time. In the general set up of the permeameter with the specimen the nylon papers are always placed separately on top and bottom of the specimen. Hence, the tailing observed in Experiments No 3 and 5 is due to the porous stones.

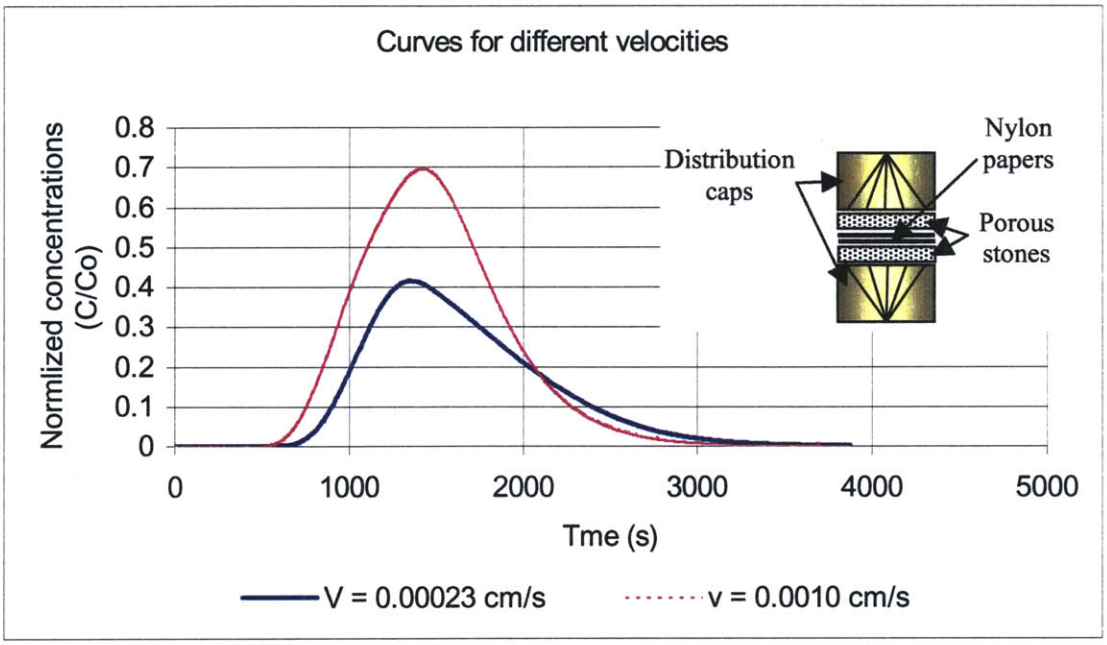

Figure 6.13: Tracer tests in permeameter without soil

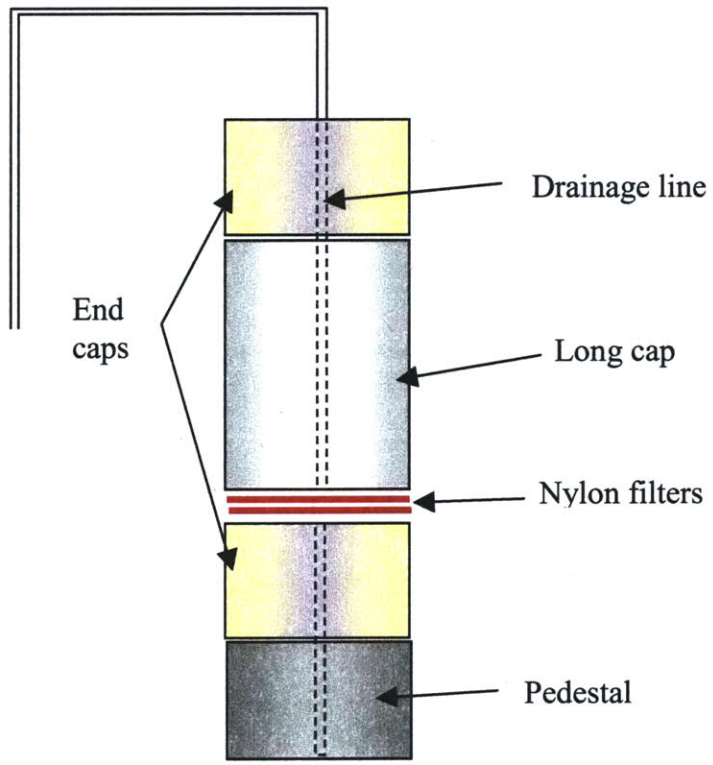

Figure 6.14: Long cap and nylon papers position in experiment No 7

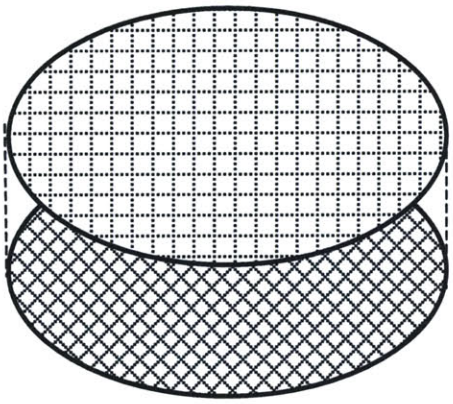

Figure 6.15: Overlaying of nylon papers

6.5.3. Influence of drainage lines

The tracer solution injection point is far away from the top of the specimen. Flow lines can affect some transport parameters such as diffusion and mass transfer coefficients. Experiments No 6 showed the effect of the flow lines on the breakthrough curves. This experiment consisted of a tracer test with only the long cap in the permeameter. The input and output pulses are shown in figure 6.16.

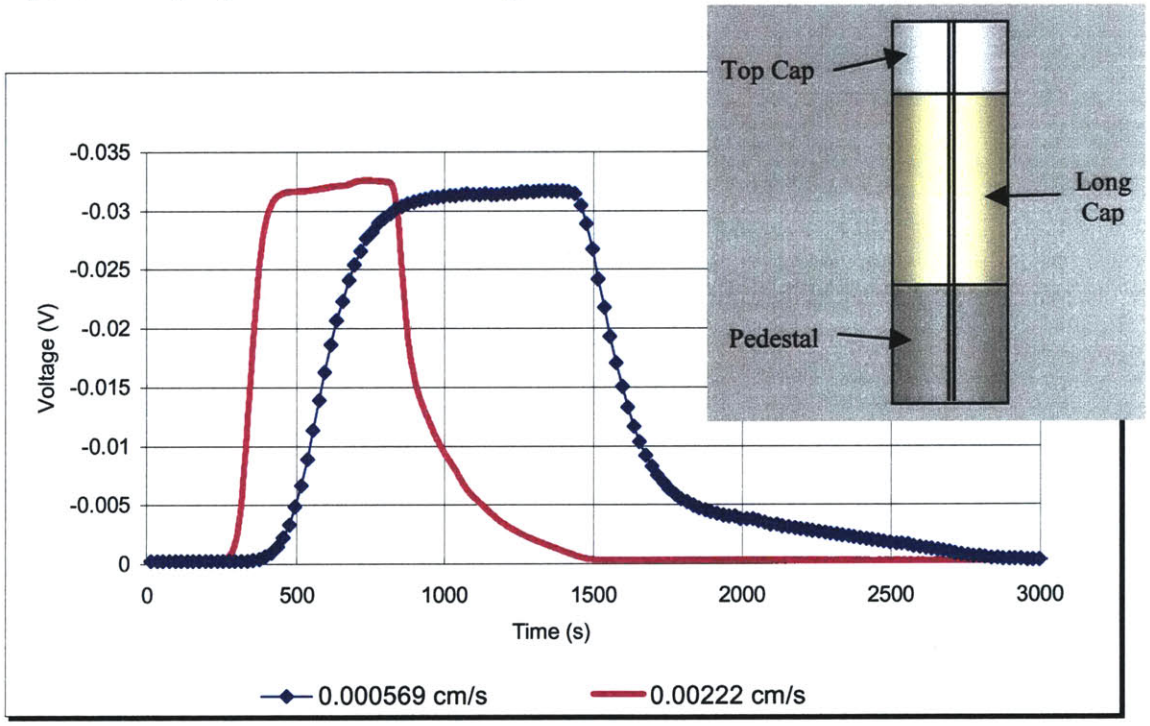

Figure 6.16: Influence of drainage lines

These results indicate that:

1. There is a small tailing on the breakthrough curves, but their influence on the results is insignificant.

2. Tracer tests were carried out at different flow rates. There are no main differences between input and output pulse shapes, and it can be concluded that drainage lines do not affect the measured diffusion coefficient.

6.5.4. Influence of flow rate

Different flow rates will give breakthrough curves with different shapes, thus different parameters. Obviously, when tracer tests are carried at high flow velocities, solute will move faster with the main flow than it will diffuse. This means that advection is the main transport process. On the other hand, when tracer tests are carried at very low flow rates the solute will move mainly due to diffusion along both the main flow paths and into the immobile zones.

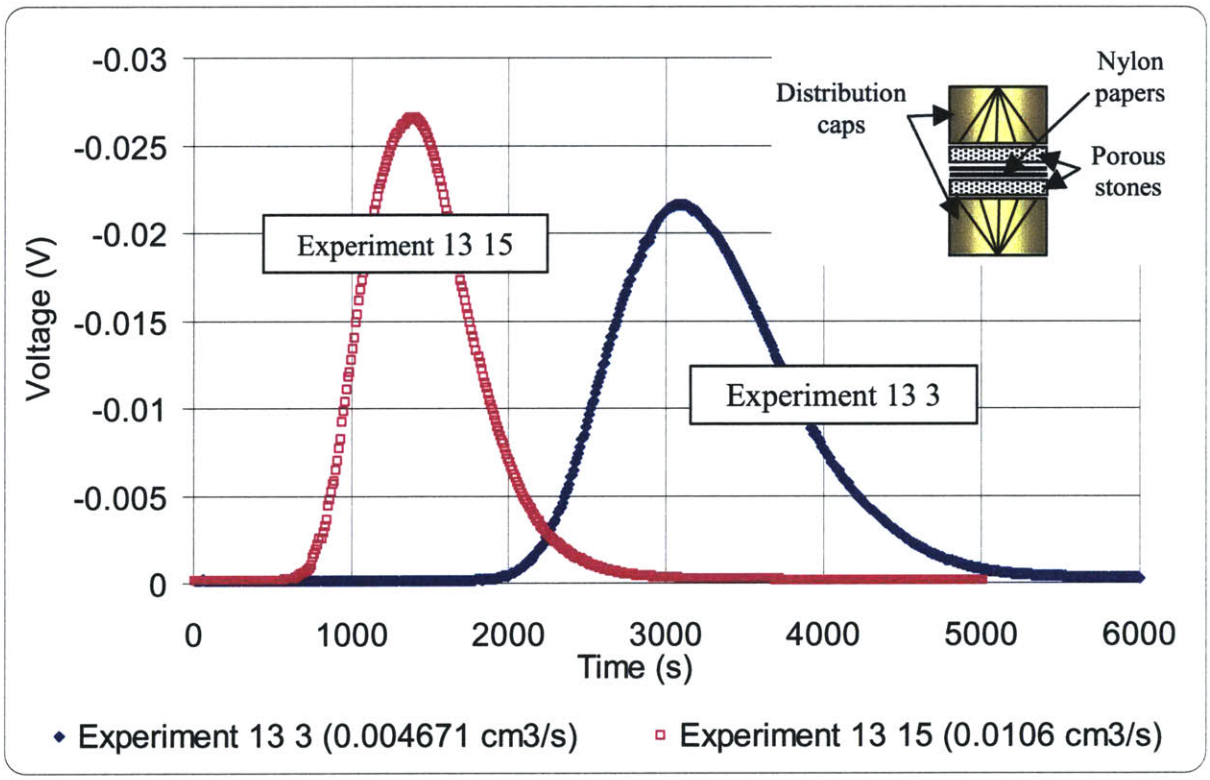

Figure 6.17: Effects of flow rate on breakthrough curves

Tracer tests 13 3 and 13 15 (figure 6.17) were carried out with the same set up, the permeameter with no specimen, but they were carried at different flow rates. Tracer test 13 3 had a flow rate of 0.004671 cm^3/s while tracer test 13 15 had a flow rate of 0.0106 cm^3/s, almost three times faster than the previous one. As can be seen in figure 6.16, breakthrough curves are similar in shape (although they are different in duration) indicating that diffusion and mass transfer are similar in both cases.

6.5.5. Influence of porous stones

The main critical parameter in the column test is the diffusion due to the permeameter elements, principally the porous stones and distribution caps, on the total diffusion value obtained with the program CXTFIT. The diffusion value can be divided two components, the diffusion due to the permeameter and the diffusion due to the soil being tested.

As discussed in Chapter 3, the diffusion value is really the hydrodynamic dispersion coefficient D_h, which is related to the dispersivity and the free molecular diffusion coefficient D_0 as:

$$D_h = D_0 + \alpha.u \tag{1}$$

where u is the pore flow velocity. The molecular diffusion causes spreading due to concentration gradients and random motion, and it can be considered constant. The dispersivity factor depends on the flow velocity of the solution and increases with it. Dispersion is caused by the heterogeneities in the equipment flow paths that create variations in flow velocity.

The Peclet Number is used to study which factor, dispersion or diffusion, is predominant during contaminant transport. Figure 6.18 gives the Peclet number and the diffusion coefficient for a series of experiments, with and without specimens. Some fits where the program gave average velocities much higher than the measured ones, such as the Experiment 15 fits and some fits for the Experiment 14, were eliminated (figure 6.19). Furthermore, the soil specimen had different lengths in order to observe the influence of specimen length in the total diffusion. The Peclet Number is defined as:

$$P_e = \frac{d_{10}.u}{D_o} \tag{2}$$

where:

d_{10}: effective size defined in Appendix B for sand. For column tests with no specimen the effective size of the porous stones is used [L]

u: average flow velocity [L/T]

D_0: molecular diffusion of NaCl which is $1.5_x\ 10^{-5}$ cm^2/s at 25°C [L^2/T]

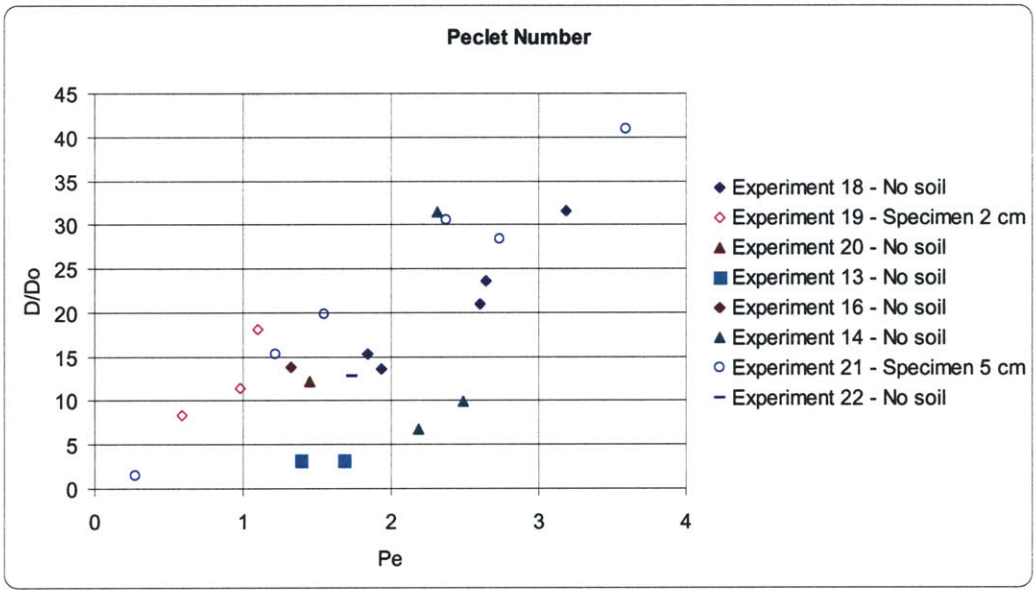

Figure 6.18: Peclet number versus D/D_0

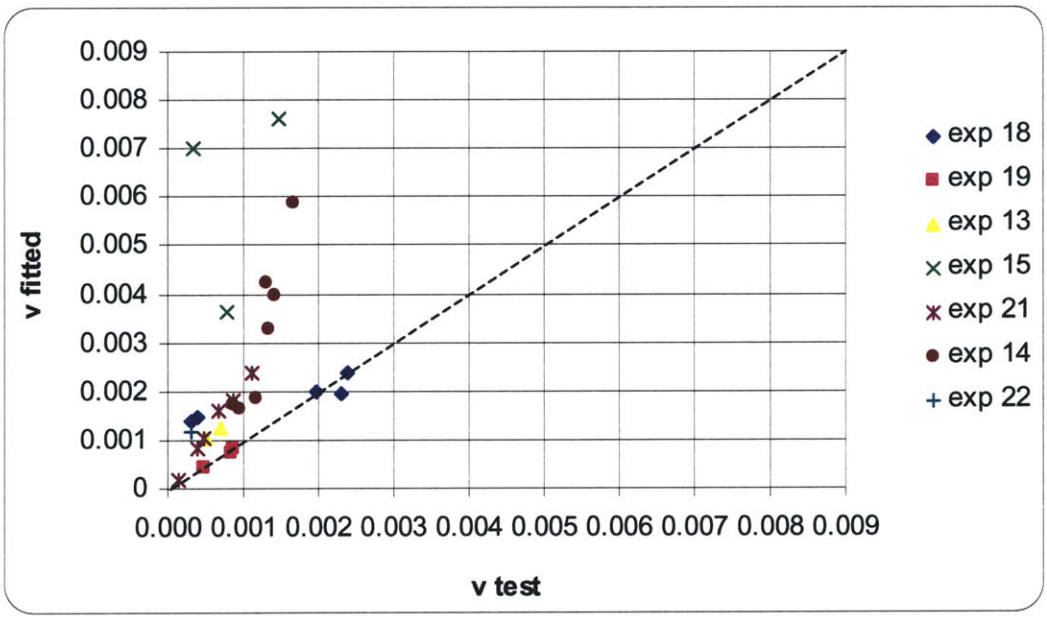

Figure 6.19: Measured versus fitted average velocities

Values of P_e less than 0.4 indicate the diffusion is predominant over the dispersion while values of Pe larger than 1 indicate that dispersion is the predominant cause of diffusion. For values between 0.4 and 1 the effects of mechanical dispersion and diffusion are of the same order of magnitude (Pfannkuch, 1969).

From the plot two important facts can be deduced:

1. Diffusion and dispersion are both present at the flow velocities the column tests were carried out. Considering that in figure 6.18 the data points can be approximated with a straight line with slope of about 6°, it is assumed that dispersion effect is generally predominant over diffusion.

2. Column tests with specimen gave similar values than column tests without specimen, but they are slightly larger, what means that the presence of soil produce additional dispersion.

The final values of diffusion and flow velocity are affected by the permeameter characteristics. The dispersivity α is calculated for the experiments with and without specimen from the Equation (3) for the hydrodynamic diffusion as:

$$\alpha = \frac{D_h - D_o}{u} \tag{3}$$

A plot with D_h-D_0 versus u is represented in figure 6.20. The slopes of the regression lines are the dispersivity values.

- Experiments without specimen: $\alpha_p = 0.1947$
- Experiments with specimen: $\alpha_s = 0.2548$

Soil dispersivity cannot be calculated by subtracting the permeameter dispersivity. A new equation that separates both diffusion coefficients needs to be developed. In these cases, an overall value can be assumed, independent of the position of different material's position with respect to the flow direction, as it is shown in figure 6.21.

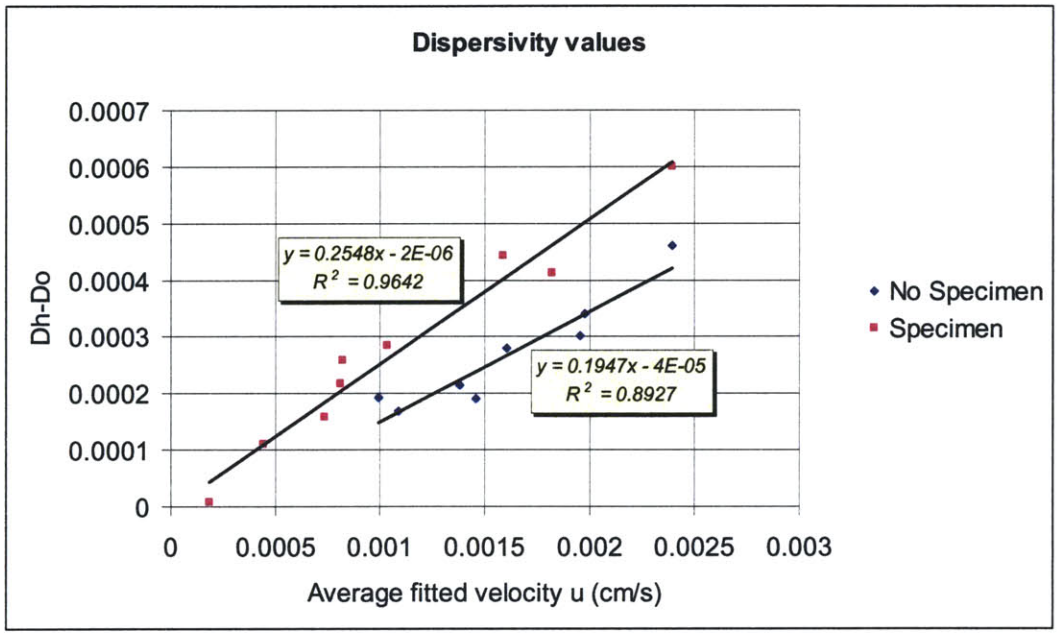

Figure 6.20: Dispersivity values for experiments with and without specimen

The final dispersivity observed on the breakthrough curve is almost the same regardless of the soil's position and due mainly to the property of material B in both cases.

In this material, the dispersivity caused by the soil is large enough to overcome the effect of the dispersivity due to the permeameter and thus, the final values calculated with the CXTFIT program can be assumed as the values corresponding to the sand.

The soil used in all experiments was sand. For the case of organic soils, it is necessary to repeat the process and check the influence of the soil on the total dispersion observed. It is logical to think that, since organic soils have a more complex structure than sand that changes with time, the dispersion produced by them is larger than the one calculated for sands.

On the other hand, at the low velocities required for organic soil testing, the diffusion would be the predominant process.

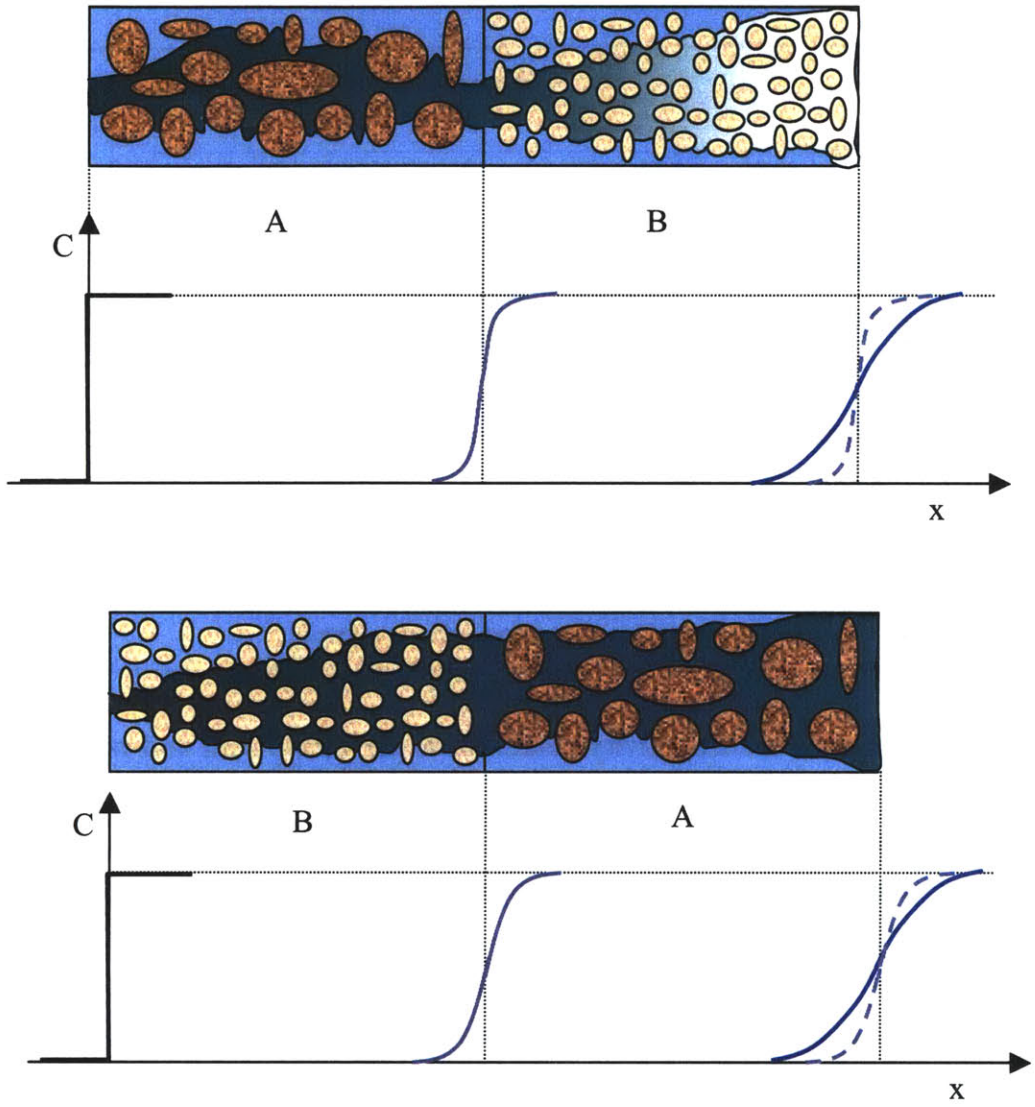

Figure 6.21: Effects of dispersion on the breakthrough curve

6.6. New equations for multi-type materials

All the deductions above are valid only for the sand type used for this research. The influence of the permeameter elements in the final parameters is a relative concept and depends mostly in the type of soil being tested. In some cases, the soil will cause a large dispersion that cancels out that produced by the permeameter. In other cases, the dispersion due to the permeameter can be large enough to overcome the dispersion in the soil. In this case, the soil dispersivity cannot be calculated.

Ideally, the most exact and accurate process would be to solve a transport equation that can encompass the permeameter and soil properties as separate parameters. These equations are usually very complicated and must be solved with the help of a computer program. Although the postulation of these types of equations is out of the scope of this research, the basic procedure is described in this part.

The conductivity probes are far from the specimen ends and their readings include the transport characteristics of the soil and the elements placed between the specimen ends and probes, which comprise the distribution caps, porous stones, nylon papers and flow pipes. For simplicity, these elements will be considered as a soil with its own transport parameters diffusion coefficient (D_p) and average flow rate (u_p). Figure 6.22 shows the simplified model used in developing the equations.

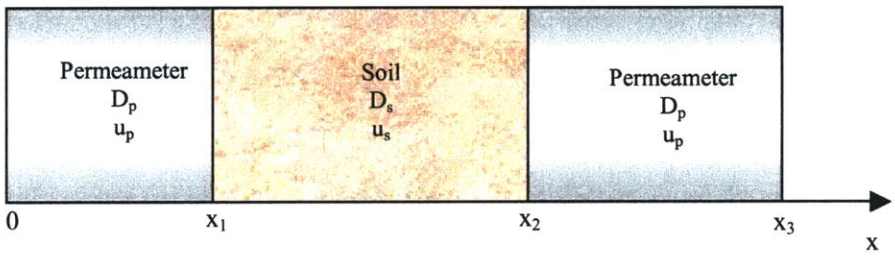

Figure 6.22: Set up simplification

For an overview, the most simplified solution of the equations described in Chapter 3 applied to One-Region materials is used (Bedient, 1999). This solution is given for a continuous source (or step input injection type) with an input tracer of concentration C_0. This solution is only valid for semi-infinite column length. In the case considered here, each of the materials may not be long enough for this assumption to be true, but for simplicity it is considered so. The equations that give the contaminant concentration in each type of material are:

- *For $0<x<x_1$*

$$C_1 = \frac{1}{2} C_0 .erfc\left(\frac{x-u_p}{2\sqrt{D_p t}}\right) + \exp\left(\frac{u_p .x}{D_p}\right) erfc\left(\frac{x+u_p .t}{2\sqrt{D_p .t}}\right) \quad (4)$$

- *For $x_1<x<x_2$*

$$C_2 = \frac{1}{2}\left(\frac{1}{2}C_0.erfc\left(\frac{x_p - u_p}{2\sqrt{D_p t}}\right) + \exp\left(\frac{u_p.x_1}{D_p}\right)erfc\left(\frac{x_1 + u_p.t}{2\sqrt{D_p.t}}\right)\right).$$
$$\left(erfc\left(\frac{(x - x_1) - u_s t}{2\sqrt{D_s t}}\right) + \exp\left(\frac{u_s.(x - x_1)}{D_s}\right).erfc\left(\frac{(x - x_1) + u_s.t}{2\sqrt{D_s.t}}\right)\right) \quad (5)$$

Note that the concentration at the boundaries x_1 and x_2 is considered constant. In actuality, due to the hydrodynamic dispersion, they will not be constant and will have the shape shown in figure 6.21.

The equation that gives the concentration at the end of the system, x_3 is:

$$C_3 = \frac{1}{2}\frac{1}{2}\left(\frac{1}{2}C_0.erfc\left(\frac{x_1 - u_p}{2\sqrt{D_p t}}\right) + \exp\left(\frac{u_p.x_1}{D_p}\right)erfc\left(\frac{x_1 + u_p.t}{2\sqrt{D_p.t}}\right)\right).$$
$$\left(erfc\left(\frac{(x_2 - x_1) - u_s t}{2\sqrt{D_s t}}\right) + \exp\left(\frac{u_s.(x_2 - x_1)}{D_s}\right).erfc\left(\frac{(x_2 - x_1) + u_s.t}{2\sqrt{D_s.t}}\right)\right). \quad (6)$$
$$\left(erfc\left(\frac{(x_3 - x_2) - u_p t}{2\sqrt{D_p t}}\right).\exp\left(\frac{u_p.t}{D_p}\right).erfc\left(\frac{(x_3 - x_2) + u_p t}{2\sqrt{D_p t}}\right)\right)$$

Alternatively, more simplify:

$$C_3 = \frac{1}{8}C_0.[erfc(A) + \exp(A').\text{erfc}(A'')].[erfc(B) + \exp(B').\text{erfc}(B'')].[erfc(C) + \exp(C').erfc(C'')] \quad (7)$$

If the equation that gives the concentration at x_3 has a general expression of:

$$C_3 = \frac{1}{2}C_0\left(erfc\left(\frac{x - u_s.t}{2\sqrt{D t}}\right) + \exp\left(\frac{u_s.x}{D}\right).erfc\left(\frac{x + u_s.t}{2\sqrt{D t}}\right)\right) \quad (8)$$

where u_s and D are the values that can be measured and calculated directly from the column test result.

The relationships between $D_{s,p}$ and D can be seen by equating equations (7) and (8):

$$4.\left(erfc\left(\frac{x-u_s.t}{2\sqrt{D\,t}}\right)+\exp\left(\frac{u_s.x}{D}\right).erfc\left(\frac{x+u_s.t}{2\sqrt{D\,t}}\right)\right)= \tag{9}$$
$$=\left[erfc(A)+\exp(A').\mathrm{erfc}(A'')\right].\left[erfc(B)+\exp(B').\mathrm{erfc}(B'')\right].\left[erfc(C)+\exp(C').erfc(C'')\right]$$

To find D_s, D and D_p must be known.

6.7. Influence of injection type on CXTFIT program results

CXTFIT program allows for different types of solute injection. The step and pulse injection are the only two types that can be accomplished with the permeameter configuration. To study the influence of the injection type the permeameter was set up without specimen and the two different types of injection were carried out. Both breakthrough curves were then analyzed with the computer program. The results indicated that the permeameter parameters are very similar in both cases (see table 6.4).

There is no preference in the use of one or the other type of injection, but in some cases were the flow rates are low and the experiment should be left running overnight, it is more convenient the step input since it does not require the waiting time that is needed for a pulse of a desirable time length.

	Step	Pulse
Flow rate (cm/s)	0.001977	0.002393
Diffusion	0.0003566	0.0004742
Beta	1	1
Omega	0.0000001	0.0000001
D/v	0.1803743	0.1981613

Table 6.4: Influence of injection type in Experiment 18

Chapter 7: Conclusions and recommendations

7.1. Introduction

Over the past decades, manufacturing industries buried their refuse and waste as a common practice. There was no waste management and thus the normal practice was the disposal of waste in uncontrolled landfills or dumping it on surface soils. In addition to this, liquid hazardous waste was released to rivers and water streams. Wastes originating from metal treatments were, and are still, disposed of in lagoons closed by embankments or in large landfills.

Many toxic wastes were dumped or buried in organic soil, since it was commonly thought that this type of soil could act as a barrier and absorb substances into its matrix, preventing then from migration. Wetlands, for example, have been extensively used as toxic waste repositories because these soils can remove contaminants from the water and store them, and this characteristic made wetlands attractive sites for toxic waste storage and water treatment. Despite this characteristic, the nature of organic soils is very complicated and not well known, since they are Dual-Porous Media; thereby their use as toxic waste repositories is not feasible without an adequate monitoring and management plant.

The main objective of this research is the improvement of the modified permeameter developed in the MIT by Ramsay (1990) and used by Aref (1999) to obtain the transport parameters of peat. This permeameter was designed to allow measurement of the hydraulic parameters that characterize wetlands deposits. The permeameter has been modified and adapted so any kind of soil, particularly organic soils, can be tested and accurate results can be obtained with the new procedures.

7.2. Equipment and protocol improvements

To improve the permeameter, is necessary to understand the influence of the permeameter elements on the results from tracer tests and how can they be eliminated to end up with only the parameters that characterize the soil being tested. The main improvements attained in this research can be divided in two groups:

1. Improvement of tracer tests results from physical modification of permeameter.
2. Improvement of tracer tests results from testing procedure modifications.

The improvements in some of the testing procedures are directly related to the changes in the permeameter configuration. The main changes in the configuration that affect the protocol are summarized next.

a) *Change of injection point of tracer solution*: to avoid solute accumulation in the lines that connects the main flow pipes with the pressure transducers, a new injection point is used. Before this new development there were two flow lines, one for the salty water and another for the fresh water. Consequently, not all the salty water lines could be washed out by fresh water. With the new configuration, the salty solution is injected into the fresh water line through a three-way valve so all the zones that can be in contact with the salty solution are accessible by the fresh water, and thus they can be washed out.

Due to this new configuration the pressure transducer that was used to measure the tracer solution pressures was disabled, and only one pressure transducer is used to measure pressures in the fresh and salty water lines.

b) Reverse of flow direction: during the tracer experiments even after the probes were re-platinized it was observed that the pedestal probe lost sensibility with time while the top cap probes were stable for the same periods of time. It was decided to reverse the flow so the top cap probes read the breakthrough curves. Although this new disposition requires one to exchange the valves that were used connect the top cap to the water pots and the pedestal to the Volume Change Device, the old configuration can still be used for the back saturation procedures and, after this is complete, the pipes can be exchanged.

Some procedures changed regardless the new configuration to improve results:

a) *Curve calibration of conductivity probes:* normally, the calibration curves are represented in log-log scale, where the data points relating conductivities of the solutions with concentration can be approximated with a straight line. With this procedure, it is not possible to include as a data point to construct the curves the one corresponding to zero concentration, that would be the conductivity of distilled water used in the column tests as fresh water to flush the lines and specimen. For this reason, normal scales, were the conductivity of the distilled water correspond to zero concentration, are used. In this case, the data points can also be approximated with a straight line.

b) *CXTFIT program used to fit pulse and step injection:* same results for the same soils were obtained using a pulse or step injection. Thus, either of these inputs can be used depending on the convenience of the circumstance.

c) *Relation between specimen length and injection time:* for a Two-Region soil there is an optimum injection time for each specimen length at which the solute has time to interact with the immobile zones in the soil so the parameters for these type of soils can be accurately obtained. It was found that injection times that input into the specimen a solution volume of about 25% the specimen total pore volume, are the most reliable values for interpretation of results using the CXTFIT program. Note that, for step injections, the solute can always interact with the immobile zones despite the specimen length.

7.2.1. Conductivity probes re-platinization

The major improvement in the permeameter was the re-platinization of the electrical conductivity probes. Good preservation of the probes ensures accurate conductivity readings, which are essential for obtaining precise results. Impurities and constant immersion in water alter the electrodes surfaces. Probes need to be plated every one or two years to rebuild the electrodes original surface, and be carefully stored when they are not in use.

The pedestal probe was re-plated, while a new conductivity probe for the top cap line was built. The new probes proved to be more accurate than the re-plated one, and more stable over time. It was then decided to reverse the flow direction and use the new probe to measure the breakthrough curve.

7.3. Recommendations

Recommendations for a better testing procedure performance are summarized in the following paragraphs:

1. To complete the procedure it is necessary for development of new method that allows one to input the permeameter parameters in order to obtain the parameters that correspond only to the soil being tested. Due to the complex formula needed in the problem solving

of these type of processes, it is recommended that this is done via the implementation of a computer program.

2. Development of new types of electrical conductivity probes that are less sensitive with time and more resistant, so their properties will last for longer periods of time. New probes with these properties will require less maintenance.

3. The porous stones are the principal element in the permeameter producing erroneous dispersion. It is recommended the use a different type of porous stones that produce less dispersion, without loosing their main purpose of distributing the flow along the specimen cross-section area. Furthermore, it is advisable to substitute them by other element of the same characteristics that can avoid dispersion.

References

Aref, A.A. *"Flow and Transport in Wetland Deposits (1999)"*. PhD Thesis. Massachusetts Institute of Technology, Cambridge, MA.

Barry, D.A., Culligan, P.J., Bajracharya, K. *"Mass transfer in soils with local stratification of hydraulic conductivity (1994)"*. Water Resources Research, Vol 30, No 11, pp 289-2900.

Bear J. and Verruijt, A. *"Modeling Groundwater Flow and Pollution (1987)"*. D. Residel Publishing Company, Dordrecht, Holland.

Bear, J. *"Hydraulics of Groundwater (1979)"*. New York. McGraw-Hill International Book Co. US.

Bedient , P.B., Rifai, H.S., Newell, C.J. *"Ground water contamination : transport and remediation (1994)"*. Upper Saddle River, NJ. Prentice Hall PTR. US.

Buol S.W *"Soil genesis and classification, 4th edition (1997)"*. Ames Iowa State University Press, US.

De Lima, V., Olimpio, J.C. *"Hydrogeology and simulation of Groundwater Flow at Superfund Site Wells G and H. Woburn, MA (1989)"*. U.S. Geological Survey, Water Resources Investigation Report. Boston, MA. pp 89-4058.

Downing, D. *"Groundwater - our hidden asset (2000)"*. Ed. British Geological Survey. Keyworth, Nottingham, NG12 5GG. UK.

Evans, J.C. and Fang, H.Y. *"Triaxial Permeability and strength Testing of Contaminate soils (1988)"*. Advance Triaxial Testing of Soils and Rocks, ASTM STP 977. American Society for Testing and Materials. Philadelphia. US. pp 387-404.

Everett, E. *"Pedogenesis y taxonomía del suelo. II. Las Órdenes Del Suelo (1983)"*. Progresos en taxonomía del suelo. Elsevier, Amsterdam.

Freeze, R. A. *"Groundwater (1979)"*. Englewood Cliffs, N.J. Prentice-Hall, US.

Fried, Jean J. *"Groundwater pollution: theory, methodology, modeling, and practical rules (1975)".* Amsterdam ; New York : Elsevier Scientific Pub. Co. US.

Grathwohl, P. *"Diffusion in natural porous media: contaminant transport, sorption/desorption and dissolution kinetics (1988)".* Boston : Kluwer Academic Publishers.

Griffiren, J.W., Barry, D.A., Parlange, J.Y. *"Interpretation of Two-Region Model parameters (1998)".* Water Resources Research, Vol 34, No 3; pp 373-384.

Hag, R.S., Price, J.S. *"A field scale, natural gradient solute transport experiment in peat at a Newfoundland blanket bog (1995)".* Journal f Hydrology. Ed Elsevier, pp 171-184.

Head. K.H. *"Soil Laboratory Testing. Vol 3 (1985)".* Pentech Press, London. UK.

Landva, A.O., Pheeney, P.E. *"Peat fabric and structure (1980)".* Canada Geotechnical Journal, pp 416-435.

Lewandowski, A. *"Organic Matter Management, (2000)"* Soil management Series. University of Minnesota. US.

Loxham, M., Burghardt, W. *"Peat as a barrier to the spread of micro-contaminants to the groundwater (1983)".* Proc. Int. Symposium on Peat Utilization. Bemidhi State University, Minnesota.

McLaughlin, D., Kinzerbach, W. and Ghassemi, F. *"Modelling Subsurface Flow and Transport (1993)".* Modelling Change in Environmental Systems. John Wiley & Sons Ltd.

Myette, C.F., Olimpio, J.C., Johnson, D.G. *"Area of Influence and Zone of Contribution to Superfund Sites Wells G and H, Woburn, MA (1987)".* U.S. Geological Survey, Water Resources Investigation Report. Boston, MA. pp 87-4100.

Paustian, P. *"Microbiology Textbook (2000)"* Ed. University of Wisconsin-Madison. US.

Olsen. H.W., Willden, A.T., Kiausalas, N.J., Nelson, K.R., Poe, E.P. *"Volume-controlled Hydraulic Property Measurements in Triaxial Systems (1994)"*. Hydraulic conductivity and Waste contaminant Transporting soil, ASTM STP 1142. American Society for Testing and Materials. Philadelphia. US.

Olsen. H.W., Rice, T.L., Nichols, R.W. *"Measuring Effects of Permeant Composition on Pore-Fluid Movement in Soils"*. Ground Water Contamination: Field Methods, ASTM STP 963. American Society for Testing and Materials. Philadelphia. US. pp 331-342.

Price, J.S., Woo, M. *"Wetlands as waste repositories? Solute transport in peats (1986) "*. Student Conference Proceedings. Department of Geography, McMaster University, Ontario.

Rail, C.D. *"Groundwater contamination, v.1. (2000)"*. Lancaster, Pa. : Technomic Pub.

Ramsay, W.B. *"A Modified Permeameter for Physical Characterization of Parameters Affecting Contaminant Transport through Wetlands Deposits (1996)"*. Master of Science Thesis. Massachusetts Institute of Technology, Cambridge, MA.

Reiken, G. Kale, S.P., Fuehr, F. *"Distribution Patterns of Organic Carbon in Soils and its Role in Preferential Movement of Brilliant Blue in a Structured Silty Soil (1996)"*. Science Of Soils, Rel. 1.

Shackelford, C.D. and Rowe, R.K. *"Contaminant Transport Modelling (1998)"*. Environmental Geotechnics, pp 939-956. Balkema, Rotterdam.

Shackelford, C.D. *"Waste-soil interactions that alter hydraulic conductivity (1994)"*. Hydraulic conductivity and Waste contaminant Transport in soil, ASTM STP 1142. American Society fo Testing and Materials. Philadelphia. US.

Siegel, D.I., Glaser P.H., *"Groundwater flow in Bog-Fen complex, Lost River Peat land, Northern Minnesota (1987)"*. Journal of Ecology, No 75, pp 743-754.

Sullivan, P. *"Sustainable Soil Management (2001)"* Soil System Guide. NCAT Agriculture Specialist. Arkansas. US.

Tan, K. *"Environmental soil science, 2nd ed (1994)."* New York. M. Dekker,US.

Toride, N. Leij, F.J., Van Genuchten, M.T. *"The CXTFIT code for estimating transport parameters from laboratory or field tracer experiments, Version 2.0. (1995)".* U.S. Salinity Laboratory, Agricultural Research Service, U.S. Department of Agriculture, Research Report 137.

Yong, R.N., Mohamed A.M.O. and Warkentin, B.P. *"Principles of Contaminant Transport in Soils (1992)".* Elsevier Science Publishers, Amsterdam.

Appendix A: Sand Characterization

A.1. Sieve Analysis

The sieve analysis test is a particle size analysis for coarse soils. Since the sand used in tests is a coarse soil the sieve analysis is appropriate. Results are presented in table A.1, and its graphical representation, the particle size distribution curve, in figure A.1. The ASTM procedures were used for the characterization of the sand's physical properties.

Weight of oven dry sample = ***577.7***

Sieve No	Sieve opening (mm)	Sieve Weight (g)	Weight sieve + retained (g)	Weight retained (g)	Percent of soil retained (%)	Cumulate percent retained	Percent finer (%)
25	0.71	503.2	517.3	14.1	2.4	2.4	97.6
40	0.425	373.15	576	202.85	35.2	37.6	62.4
60	0.25	363.55	671.7	308.15	53.5	91.1	8.9
120	0.125	343	393.2	50.2	8.7	99.8	0.2
200	0.075	350.6	351.7	1.1	0.2	100.0	0.0
Pan	-	436.6	436.6	0	0.0	100.0	0.0
			Total weight soil =	***576.4***			

Table A.1: Sieve analysis results

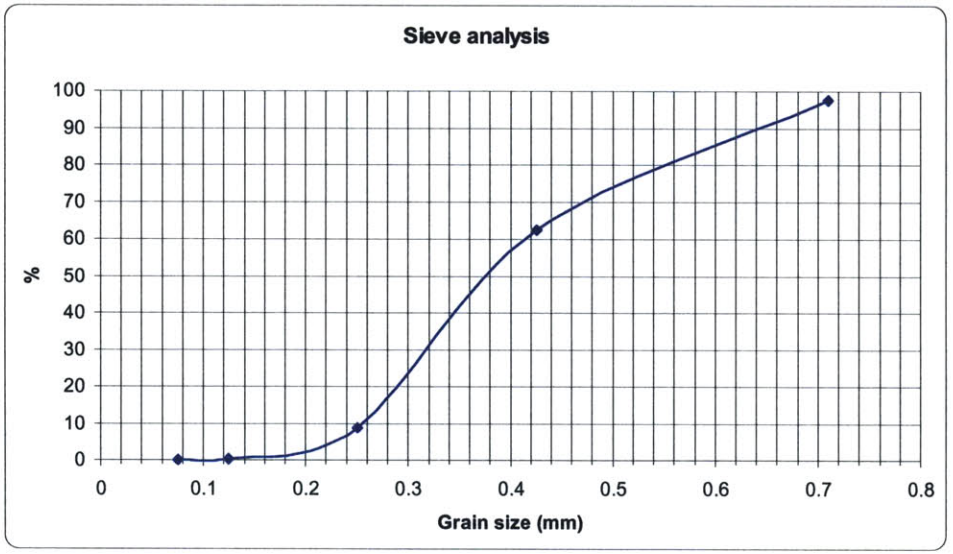

Figure A.1: Distribution curve for sand

Since the particle sizes are comprised between 2 and 0.06 mm, this soil is classified as SP sand. Its shape indicates uniform-graded sand with a uniformity coefficient (ratio between D_{60} and D_{10}) of 1.63.

A.2. Solute sorption coefficient

Soil is placed in several containers each of them having solute solutions of different concentrations. Solute concentration changes are measured over time. The results are presented on next table and in figure A.2.

Final Concentrations (g/l)

No soil

Calibration Curve Equation (No soil)

$Y = 1.10391\ X + 0.15648$

Container No	1	2	3
A	0.072	0.946	10.215
B	0.074	0.952	10.282

first measure: 0 hour

Calibration Curve Equation (0 Hours))

$Y = 1.09454\ X + 0.16326$

Container No	1	2	3
A	0.078	0.952	10.102
B	0.078	0.934	10.146

second measure: 1 hour

Calibration Curve Equation (1 Hours))

$Y = 1.09454\ X + 0.16326$

Container No	1	2	3
A	0.078	0.958	10.088
B	0.079	0.940	10.153

Last measure: 24 hour

Calibration Curve Equation (1 Hours))

$Y = 1.09568\ X + 0.15043$

Container No	1	2	3
A	0.078	0.965	10.156
B	0.079	0.941	10.120

Table A.2: Sorption Coefficient calculations

The differences between the initial (0 hours) and final (24 hours) solute concentrations indicate the amount of solute sorbed onto the solid phase. Knowing the solution volume and soil weight, the amount of solute sorbed per mass of solid can be represented versus the concentration of solute in the solution.

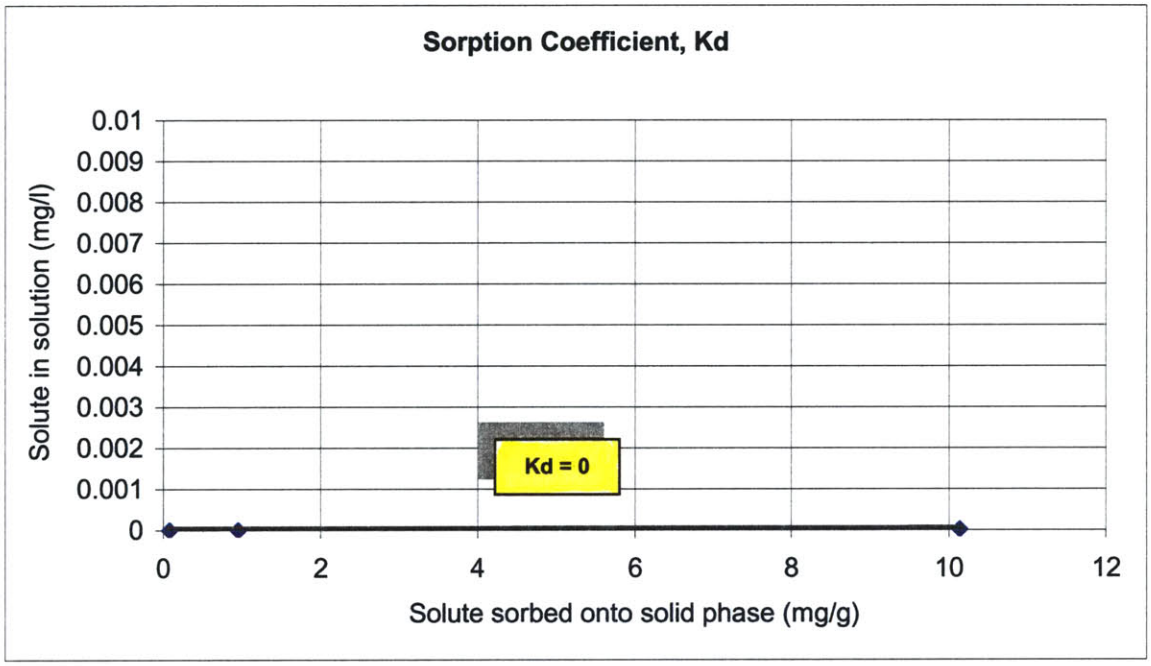

Figure A.2: Partition coefficient of sand

The partition coefficient is zero in this case, since the Sodium Chlorine used as solute is a non-reactive element. Therefore, the retardation factor is 1.

A.3. Specific Gravity

Calculations of the Specific Gravity, following the ASTM procedure, are given in table A.3. The specific gravity values allow the calculation of the specimens porosity and therefore the pore flow velocity, a value that the CXTFIT program requires as an input.

Specific gravity calculations

Experiment No:	1
Date:	30-May-00
Type of soil:	Sand Type 1
Comments:	

Flask No	1	2	3
M_B	174.38	166.2	171.13
M_{B+W}	672.1	664.2	669.1
T_1 (C)	24.8	24.4	24.3
γ_{wt1} (g/ml)	0.9940990	0.9920000	0.9942250
$M_{B+W+S(T2)}$	733.9	726.1	731.1
T_2	22.8	22	22.6
M_S	100.1	99.93	100
γ_{wt2} (g/ml)	0.9972499	0.9977730	0.9942250

Calculations

Falsk No	1	2	3
Volume of flask,ml	500.67	502.02	500.86
Specific gravity at T_2	2.614	2.628	2.632
Specific gravity at 20C	2.611	2.627	2.621

Specific gravity of soil

Average value, S.G	**2.62**
Standart deviation	*0.007836339*

Table A.3: Specific gravity calculations for sand

Appendix B: Column Test Procedures

B.1. Travel Time calculations

Tables B.1 and B.2 give travel time values that correspond to the experiments before and after the last equipment modification consisting in a new conductivity probes, i.e., before and after Experiment 17.

Experiment No	Average linear velocity (cc/s)	Flow rate (cm/s)	Travel time (s)	Volume (cc)	Travel time factor (Txv)
9 2	0.0042	0.000422535	1990	8.358	0.84084507
9 4	0.0066	0.000663984	1180	7.788	0.783501006
10 1	0.0049	0.000492958	1530	7.497	0.754225352
13 1	0.005	0.000503018	1560	7.8	0.784708249
13 2	0.0048	0.000482897	1610	7.728	0.777464789
13 3	0.0047	0.000472837	1600	7.52	0.756539235
13 4	0.0031	0.000311871	2410	7.471	0.751609658
13 5	0.0056	0.00056338	1410	7.896	0.794366197
13 7	0.0068	0.000684105	1140	7.752	0.779879276
13 9	0.0092	0.000925553	850	7.82	0.786720322
13 10	0.0093	0.000935614	860	7.998	0.804627767
13 11	0.0089	0.000895372	866	7.7074	0.775392354
13 13	0.0092	0.000925553	900	8.28	0.832997988
13 14	0.0092	0.000925553	900	8.28	0.832997988
13 15	0.0106	0.001066398	750	7.95	0.799798793
13 16	0.0076	0.000764588	1030	7.828	0.787525151
13 17	0.0073	0.000734406	1150	8.395	0.844567404
13 18	0.0082	0.00082495	1010	8.282	0.833199195
					0.795609211

Table B.1: Travel Time Calculation for Experiments 1 to 17

Experiment No	Linear velocity (cm/s)	Flow rate(cc/s)	Travel time (s)	Volume (cm)	Travel Time Factor (Txv)
18 1	0.000482897	0.0048	1560	7.488	0.75331992
18 3	0.000311871	0.0031	2480	7.688	0.773440644
18 4	0.000176056	0.00175	4640	8.12	0.816901408
18 5	0.00033031	0.003283279	2340	7.68287286	0.772924835
18 6	0.000100111	0.000995105	7890	7.85137845	0.789877108
18 7	0.000469334	0.00466518	1710	7.9774578	0.802561147
18 8	0.000400525	0.003981214	2010	8.00224014	0.80505434
18 9	0.000522256	0.005191226	1530	7.94257578	0.799051889
18 10	0.000548321	0.005450309	1500	8.1754635	0.822481237
					0.792845836

Table B.2: Travel Time Calculation for Experiments 18 to 20

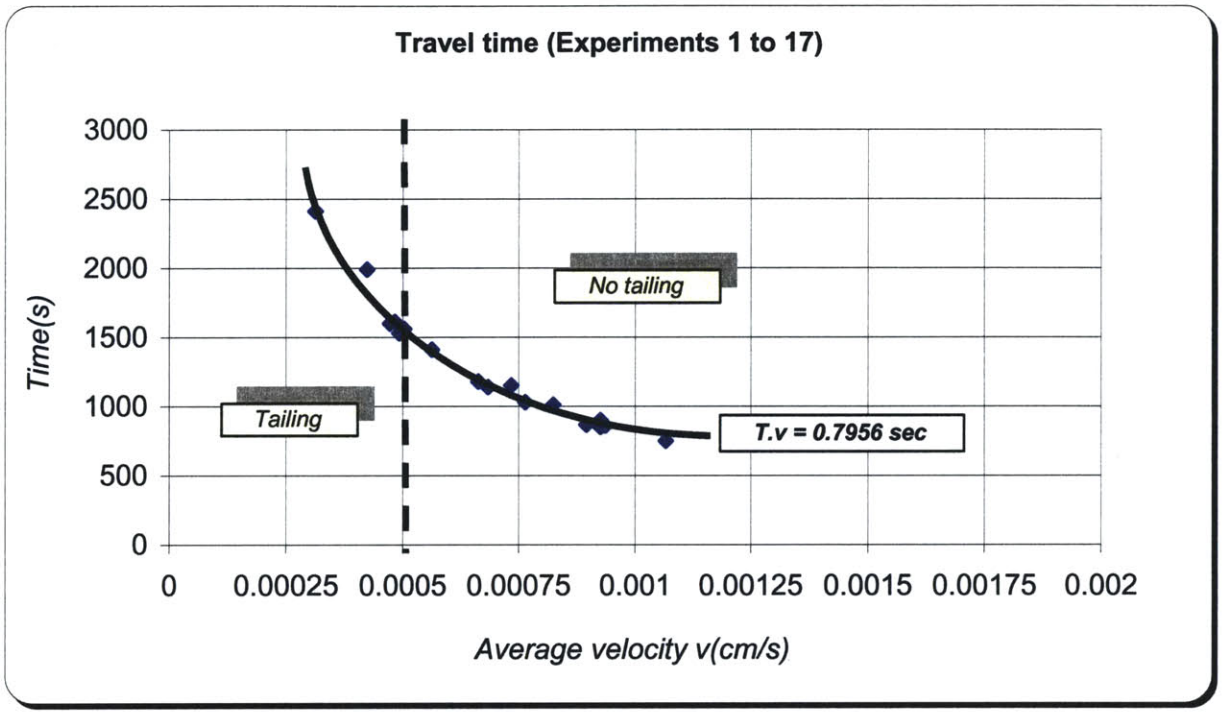

Figure B.1: Travel Time Equation Experiments 1 to 17

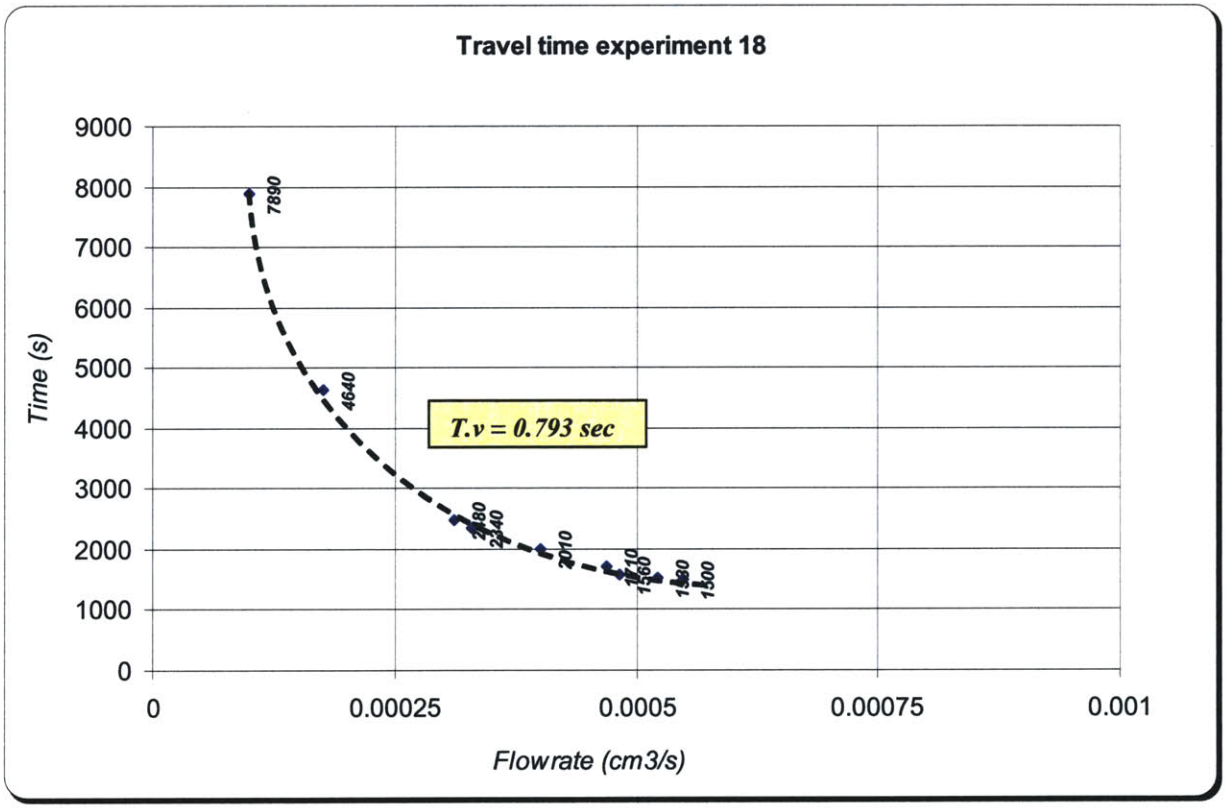

Figure B.2: Travel Time Equation Experiments 18 to 20

B.2. Conductivity Probes calibration

Calibration Probes curves after the platinization are as shown below. Note the use of non-logarithm axis so the distilled water conductivity equals zero concentration.

Concentrations (g/l)	Volts (V)
0	-0.000630112
0.1	-0.004974565
0.2	-0.00994913
0.3	-0.014370965

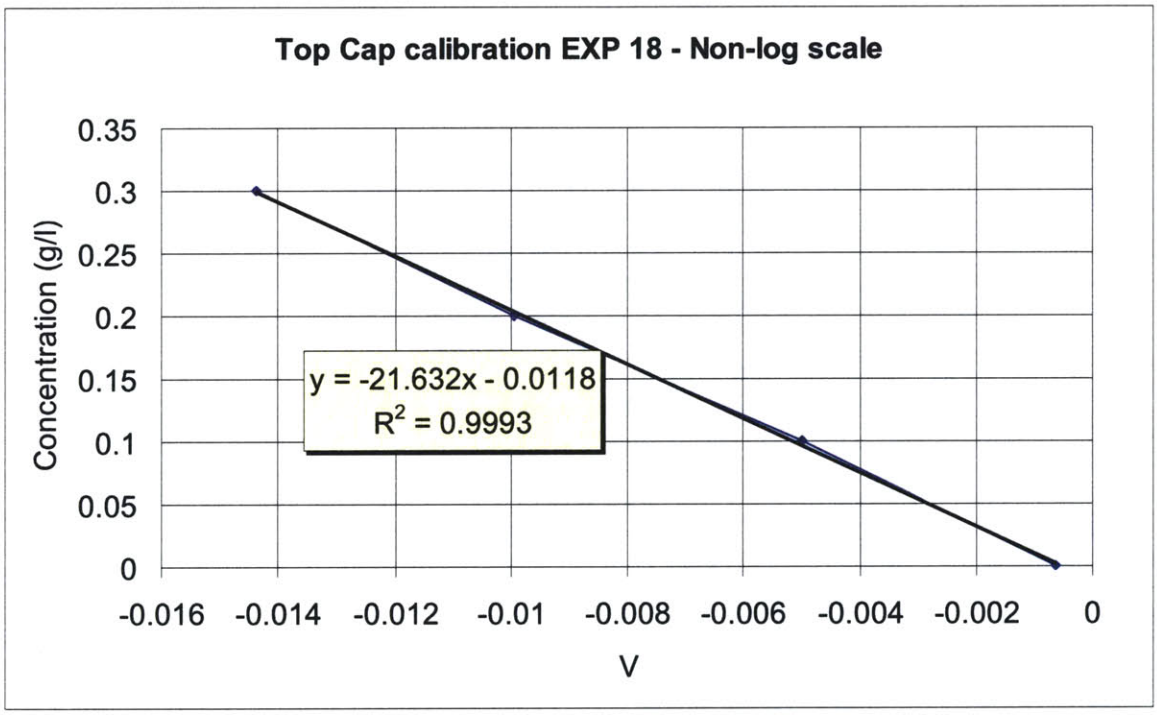

Figure B.3: Example of Calibration Curve for Top Cap Probe in Experiment No 18

Concentrations (g/l)	Volts (V)
0	-0.001658188
0.1	-0.023214636
0.2	-0.044771084
0.3	-0.066880261

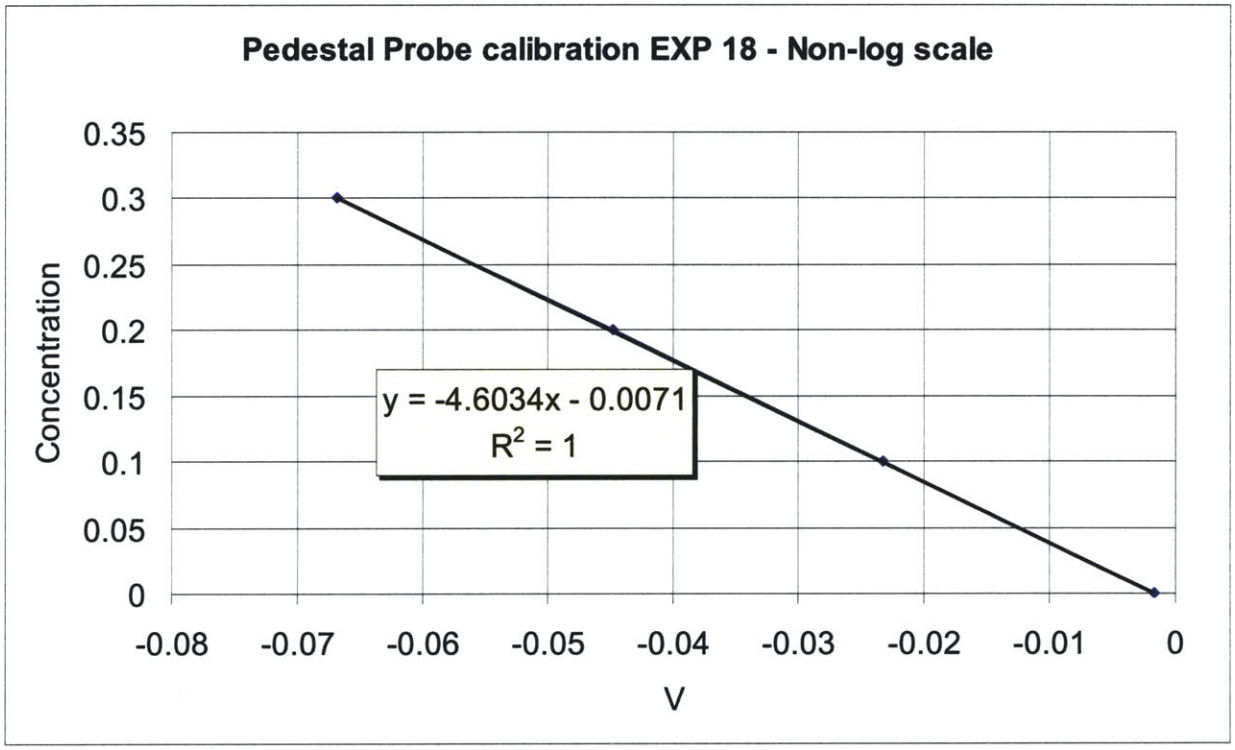

Figure B.4: Example of Calibration Curve for Pedestal Probe in Experiment No 18

B.3. VCD Linear Range and Calibration Factor

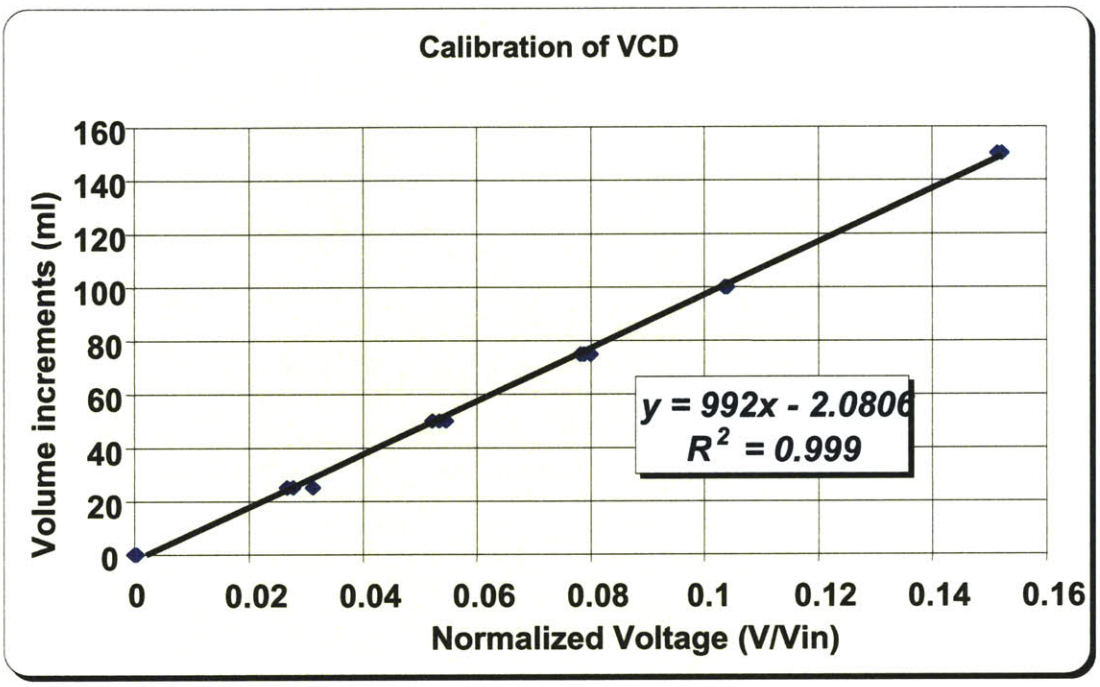

Figure B.5: Volume Change Device calibration

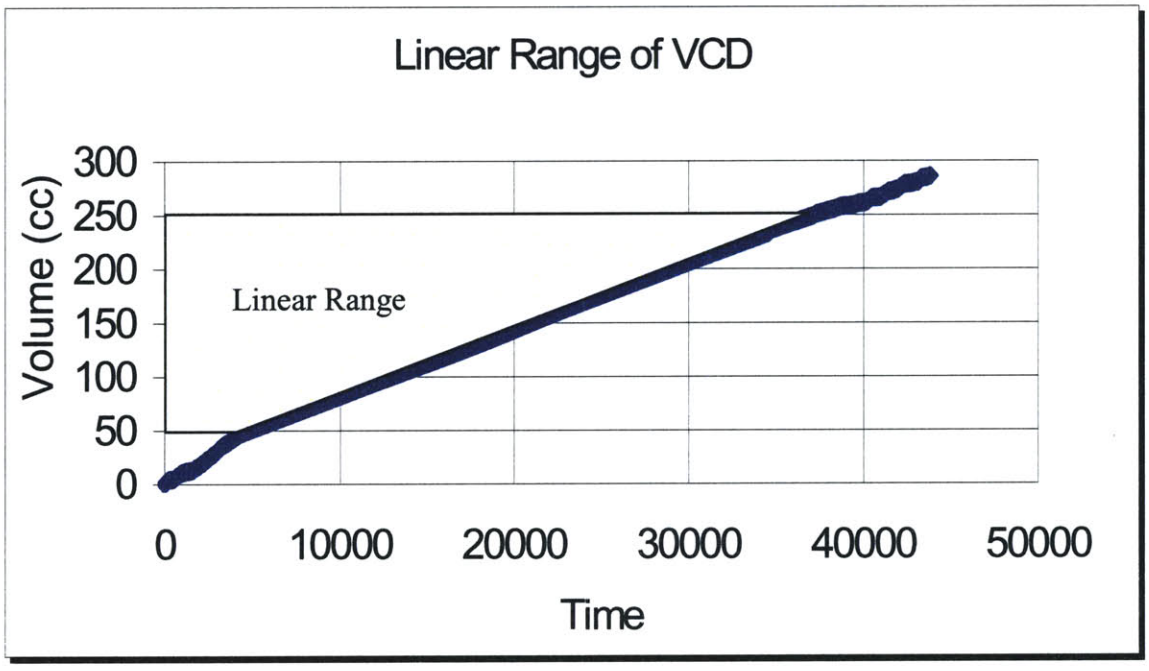

Figure B.6: Volume Change Device working rage

B.4. Specimen set up guide

Experiment No:_____

Soil Type:_____

Date:_____

Set up Specimen

- ☐ Fill lines with appropriate fluid (review line between top cap and pedestal).
- ☐ Sonicate filter papers and porous stones for 30 min.
- ☐ Set specimen with the *triaxial cell sand* equipment.

  - ✤ Grease pedestal and place protector membrane on it.
  - ✤ Leave a small amount of water on pedestal, open PT to pedestal and measure the *zero*:

    Pedestal Zero: _____ ***mV***

  - ✤ Open the inlet line to the pedestal with pots valve close when there is still a small amount of water on it and read the zero:

    Inlet water Zero (2): _____ ***mV***

  - ✤ Place cap, porous stone and filter paper on pedestal in membrane.
  - ✤ Place metal armors around membrane and connect to vacuum pump.
  - ✤ Measure the *total mass* of sand available, *height* and *diameter* of specimen (use caliper).

No Reading	1	2	3
Height (mm)			
Diameter (mm)			

✤ Place sand to the required height. You can use one of the two methods:

1. Raining method
2. Dumping a known weight of sand and compact it to the required height.

✤ Weight of specimen:

Weight before set up (1), g	
Weight after set up (2), g	
Weight of specimen (1) – (2), g	

✤ Place filter paper and porous stone on top of specimen. Before, take excess of sand with a sharp end device.

❑ Place prophylactic membranes. Firs place one and secure it to the pedestal with two O-ring. Then, place second one and secure it with a O-ring in the middle of the two first.

❑ Place protector membrane on top cap and upper cap. Place it in the membrane on the porous stone carefully. Screw top cap to the influent line.

❑ Secure prophylactics membrane to the top cap in the same manner that on the pedestal.

❑ Attach chambre to base of cell and fill with distilled water.

❑ Take *cell transducer zero* when chamber is half filled.

Cell Zero: _____ ***mV***

Vin: _____ ***mV***

❑ Pass three pore volumes of water through the specimen from bottom to top of specimen to wash any air bubble in the specimen.

Back Saturation

❑ Close all valves

❑ Increase cell pressure in 0.5 ksc plus a value of, at least, 0.1 ksc so it will have positive effective stress. For it, follow the values of mV corresponding to the 0.5 ksc increase.

	Calibration Factors	Zeros (mV)	Increments 0.1 ksc (mV)	Increments 0.5 ksc (mV)
Inlet water	**-701.859**		-	
Cell pressure transducer	**-701.822**			

$$Increment\ (mV) = \Delta ksc * Vin * 1000/C.F.$$

Pressure increments		Voltage increments (mV)	
Cell pressure (ksc)	Inlet water pressure (ksc)	Cell pressure (ksc)	Inlet water pressure (ksc)
0.1	0		
0.6	0.5		
1.1	1		
1.6	1.5		
2.1	2		
2.6	2.5		
3.1	3		
3.6	3.5		
4.1	4		

❑ Increase pressure in FW pot by 0.5 ksc.

❑ Open cell valve and top cap valve at the same time. Link pedestal valve to top cap line.

❑ Wait for pressures to equilibrate.

❑ When pressure in FW pot is 4 ksc, check B value:

- ❖ Increases only cell pressure 0.25 ksc.
- ❖ Open only cell valve while pedestal and top cap vales are close and no drainage of water out the specimen in allowed. If sample is saturated, pore pressure (pedestal PT) should increase in 0.25 ksc.

Rising specimen

❑ Close all valves

❑ Check pressure on pedestal

❑ Switch pedestal PT to the effluent line, that it will be connected to the VCD.

❑ Move piston up until pressure on line is equal to pressure on pedestal.

❑ Stop pump, open all valves and move motor to suck to the required voltage or to obtain a desired pressure on pedestal, whatever method is used to set a gradient through the specimen.

Appendix C: CXTFIT files

C.1. Inverse problem

All the fits shown below correspond to a One Region Model (0RM) fit. Same breakthrough curves were fits with the Two-Region Model (TRM) obtaining the same values of flow velocity and diffusion than the ones obtained with the ORM FIT. The values of the mass transfer and partition coefficient that indicates a Two Region Soil were in all cases 0 and 1, respectively. This means that there is no diffusion between a mobile and immobile region (thus it is assume there are no immobile zones) and that all the pores are actually mobile zones.

The input files include the calculated flow rate and known injection times. Although the average flow is calculated in the column tests, the program is allowed to fit it. It also fits the diffusion coefficient whereas the retardation and decay coefficients are assumed as 1 (no retardation) and 0 (no decay).

C.1.1. Step Injection

Input file

```
1
*** BLOCK A: MODEL DESCRIPTION ***********************************************
"One region model. Theoretical model"
"(UNITS: cm, s, normalized concentration)  "
INVERSE    MODE      NREDU
   1         1         1
 MODC       ZL(specimen lenght cm)
   1        4
*** BLOCK B: INVERSE PROBLEM *************************************************
  MIT       ILMT    MASS
  50        0        0
*** BLOCK C: TRANSPORT PARAMETERS ********************************************
    V(cm/S)    D(cm2/s)       R(-)      Mu1
0.0003111   0.000025         1.0        0
     1           1             0         0
*** BLOCK D: BVP; MODB=0 ZERO; =1 Dirac.; =2 STEP; =3 A PULSE  ***********
  MODB (Reduced Conc.& time) =4 MULTIPLE; =5 EXPONENTIAL; =6 ARBITRARY
    2
    1
*** BLOCK E: IVP; MODI=0 ZERO; =1 CONSTANT; =2 STEPWISE; =3 EXPONENTIAL **
  MODI
    0
*** BLOCK F: PVP; MODP=0 ZERO; =1 CONSTANT; =2 STEPWISE; =3 EXPONENTIAL **
  MODP
```

```
    0
*** BLOCK G: DATA FOR INVERSE PROBLEM ************************************
"INPUTM =0; Z,T,C  =1; T,C FOR SAME Z  =2; Z,C FOR SAME T"
1
4
"TIME                CONC      (Give ""0 0 0"" after last data set.)"
18     0
48     0.008205738
78     0.008880603
108    0.008866398
138    0.00801292
168    0.007916511
198    0.007048828
228    0.007916511
258    0.007324169
288    0.00848084
318    0.00848084

*** *** *** ***

56598 0.978816358
56628 0.979203274
56658 0.993228973
0      0      0
```

Output file

```
$

      ************************************************************************
      *                                                                      *
      *      CXTFIT VERSION 2.1 (4/17/99)                                    *
      *      ANALYTICAL SOLUTIONS FOR ONE-DIMENSIONAL CDE                    *
      *      NON-LINEAR LEAST-SQUARES ANALYSIS                               *
      *                                                                      *
      *      "One region model. Theoretical model"                           *
      *      "(UNITS: cm, s, normalized concentration)   "                   *
      *                                                                      *
      *      DATA INPUT FILE:  22 1.IN                                       *
      *                                                                      *
      ************************************************************************


      MODEL DESCRIPTION
      =================
         DETERMINISTIC EQUILIBRIUM CDE (MODE=1)
         FLUX-AVERAGED CONCENTRATION
         REAL TIME (t), POSITION(x)
           (D,V,mu, AND gamma ARE ALSO DIMENSIONAL)


      INITIAL VALUES OF COEFFICIENTS
      ==============================
```

```
NAME         INITIAL VALUE   FITTING
 V........      .3111E-03       Y
 D........      .2500E-04       Y
 R........      .1000E+01       N
 mu.......      .0000E+00       N


BOUNDARY, INITIAL, AND PRODUCTION CONDITIONS
============================================
  STEP INPUT OF CONC. =    1.0000
  SOLUTE FREE INITIAL CONDITION
  NO PRODUCTION TERM


PARAMETER ESTIMATION MODE
=========================
  MAXIMUM NUMBER OF ITERATIONS =   50


ITER      SSQ         V....      D....
 0     .2393E+03   .311E-03   .250E-04
 1     .1301E+03   .395E-03   .115E-03
 2     .3765E+02   .559E-03   .494E-03
 3     .8806E+01   .837E-03   .118E-02
 4     .1713E+01   .112E-02   .493E-03
 5     .7521E+00   .115E-02   .134E-03
 6     .6128E+00   .114E-02   .184E-03
 7     .6093E+00   .114E-02   .194E-03
 8     .6093E+00   .114E-02   .195E-03
 9     .6093E+00   .114E-02   .195E-03


COVARIANCE MATRIX FOR FITTED PARAMETERS
=======================================
           V....  D....
    V....  1.000
    D....  -.110  1.000

  RSQUARE FOR REGRESSION OF OBSERVED VS PREDICTED = .99293665
     (COEFFICIENT OF DETERMINATION)

  MEAN SQUARE FOR ERROR (MSE) =    .3229E-03


NON-LINEAR LEAST SQUARES ANALYSIS, FINAL RESULTS
================================================

                                                 95% CONFIDENCE LIMITS
 NAME       VALUE      S.E.COEFF. T-VALUE        LOWER         UPPER
 V....   .1141E-02   .1989E-05 .5734E+03    .1137E-02     .1144E-02
 D....   .1952E-03   .3302E-05 .5913E+02    .1888E-03     .2017E-03


------------------ORDERED BY COMPUTER INPUT------------------
```

$	NO	DISTANCE	TIME	CONCENTRATION OBS	CONCENTRATION FITTED	RESI-DUAL
	1	4.0000	18.0000	.0000	.0000	.0000
	2	4.0000	48.0000	.0082	.0000	.0082
	3	4.0000	78.0000	.0089	.0000	.0089
	4	4.0000	108.0000	.0089	.0000	.0089
	5	4.0000	138.0000	.0080	.0000	.0080
	6	4.0000	168.0000	.0079	.0000	.0079
	7	4.0000	198.0000	.0070	.0000	.0070
		*** ***	*** ***	*** ***	*** ***	***
	***	4.0000	56358.0000	.9947	1.0000	-.0053
	***	4.0000	56388.0000	.9777	1.0000	-.0223
	***	4.0000	56418.0000	.9948	1.0000	-.0052
	***	4.0000	56448.0000	.9860	1.0000	-.0140
	***	4.0000	56478.0000	.9860	1.0000	-.0140
	***	4.0000	56508.0000	.9859	1.0000	-.0141
	***	4.0000	56538.0000	.9788	1.0000	-.0212
	***	4.0000	56568.0000	.9944	1.0000	-.0056
	***	4.0000	56598.0000	.9788	1.0000	-.0212
	***	4.0000	56628.0000	.9792	1.0000	-.0208
	***	4.0000	56658.0000	.9932	1.0000	-.0068

Breakthrough curve and ORM Fit

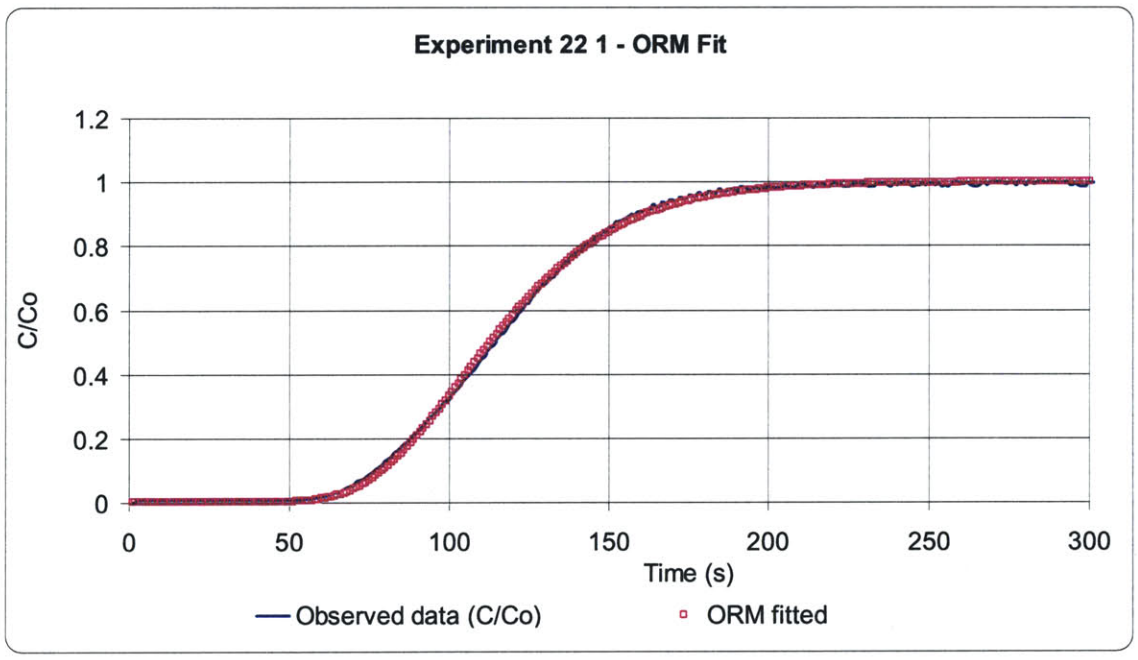

Figure C.1: Example of breakthrough curve and ORM fit for step injection

C.1.2. Pulse injection

Input file

```
1
*** BLOCK A: MODEL DESCRIPTION ***********************************************
"One region model. Theoretical model"
"(UNITS: cm, s, normalized concentration)  "
INVERSE    MODE      NREDU
   1         1         1
 MODC       ZL(specimen lenght cm)
   1        4
*** BLOCK B: INVERSE PROBLEM *************************************************
  MIT       ILMT    MASS
  50        0        0
*** BLOCK C: TRANSPORT PARAMETERS ********************************************
    V(cm/S)    D(cm2/s)       R(-)      Mu1
 0.0024        0.00025         1.0        0
     1            1             0        0
*** BLOCK D: BVP; MODB=0 ZERO; =1 Dirac.; =2 STEP; =3 A PULSE  ***********
  MODB (Reduced Conc.& time) =4 MULTIPLE; =5 EXPONENTIAL; =6 ARBITRARY
    3
   1.0    3000
*** BLOCK E: IVP; MODI=0 ZERO; =1 CONSTANT; =2 STEPWISE; =3 EXPONENTIAL **
  MODI
    0
*** BLOCK F: PVP; MODP=0 ZERO; =1 CONSTANT; =2 STEPWISE; =3 EXPONENTIAL **
  MODP
    0
*** BLOCK G: DATA FOR INVERSE PROBLEM ***********************************
"INPUTM =0; Z,T,C  =1; T,C FOR SAME Z  =2; Z,C FOR SAME T"
1
4
"TIME              CONC     (Give ""0 0 0"" after last data set.)"
731   0.033795618
761   0.035119186
791   0.035543137
821   0.037657718
851   0.039092802
881   0.043089578

***   ***   ***

3161  0.98813505
3191  0.993678368
3221  0.991316809
3251  0.992537588
3281  0.994158711
3311  0.994166974
3341  0.995307592
3371  0.996508297
3401  0.996228128
3431  0.996408236
```

```
3461   0.996868519
3491   0.997488914
3521   0.99667613
3551   0.996396017
3581   0.996396017

***    ***    ***

5921   0.042452315
5951   0.042081237
5981   0.04133946
6011   0.040933464
6041   0.040174845
6071   0.040051401
6101   0.039584604
6131   0.039091297
6161   0.037595235
0      0      0
```

Output file

```
$

      ************************************************************************
      *                                                                      *
      *     CXTFIT VERSION 2.1 (4/17/99)                                     *
      *     ANALYTICAL SOLUTIONS FOR ONE-DIMENSIONAL CDE                     *
      *     NON-LINEAR LEAST-SQUARES ANALYSIS                                *
      *                                                                      *
      *     "One region model. Theoretical model"                            *
      *     "(UNITS: cm, s, normalized concentration)  "                     *
      *                                                                      *
      *     DATA INPUT FILE:  18 1.in                                        *
      *                                                                      *
      ************************************************************************


      MODEL DESCRIPTION
      =================
         DETERMINISTIC EQUILIBRIUM CDE (MODE=1)
         FLUX-AVERAGED CONCENTRATION
         REAL TIME (t), POSITION(x)
           (D,V,mu, AND gamma ARE ALSO DIMENSIONAL)


      INITIAL VALUES OF COEFFICIENTS
      ==============================
      NAME         INITIAL VALUE   FITTING
       V........      .2400E-02       Y
       D........      .2500E-03       Y
       R........      .1000E+01       N
       mu.......      .0000E+00       N
```

```
BOUNDARY, INITIAL, AND PRODUCTION CONDITIONS
============================================
  SINGLE PULSE OF CONC. =    1.0000 & DURATION = 3000.0000
  SOLUTE FREE INITIAL CONDITION
  NO PRODUCTION TERM


PARAMETER ESTIMATION MODE
=========================
  MAXIMUM NUMBER OF ITERATIONS =   50


ITER     SSQ        V....     D....
 0    .4460E+00  .240E-02  .250E-03
 1    .9060E-01  .240E-02  .406E-03
 2    .6575E-01  .239E-02  .466E-03
 3    .6540E-01  .239E-02  .474E-03
 4    .6539E-01  .239E-02  .474E-03
 5    .6539E-01  .239E-02  .474E-03


COVARIANCE MATRIX FOR FITTED PARAMETERS
=======================================
           V....  D....
    V....  1.000
    D....  -.121  1.000

  RSQUARE FOR REGRESSION OF OBSERVED VS PREDICTED = .99746028
     (COEFFICIENT OF DETERMINATION)

  MEAN SQUARE FOR ERROR (MSE) =   .3633E-03


NON-LINEAR LEAST SQUARES ANALYSIS, FINAL RESULTS
================================================

                                                95% CONFIDENCE LIMITS
 NAME      VALUE     S.E.COEFF. T-VALUE      LOWER        UPPER
 V....  .2393E-02   .4734E-05 .5055E+03   .2384E-02    .2402E-02
 D....  .4742E-03   .8387E-05 .5654E+02   .4577E-03    .4908E-03


------------------ORDERED BY COMPUTER INPUT-------------------
                                        CONCENTRATION          RESI-
$    NO    DISTANCE       TIME        OBS        FITTED        DUAL
      1      4.0000    731.0000       .0338       .0049        .0289
      2      4.0000    761.0000       .0351       .0073        .0278
      3      4.0000    791.0000       .0355       .0105        .0251
      4      4.0000    821.0000       .0377       .0146        .0231
      5      4.0000    851.0000       .0391       .0198        .0193
      6      4.0000    881.0000       .0431       .0261        .0170
```

***	***	***	***	***	***	***	***	***	***	***
91	4.0000	3431.0000	.9964	.9940	.0024
92	4.0000	3461.0000	.9969	.9945	.0024
93	4.0000	3491.0000	.9975	.9949	.0026
94	4.0000	3521.0000	.9967	.9953	.0014
95	4.0000	3551.0000	.9964	.9956	.0008
96	4.0000	3581.0000	.9964	.9957	.0007
97	4.0000	3611.0000	.9956	.9958	-.0002
98	4.0000	3641.0000	.9931	.9955	-.0024
99	4.0000	3671.0000	.9908	.9950	-.0042
100	4.0000	3701.0000	.9883	.9940	-.0057
101	4.0000	3731.0000	.9847	.9925	-.0079

***	***	***	***	***	***	***	***	***	***	***
175	4.0000	5951.0000	.0421	.0225	.0195
176	4.0000	5981.0000	.0413	.0208	.0205
177	4.0000	6011.0000	.0409	.0192	.0218
178	4.0000	6041.0000	.0402	.0177	.0225
179	4.0000	6071.0000	.0401	.0163	.0238
180	4.0000	6101.0000	.0396	.0150	.0246
181	4.0000	6131.0000	.0391	.0138	.0253
182	4.0000	6161.0000	.0376	.0127	.0249

Breakthrough curve and fitted curve

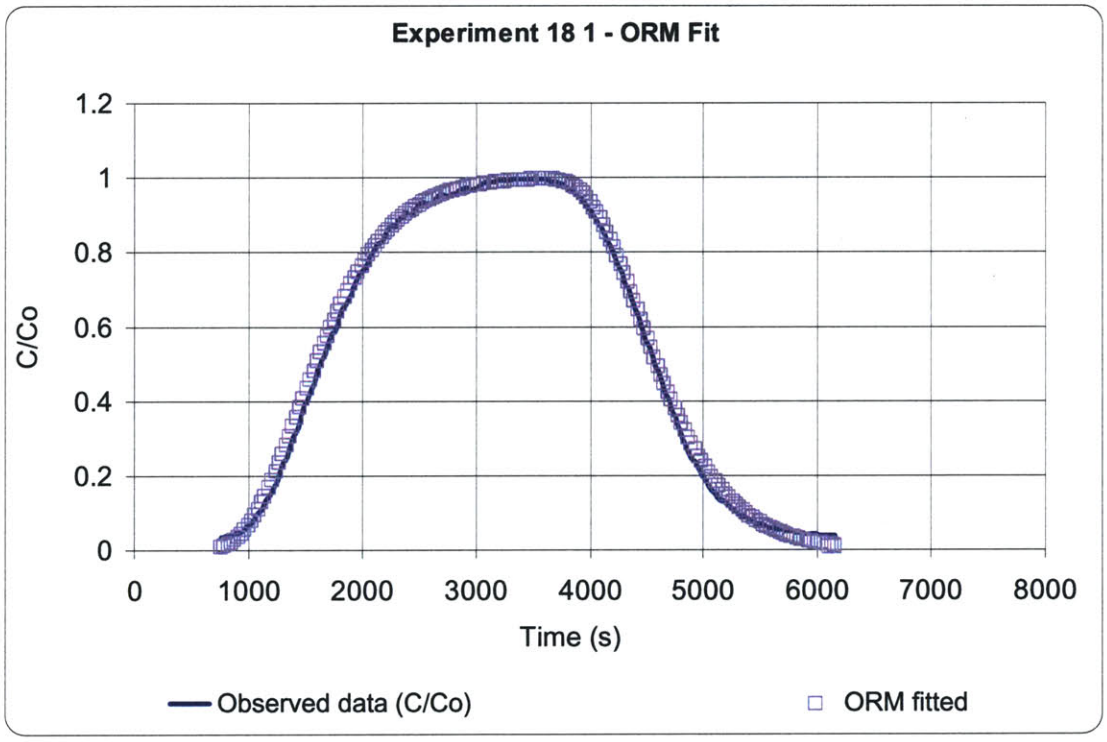

Figure C.2: Example of breakthrough curve and ORM fit for pulse injection

C.2. Best injection times for TRM fit

Next, tables and graphics show the best injection time for a good TRM fit for different specimen heights. The breakthrough curves were obtained theoretically from the CXTFIT program where the specimen height, average flow velocity and transport parameters (R, D, α and T) were specified, and the corresponding breakthrough curve obtained with the direct problem solving capabilities of the program. Several breakthrough curves for different injection times were obtained.

The breakthrough curves were then fitted as explained in the previous section. Results are summarized in tables and graphs.

Height: 5 cm				
Injection time (d)	**Diffusion (cm2/d)**	**Beta**	**Omega**	**Alpha**
Original values	1.3	0.75	0.6475	0.259
0.5	1.295	0.7493	0.6507	0.26028
1	1.305	0.7509	0.6439	0.25756
5	1.302	0.7504	0.6459	0.25836
10	1.303	0.7505	0.6456	0.25824

Table C.1: TRM Fit results for specimen of 5 cm height

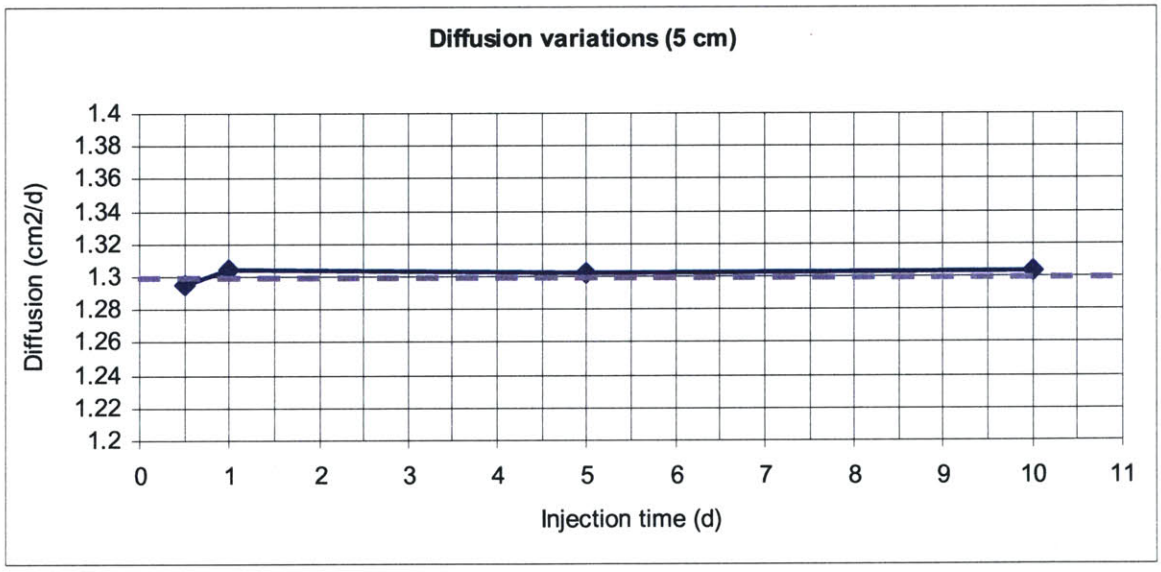

Figure C.3: TRM diffusion fit results for specimen of 5 cm height

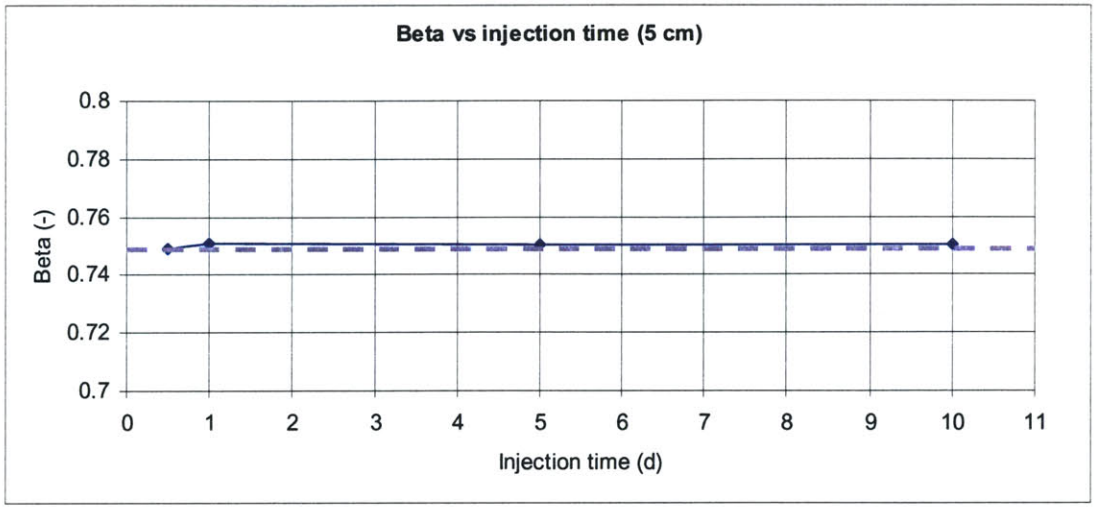

Figure C.4: TRM beta fit results for specimen of 5 cm height

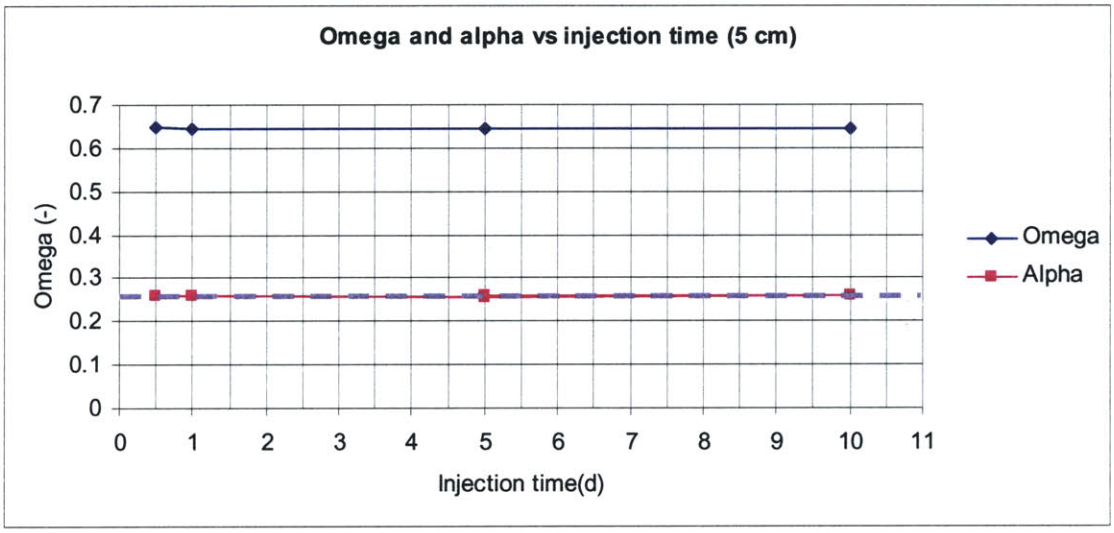

Figure C.5: TRM omega and alpha fit results for specimen of 5 cm height

Height: 10 cm				
Injection time (d)	**Diffusion (cm2/d)**	**Beta**	**Omega**	**Alpha**
Original values	1.3	0.75	0.777	0.2590
0.5	1.294	0.7496	0.7789	0.2596
1	1.298	0.7503	0.7735	0.2578
3	1.298	0.7503	0.7503	0.2501
5	1.299	0.7504	0.7734	0.2578

Table C.2: TRM Fit results for specimen of 10 cm height

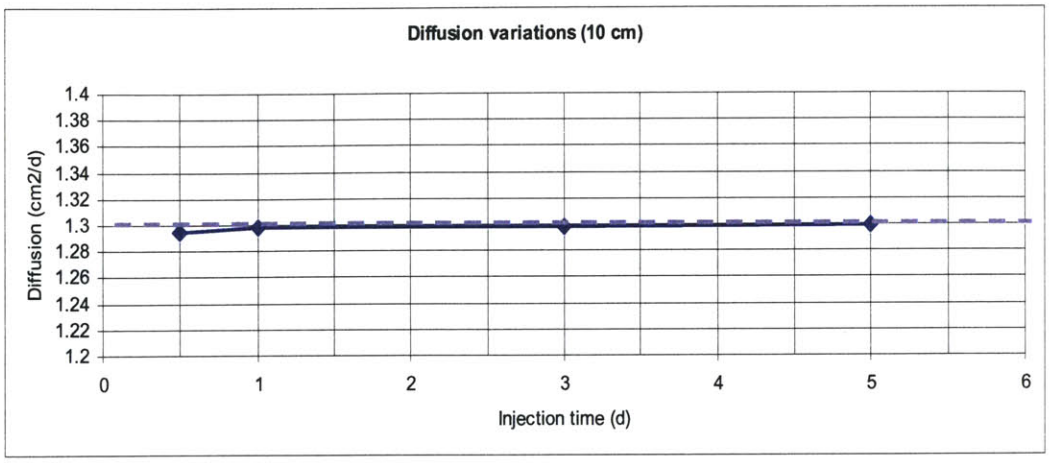

Figure C.6: TRM diffusion fit results for specimen of 10 cm height

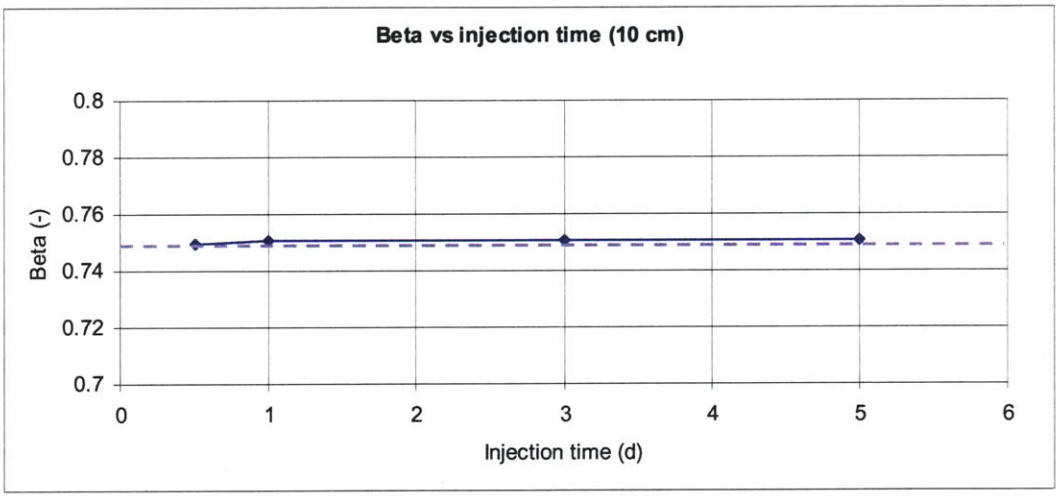

Figure C.7: TRM beta fit results for specimen of 10 cm height

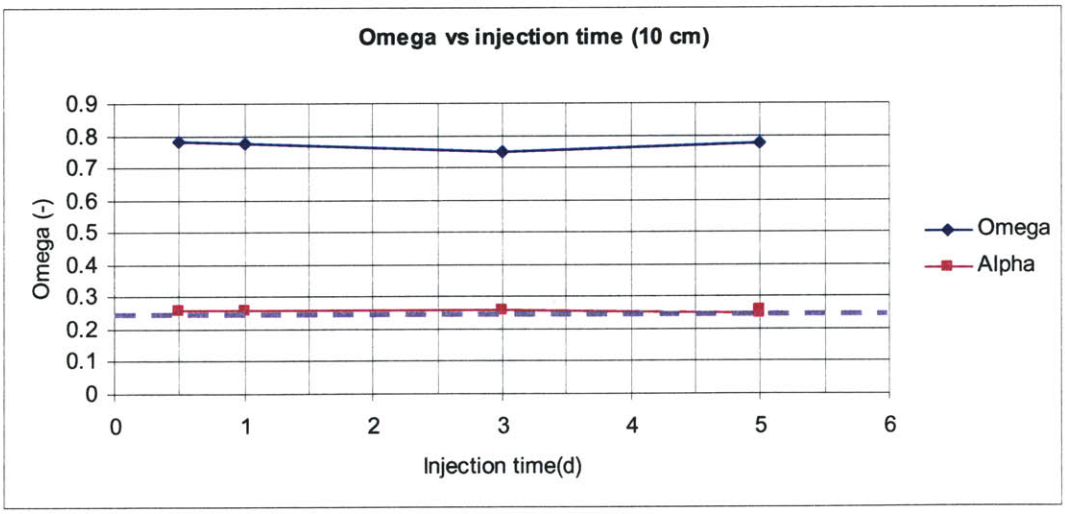

Figure C.8: TRM omega and alpha fit results for specimen of 10 cm height

Height: 20 cm				
Injection time (d)	Diffusion (cm2/d)	Beta	Omega	Alpha
0	1.3	0.75	2.59	0.2590
0.5	1.323	0.7535	2.441	0.2441
1	1.275	0.747	2.539	0.2539
3	1.286	0.7483	2.518	0.2518
5	1.309	0.7519	2.471	0.2471
10	1.289	0.7487	2.512	0.2512

Table C.3: TRM Fit results for specimen of 20 cm height

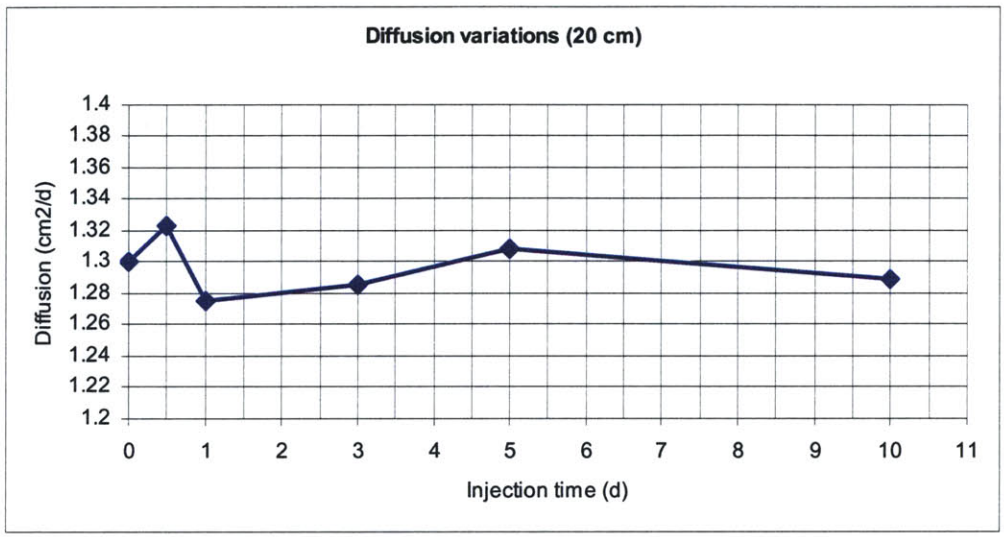

Figure C.9: TRM diffusion fit results for specimen of 10 cm height

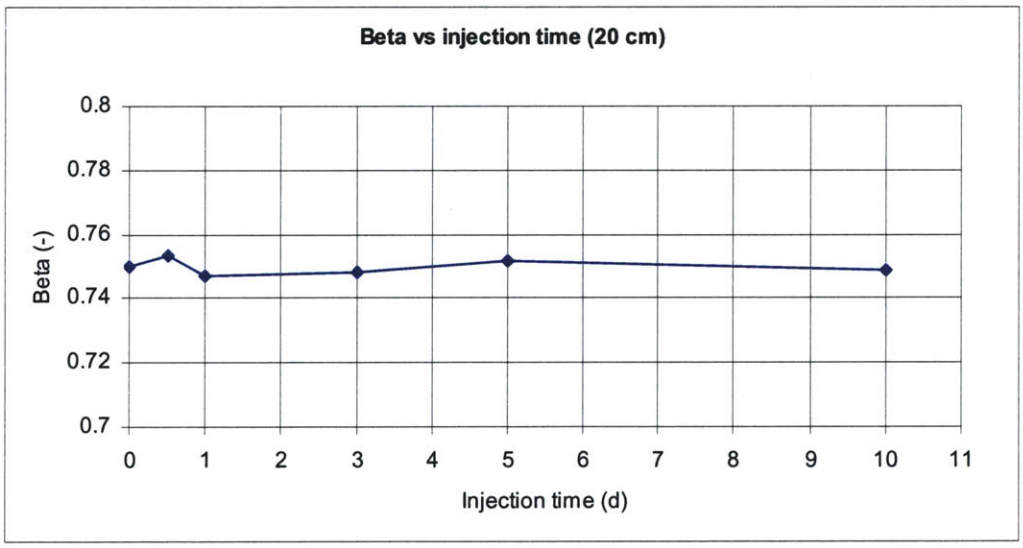

Figure C.10: TRM beta fit results for specimen of 10 cm height

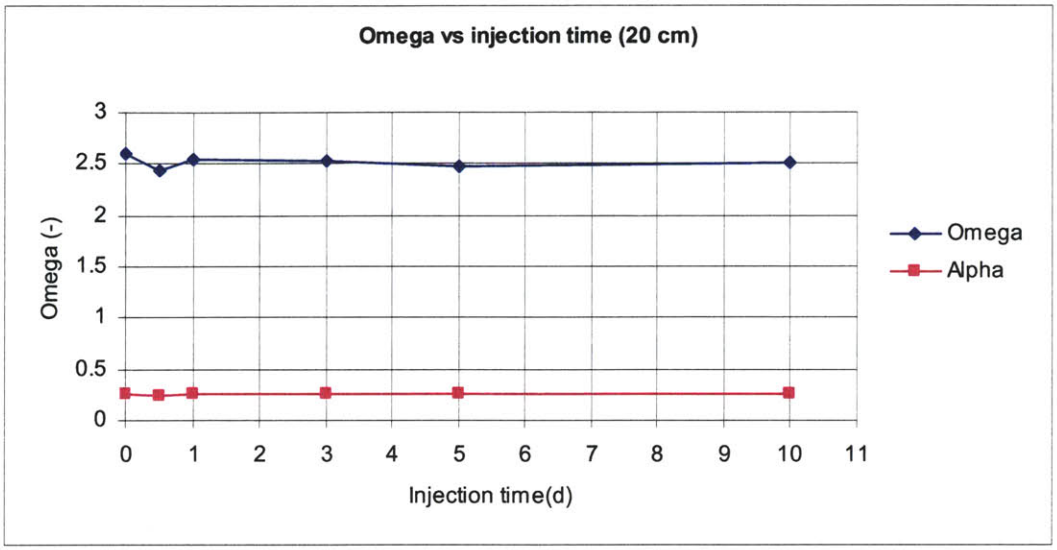

Figure C.11: TRM omega and alpha fit results for specimen of 10 cm height